PACIFIC EARTHQUAKE ENGINEERING
RESEARCH CENTER

Probabilistic Seismic Hazard Analysis and Selecting and Scaling of Ground-Motion Records

A Report for the "Quantifying the Performance of Retrofit of Cripple Walls and Sill Anchorage in Single-Family Wood-Frame Buildings" Project

Silvia Mazzoni
University of California, Los Angeles

Nicholas Gregor
N. Gregor Consulting

Linda Al Atik
L. AlAtik Consulting

Yousef Bozorgnia
University of California, Los Angeles

David P. Welch
Stanford University

Gregory G. Deierlein
Stanford University

PEER Report 2020/14
Pacific Earthquake Engineering Research Center
Headquarters, University of California at Berkeley

November 2020

PEER 2020/14
November 2020

Probabilistic Seismic Hazard Analysis and Selecting and Scaling of Ground-Motion Records

A Report for the "Quantifying the Performance of Retrofit of Cripple Walls and Sill Anchorage in Single-Family Wood-Frame Buildings" Project

Silvia Mazzoni
University of California, Los Angeles

Nicholas Gregor
N. Gregor Consulting

Linda Al Atik
L. AlAtik Consulting

Yousef Bozorgnia
University of California, Los Angeles

David P. Welch
Stanford University

Gregory G. Deierlein
Stanford University

PEER Report 2020/14
Pacific Earthquake Engineering Research Center
Headquarters at the University of California, Berkeley

November 2020

ABSTRACT

This report is one of a series of reports documenting the methods and findings of a multi-year, multi-disciplinary project coordinated by the Pacific Earthquake Engineering Research Center (PEER and funded by the California Earthquake Authority (CEA). The overall project is titled "*Quantifying the Performance of Retrofit of Cripple Walls and Sill Anchorage in Single-Family Wood-Frame Buildings*," henceforth referred to as the "PEER–CEA Project."

The overall objective of the PEER–CEA Project is to provide scientifically based information (e.g., testing, analysis, and resulting loss models) that measure and assess the effectiveness of seismic retrofit to reduce the risk of damage and associated losses (repair costs) of wood-frame houses with cripple wall and sill anchorage deficiencies as well as retrofitted conditions that address those deficiencies. Tasks that support and inform the loss-modeling effort are: (1) collecting and summarizing existing information and results of previous research on the performance of wood-frame houses; (2) identifying construction features to characterize alternative variants of wood-frame houses; (3) characterizing earthquake hazard and ground motions at representative sites in California; (4) developing cyclic loading protocols and conducting laboratory tests of cripple wall panels, wood-frame wall subassemblies, and sill anchorages to measure and document their response (strength and stiffness) under cyclic loading; and (5) the computer modeling, simulations, and the development of loss models as informed by a workshop with claims adjustors.

This report is a product of Working Group 3 (WG3), Task 3.1: *Selecting and Scaling Ground-motion records***.** The objective of Task 3.1 is to provide suites of ground motions to be used by other working groups (WGs), especially Working Group 5: Analytical Modeling (WG5) for Simulation Studies. The ground motions used in the numerical simulations are intended to represent seismic hazard at the building site. The seismic hazard is dependent on the location of the site relative to seismic sources, the characteristics of the seismic sources in the region and the local soil conditions at the site. To achieve a proper representation of hazard across the State of California, ten sites were selected, and a site-specific probabilistic seismic hazard analysis (PSHA) was performed at each of these sites for both a soft soil (V_{s30} = 270 m/sec) and a stiff soil (V_{s30} =760 m/sec). The PSHA used the UCERF3 seismic source model, which represents the latest seismic source model adopted by the USGS [2013] and NGA-West2 ground-motion models. The PSHA was carried out for structural periods ranging from 0.01 to 10 sec.

At each site and soil class, the results from the PSHA—hazard curves, hazard deaggregation, and uniform-hazard spectra (UHS)—were extracted for a series of ten return periods, prescribed by WG5 and WG6, ranging from 15.5–2500 years. For each case (site, soil class, and return period), the UHS was used as the target spectrum for selection and modification of a suite of ground motions. Additionally, another set of target spectra based on "Conditional Spectra" (CS), which are more realistic than UHS, was developed [Baker and Lee 2018]. The Conditional Spectra are defined by the median (Conditional Mean Spectrum) and a period-dependent variance. A suite of at least 40 record pairs (horizontal) were selected and modified for each return period and target-spectrum type. Thus, for each ground-motion suite, 40 or more record pairs were selected using the deaggregation of the hazard, resulting in more than 200 record pairs per target-spectrum type at each site. The suites contained more than 40 records in case some were

rejected by the modelers due to secondary characteristics; however, none were rejected, and the complete set was used.

For the case of UHS as the target spectrum, the selected motions were modified (scaled) such that the average of the median spectrum (RotD50) [Boore 2010] of the ground-motion pairs follow the target spectrum closely within the period range of interest to the analysts. In communications with WG5 researchers, for ground-motion (time histories, or time series) selection and modification, a period range between 0.01–2.0 sec was selected for this specific application for the project. The duration metrics and pulse characteristics of the records were also used in the final selection of ground motions. The damping ratio for the PSHA and ground-motion target spectra was set to 5%, which is standard practice in engineering applications.

For the cases where the CS was used as the target spectrum, the ground-motion suites were selected and scaled using a modified version of the conditional spectrum ground-motion selection tool (CS-GMS tool) developed by Baker and Lee [2018]. This tool selects and scales a suite of ground motions to meet both the median and the user-defined variability. This variability is defined by the relationship developed by Baker and Jayaram [2008]. The computation of CS requires a structural period for the conditional model. In collaboration with WG5 researchers, a conditioning period of 0.25 sec was selected as a representative of the fundamental mode of vibration of the buildings of interest in this study. Working Group 5 carried out a sensitivity analysis of using other conditioning periods, and the results and discussion of selection of conditioning period are reported in Section 4 of the WG5 PEER report entitled *Technical Background Report for Structural Analysis and Performance Assessment*.

The WG3.1 report presents a summary of the selected sites, the seismic-source characterization model, and the ground-motion characterization model used in the PSHA, followed by selection and modification of suites of ground motions. The Record Sequence Number (RSN) and the associated scale factors are tabulated in the Appendices of this report, and the actual time-series files can be downloaded from the PEER Ground-motion database Portal (*https://ngawest2.berkeley.edu/*).

ACKNOWLEDGMENT AND DISCLAIMER

ACKNOWLEDGMENT

This research project benefited from the interaction of many researchers and practitioners. The authors would like to thank the following project team members for their input and feedback Jack Baker, Henry Burton, Kelly Cobeen, Seb Ficcadenti, Bret Lizundia, Curt Haselton, Tara Hutchinson, Grace Kang, Charlie Kircher, Thor Matteson, Frank McKenna, Vahid Mahdavifar, Gilberto Mosqueda, Sharyl Rabinovici, Evan Reis, Brandon Schiller, Chia-Ming Uang, John van de Lindt, and Farzin Zareian. The assistance and feedback of the Project Review Panel consisting of Colin Blaney, Doug Hohbach, John Hooper, and Charles Scawthorn is greatly appreciated. Support from the members of the CEA Team, Shawna Ackerman, Janiele Maffei, Badie Rowshandel, and Erin Rogers, and members of their Advisory Team, Tom Heaton, Brian McDonald, John Osteraas, and Keith Porter, is gratefully acknowledged.

DISCLAIMER

This research study was funded by the California Earthquake Authority (CEA). The support of the CEA is gratefully acknowledged. The opinions, findings, conclusions, and recommendations expressed in this publication are those of the authors and do not necessarily reflect the views of CEA, Pacific Earthquake Engineering Research Center (PEER), members of the Project Team, or the Regents of the University of California.

TABLE OF CONTENTS

LIST OF TABLES

LIST OF FIGURES

1 Introduction

1.1 PROJECT OVERVIEW

This report is one of a series of reports documenting the methods and findings of a multi-year, multi-disciplinary project coordinated by the Pacific Earthquake Engineering Research Center (PEER) and funded by the California Earthquake Authority (CEA). The overall project is titled "*Quantifying the Performance of Retrofit of Cripple Walls and Sill Anchorage in Single-Family Wood-Frame Buildings*," henceforth referred to as the "PEER–CEA Project."

The overall objective of the PEER–CEA Project is to provide scientifically based information (e.g., testing, analysis, and resulting loss models) that measure and assess the effectiveness of seismic retrofit to reduce the risk of damage and associated losses (repair costs) of wood-frame houses with cripple wall and sill anchorage deficiencies as well as retrofitted conditions that address those deficiencies. Tasks that support and inform the loss-modeling effort are: (1) collecting and summarizing existing information and results of previous research on the performance of wood-frame houses; (2) identifying construction features to characterize alternative variants of wood-frame houses; (3) characterizing earthquake hazard and ground motions at representative sites in California; (4) developing cyclic loading protocols and conducting laboratory tests of cripple wall panels, wood-frame wall subassemblies, and sill anchorages to measure and document their response (strength and stiffness) under cyclic loading; and (5) the computer modeling, simulations, and the development of loss models as informed by a workshop with claims adjustors.

Within the PEER–CEA Project, detailed work was conducted by seven Working Groups, each addressing a particular area of study and expertise, and collaborating with the other Working Groups. The seven Working Groups are as follows:

Working Group 1: Resources Review

Working Group 2: Index Buildings

Working Group 3: Ground-Motion Selection and Loading Protocol

Working Group 4: Testing

Working Group 5: Analytical Modeling

Working Group 6: Interaction with Claims Adjustors and Catastrophe Modelers

Working Group 7: Reporting

This report is a product of the Working Group denoted in bolded text above.

This report is a product of the Working Group 3 (WG3): *Ground Motions and Loading Protocol*. Specifically, the report focused on the characterization of seismic hazard and subsequent selection and scaling of ground motions for use by other working groups in structural analysis of wood-frame dwellings.

1.2 BACKGROUND

The overall goal of the PEER–CEA Project was to develop the difference between the "fragility function" of unretrofitted versus that of retrofitted cripple wall wood-frame buildings. This difference in the fragility functions is then to be used by the CEA to adjust premium rates for earthquake insurance. In this scope, a fragility function is for given level of a ground-motion intensity measure (IM). The very common IM used in the earthquake financial loss practice is response spectrum. Thus, the fragility functions to be developed in this project are for a given level of spectral ordinates and not for a specific value of response spectral ordinate. Therefore, a specific value of a spectral ordinate is less important in this project as compared to the shape of the target response spectra used in the analysis. As elaborated below, target response spectra of varying amplitudes (ordinates) were developed and then used to select and scale ground-motion records.

The objective of Working Group 3 (WG3), Task 3.1, Ground-Motion Selection and Modification, was to provide suites of ground motions to be used by other working groups—particularly WG5—for numerical simulations of wood-frame buildings for the PEER–CEA Project. The results of the computer simulations in WG5 were then used by WG6 to develop "fragility functions" for retrofitted and unretrofitted buildings. The methodology and framework of developing such "fragility functions" is documented in WG6's report.

Fragility functions, derived from results of a suites of ground-motion simulations, prescribe the probability of exceeding a specified engineering demand parameter, EDP, (such as interstory drift) *as a function of an input IM* (i.e., spectral acceleration at a particular period). To develop fragility functions, the numerical simulations use a nonlinear structural model subjected to ground motions of *varying intensity*, as is done in an incremental dynamic analysis (IDA) [Vamvatsikos and Cornell 2002], or a variation of it known as "stripe analysis"; see, e.g., Baker [2015]. The variation of intensity can be done by either scaling a suite of ground motions by a constant of increasing value or developing different suites of motions for different hazard levels (i.e., a hazard-consistent suite). The scope of WG3, Task 3.1, was to develop the hazard-consistent ground-motion suites.

Hazard-consistent ground-motion suites are based on probabilistic seismic hazard analysis, which is site-specific. The scope of the PEER–CEA Project was to develop fragility functions that are applicable to the entire state of California. Thus, to achieve a proper representation of hazard across the state of California, various alternatives and choices of sites and parameters for ground-motion hazard and selection and modification were considered and discussed with members of WG3, WG5, and WG6, as well as outside experts.

Considering the general framework of the project and the intended use of the ground motions for the project (summarized above), and yet he need to narrow down ranges of various parameters for seismic hazard and ground motions, a Panel Meeting was held on March 13, 2017 [Appendix C.1 of this report]. The Panel participants represented members from all the working groups in the project and resulted in a series of decisions and action items on the general scope of seismic hazards and ground motions as listed in Appendix C.2 of this report. Below is a summary of discussions, decisions, and action items arrived at because of the Panel meeting.

1. Site selection: To ensure a proper representation of the risk in the state of California, the Panel decided that the seismic hazard be computed for several different sites in the state. The selection of the sites would be based on selecting different representative seismic settings as well as different building populations across the state. Panel participants discussed various issues related to selection of sites, including the number of sites and soil conditions. The Panel's consensus was that ten sites should be selected for the seismic-hazard analysis and ground-motion selection. The simulation results from these ten sites would then be evaluated by the WG5 to determine whether all sites should be used or, if not, which should be selected. For each site, the hazard was computed for two soil conditions: "Rock" (or stiff soil), V_{s30} = 760 m/sec, and "Soil", V_{s30} = 270 m/sec. Although hazard analysis and ground-motion selection were carried out for both "rock" and "soil" conditions, communications with the CEA revealed that the "soil" condition dominates most sites in the portfolio. The Panel's consensus was also to exclude sites in very northwest of California (e.g., the area around Eureka), which is not representative of the rest of the state, and the building population at that location is low when compared to the remainder of the state. Thus, the selected sites are predominantly affected by shallow crustal earthquakes. The selected sites are discussed in more details in this report.
2. Considering the fact that the period of interest for wood-frame buildings is generally short, the Panel members cautioned WG3 that: "*Keep period range of interest into account when evaluating spectra (T < 1 sec)*" to be consistent with the building type being evaluated. Based on this constraint, the following comments can be made:
    a. The ground-motion suites contain records both with and without directivity pulses. Working Group 5 has investigated the fraction of the selected recordings with pulses as compared with those in literature, and concluded that: "*The results of the study show that the WG3 ground-motion sets have an increasing number of pulse records with increasing seismic intensity or return period. Selected sites show reasonable agreement in terms of the fraction of pulse records when comparing to relationships published in the literature.*" The WG5 investigation is presented in Chapter 3 and Chapter 4 of this report.
    b. Since the period of interest is relatively short, only the default long-period basin effects modeled in the NGA-West2 ground-motion models (e.g., Campbell and Bozorgnia (2014)] were considered in the PSHA; see Section 2.3 of this report.
3. Number of ground-motion suites at each site: The Panel's consensus was to have 40 pairs of horizontal records for each ground-motion suite at each hazard level and site combination to ensure there would be enough records for an accurate estimate of EDP probabilities at each IM to obtain fragility curves without imposing excessive computational effort in the analyses. In addition, 40 records are the

typical number of records used in developing and implementing fragility curves using the Performance Assessment Calculation Tool (PACT) framework developed for *FEMA P-58* [FEMA 2012]. Characteristics of the selected "seed motions," their associated earthquake events, and other metadata are discussed in greater detail in this report and Appendix A.1, Appendix A.2, and Appendix A.3 of this report.

4. Probabilistic seismic hazard analysis is used to estimate seismic hazard at the selected sites. The Panel recommended use of computer code HAZ-45, as it is a publicly available computer code that represents the latest state of the science in seismic hazard analysis [Hale et al. 2018].

5. For PSHA, two fundamental components are needed: seismic sources (faults with seismicity characteristics) and ground-motion characterizations (estimate of the IM at site). For seismic-source characterization, the Panel recommended the use of UCERF-3 [USGS 2013] as it includes the latest seismic-source characterization for the state of California and is used by the USGS for the development of the U.S. National Seismic Hazard Maps for California [Petersen et al. 2014]. UCERF3 time-independent model is used for this study. This type of model was chosen for this project because it is more typically used for this type of probabilistic hazard analysis.

6. For the ground-motion characterization, the NGA-West2 models and motions were used [Bozorgnia et al. 2014]. The NGA-West2 models are the latest ground motion models for the shallow crustal earthquakes and are used by the USGS for the development of the U.S. National Seismic Hazard Maps for California [Petersen et al. 2014]. To maintain compatibility between the two soil conditions, the Idriss [2014] ground-motion model was not used in the PSHA because it not applicable to the soft-soil site.

7. The Panel recommended that, as a minimum, the PSHA of the selected sites with the following return periods should be considered: 72, 100, 250, 475, 1000, and 2475 years. Subsequent to the Panel meeting and after numerous internal discussions with the members of WG5 and WG6, the following return periods were selected for the PSHA: 15, 25, 50, 75, 100, 150, 250, 500, 1000, and 2500 years.

8. The Panel's consensus was not to apply the "deterministic cap" in developing the target response spectra at the selected sites; thus, the ground-motion results were based on the PSHA runs. The deterministic cap is used in developing code-compliant design spectra, while the objective of the ground-motion development in this project was to develop hazard-consistent spectra and ground motions.

9. For target spectra, the PSHA-based UHS was recommended. Use and application of the CMS was also considered. However, during the life of the project, CMS target spectra were also generated by WG3.1 and used by WG5 as explained in Section 1.3 below.

10. Because WG3 focused on the horizontal component of ground motion, vertical ground motions were not developed. The vertical component of the records can be made available if needed by the working groups.

11. The Panel recommended the use of recorded ground motions and scale them (if needed) rather than use synthetic (simulated) motions. Synthetic motions are typically used for scenarios where recorded motions are not available. The return periods considered in this project do not warrant the need for such rare records.
12. For the modification of the selected motion, WG3 used scalar scaling factors rather than the "spectral matching" process. Spectral matching is a useful practice when using a small set of ground motions. It should be noted that one advantage of scalar scaling is to maintain some degree of record-to-record variability, as well as period-to-period variability. It should also be noted that the target spectra are the results of PSHA runs, and PSHA process already includes some degree of record-to-record variability as well in its probabilistic aspect. The process of selection and scaling of motions is discussed in detail in this report.

1.3 OVERVIEW OF TASK 3.1 AND REPORT

Following the general recommendations by the Panel as summarized above, ten sites in California were selected, and PSHA was performed at each of these sites for both a softer soil (V_{s30} = 270 m/sec) and a stiffer soil/rock (V_{s30} = 760 m/sec). The PSHA used the UCERF3 source model and NGA-West2 ground-motion models, which represent the latest state-of-the-art developments in seismic hazard analysis. Both soil classes were considered for completeness: the softer soil class was expected to represent most site conditions in the population of interest, while the stiffer soil class was used as a reference class for most PSHA comparisons.

At each site and soil class, the results from the PSHA—hazard curves, hazard deaggregation, and uniform-hazard spectra (UHS)—were extracted for a series of ten return periods prescribed by WG5: 15, 25, 50, 75, 100, 150, 250, 500, 1000, and 2500 years. For each case (site, soil class, and return period), the UHS was used as the "target spectrum" for selection and modification of a suite of ground motions. In collaboration with WG5 researchers, a preliminary decision was made to select and modify 40 record pairs (H1 and H2 components) for each case. Thus, for each ground-motion suite, at least 40 record pairs were selected using the deaggregation of the PSHA results. The selected motions were then modified (scaled) such that the average spectrum (RotD50) [Boore 2010] of the ground-motion pairs follow the target spectrum closely within the period range of interest. The PSHA was carried out for periods ranging from 0.01 to 10 sec. In communications with WG5 researchers and following the Panel's general recommendations, for ground-motion time histories (or time series) selection and modification, a period range between 0.01 and 2.0 sec was selected for this specific application for the project. Per the Panel's recommendation, this period range is longer than a period of 1.0 sec to allow an effective period elongation of structural response (i.e., "softening") during the nonlinear response history ("time history") analysis by WG5. The durations of the records were also recorded for further investigation by WG5 for possible duration effects on structural models.

In record selection and modification, the most important issue is the compatibility of the response spectra with the shape of the target spectrum. Embedded in the target spectrum are various features such as style of faulting. Additionally, if we further restrict the record selection by a parameter such as style of faulting, the selection set would become smaller and consequently the scaling factors to be applied to the records may become larger.

The viscous damping ratio for the PSHA and ground-motion spectra was set to a reference value of 5%, as is typical in code-compliant ground-motion selection. Note: the 5% damping is a nominal value used as a reference for selection only. The structural models developed by WG5 considered nonlinear hysteretic behavior (and their associated energy dissipation) in addition to an adjusted "viscous damping" to compensate for non-hysteretic energy dissipation. Thus, the selection of 5% reference damping for the hazard and ground-motion analysis did not restrict in any way the actual structural analysis performed by WG5.

A recent research study suggests that damping ratios other than 5%, and possibly as large as 70%, should be used [Buyco and Heaton 2019]. Selection of a damping ratio as high as 70% for the target spectra and the impact of such a selection on the structural analysis of wood-frame buildings should be investigated in a future research project.

Once the first set of ground-motion suites based on the UHS were developed, internal and external project review prompted the investigation of possible alternative suites, such as ones using the CMS as the target and evaluating different models for the record-to-record spectrum variability within a suite. Different types of suites were developed and proposed by WG3 to WG5, which selected the suite based on the CS, where the target mean is defined by the CMS and the record-to-record variability is defined by correlations developed by Jack Baker and his research group at Stanford [Baker 2011]. The method and resulting suites of ground motions are presented in this report.

A study of the pulse characteristics of representative sites was performed and is presented in this report. The study investigates and quantifies the different methods of identifying a pulse in a record, as well as compares the fraction of pulse-like records in the ground-motion suites to empirical predictive models.

It is worth noting that the main engineering scope of the project was to develop fragility curves to be used as input by the loss modelers. In addition, the specific objective of the project was to quantify the effects of retrofit on the loss estimates. Thus, to make the comparison between retrofitted and unretrofitted cases, a relative estimate was sought rather than an absolute one. Fragility curves give the probability of exceeding a limit state—such as collapse—as a function of input intensity, such as spectral acceleration. The objective of Task 3.1, therefore, was to develop suites of ground motions with target spectra that span the range of possibilities in California to be used by WG5 to contrast performances of retrofitted versus unretrofitted structures.

This report presents a summary of the selected sites, the seismic-source characterization (SSC) model and the ground-motion characterization (GMC) model used in the PSHA, followed by selection and modification of suites of ground motions. The report contains multiple appendices with details of the PSHA results and the selected and scaled motions, as listed below:

A. Appendix A contains the products of WG3 Task 3.1, i.e., a complete set of selected and scaled ground motions at the ten sites, for ten return periods and two soil conditions (a total of 200 suites of 40 record pairs). The scale factors, record metadata, and response spectra are provided for each record. This appendix does not contain the record files themselves; these record files have been submitted to the analysts in WG5 in electronic format and they can be downloaded from the PEER Ground-motion database Portal (*https://ngawest2.berkeley.edu/*). This appendix also contains the target spectra for the two sets of ground-motion suites.

- ✓ Appendix A.1 Products for the ground-motion suite based on UHS;
- ✓ Appendix A.2 Products for the ground-motion suite based on the CS; and
- ✓ Appendix A.3 Target Spectra for the two sets of ground-motion suites: UHS and CS (Digital Appendix – Microsoft Excel File).

B. Appendix B contains the results of the PSHA. Appendix B is a digital appendix with individual Microsoft Excel files with hazard and deaggregation data for each of the 10 sites, return periods, and soil conditions. Specifically,

- ✓ Appendix B.1 includes the list of electronic files for the digital files in Appendix B.2 and Appendix B.3;
- ✓ Appendix B.2 contains the hazard curves; and
- ✓ Appendix B.3 has the UHS deaggregation results.

C. Appendix C.1 includes a summary of the discussions during the Panel Meeting held on March 13, 2017. Appendix C.2 includes a summary of discussions, decisions, and a list of action items made during the Panel Meeting held on March 13, 2017.

2 Probabilistic Seismic Hazard Analysis

The probabilistic seismic hazard assessment (PSHA) for the ten representative sites in California was performed using the Uniform California Earthquake Rupture Forecast Version 3 (UCERF3) seismic-source model [USGS 2013], and the Next Generation Attenuation for the western U.S (NGA-West2) ground-motion prediction equations (GMPEs). The PSHA was performed following the standard state-of-the-practice methodology, and the resulting UHS and deaggregation information were used for the selection of applicable time histories (i.e., “time series”) for modification (scaling) and subsequent engineering analyses.

For each of the ten site locations, two representative V_{S30} values were assigned: 270 m/sec and 760 m/sec. The value of 760 m/sec was selected as it is the “reference” site condition in the USGS National Seismic Hazard Maps, which are used in the building code and by the financial-loss modelers. The other value of 270 m/sec was selected based on the shear-wave velocity associated with typical soil conditions in California. Hazard curves were computed for a suite of 22 spectral periods spanning the range of peak ground acceleration (PGA) (i.e., 0.01 sec) to 10.0 sec. Uniform hazard spectra were computed for a suite of ten return periods (i.e., hazard levels) from 15 years to 2500 years. In addition, deaggregation results were computed for each of the PSHA cases. Herein, a representative set of results are presented for two sites. The complete set of results for the ten site locations is contained in Appendix B of this report.

In the next sections, the representative sites are defined, and an overview of the Seismic-Source Characterization (SSC) model and the Ground-Motion Characterization (GMC) model as implemented in HAZ45 computer code for PSHA is presented. The PSHA results are presented in terms of mean hazard curves at the PGA and spectral periods of 0.1, 0.2, 0.5, 1.0, 3.0, 5.0, and 10.0 sec.

2.1 REPRESENTATIVE SITES

Ten sites in California were selected as representative sites to perform the PSHA. The selection criteria were based on the relative population of major cities in California and the expected controlling seismic sources for a given location and cities in which recent historical earthquakes have occurred. Following the completion of PSHA and ground motions—and depending on the shape of the UHS at different sites—WG5 was given the option of choosing a subset of sites for further analysis. Note: the selection of the sites was based on discussions and the consensus and expertise of participants at the Panel meeting, as indicated in the “Background” section of this report.

Based on these criteria, the ten selected cities are listed in Table 2.1 and plotted in Figure 2.1. The latitude and longitude location for each city was selected based on the geographical location of its city hall.

These ten cities fall into three main regional areas of California: Northern California, the Central Valley, and Southern California. Note that locations in far Northern California were not considered based on their relatively lower population density. In addition, the expected contribution from the Cascadia interface seismic source to the hazard is considered potentially significant, which would require the inclusion of this seismic source in the PSHA studies.

Table 2.1 Location of selected sites for PSHA.

City	Region	Latitude (°)	Longitude (°)
Oakland	Northern California	37.8053046	-122.2725459
Sacramento	Central Valley	38.5818918	-121.4935297
San Francisco	Northern California	37.7792597	-122.4192646
San Jose	Northern California	37.3378484	-121.8861262
Bakersfield	Central Valley	35.3736802	-119.020492
Long Beach	Southern California	33.7680362	-118.1956387
Los Angeles	Southern California	34.0535267	-118.2429316
Northridge	Southern California	34.2280556	-118.53583
San Bernardino	Southern California	34.1045714	-117.2927641
San Diego	Southern California	32.7181497	-117.1642655

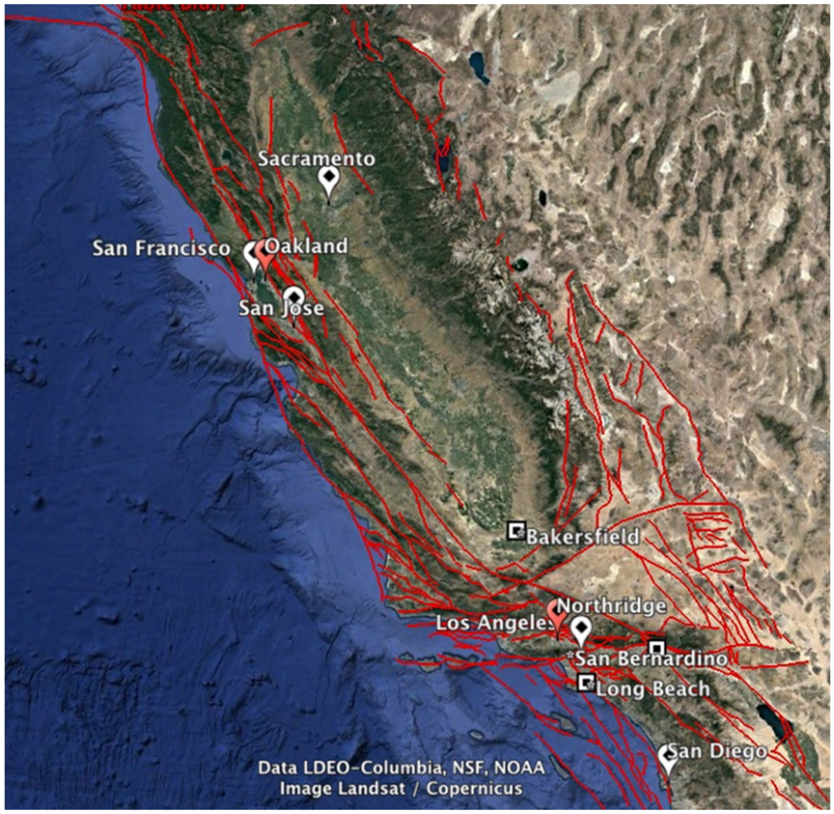

Figure 2.1 Selected Sites for PSHA + UCERF3 Sources [Google Earth 2018].

2.2 SEISMIC-SOURCE CHARACTERIZATION MODEL

The current state of knowledge seismic-source characterization (SSC) for California is based on the UCERF3 seismic-source model developed by the USGS [2013] for evaluating the hazard at the ten site locations. Note that the Cascadia Interface seismic-source model is not part of the UCERF3 source model and was not used in the analysis. Based on the ten selected site locations, it can be expected that the contribution to any of the Northern California sites locations from the Cascadia seismic source to be minimal, especially for the spectral period range of interest for this project (i.e., $T < 1$–2 sec).

The UCERF3 complex source model accounts for potential seismic events associated with both mapped and unmapped faults. This newly developed model for the California region is different from previous SSC models (e.g., UCERF2) in that the strict fault segmentation breaks were relaxed allowing for multiple fault-segment ruptures. As part of the UCERF3 SSC model, a broad range of data was used to perform a grand inversion that estimates the long-term rate of occurrence of all earthquakes of magnitude 5.0 and larger. Both planar fault segments and gridded smooth seismicity point sources were considered in this grand inversion. Mathematically, this grand inversion is somewhat straight forward; however, based on the volume of input data and as importantly the number of logic-tree branches (i.e., 1440 logic-tree branches) considered for the epistemic uncertainty (e.g., see Figure 3 of USGS [2013]), the grand inversion was performed on super computers. Two notable features of the UCERF3 SSC model are: (1) the removal of the over-prediction of earthquakes in the magnitude 6.5–7.0 range when compared to the historical seismicity catalogs; and (2) the potential for earthquakes associated with multiple fault systems as have been observed in large crustal earthquakes. A brief overview of the important features of the UCERF3 model pertinent to the PSHA performed for the selected ten sites is summarized herein.

As part of the implementation of the UCERF3 SSC model to a given site location, only seismic sources associated with fault segments and gridded point sources located within the closest maximum distance of 300 km from each site were included in the PSHA study. Scenario faults can have distances greater than 300 km if the closest point from the fault to the site is within the 300-km limit. Note that this maximum distance of 300 km is larger than is typically used for a given seismic-source model in California, but some distant seismic sources within 300 km were expected to have some contribution to the hazard. This cut-off distance of 300 km allows for the subsampling of the full dataset of rupture scenarios, while capturing the events expected to contribute to the seismic hazard at a given site location. This maximum distance of 300 km used in the analysis is also within the acceptable distance range of the ground-motion prediction equations discussed later in this report.

2.2.1 Fault Sources

The UCERF3 SSC model consists of a total of 3412 individual fault segments for the entire region of California. These individual segments were estimated based on a rupture length of approximately 7 km. Within the framework of the UCERF3 model, a minimum of at least two fault segments must rupture together to create an earthquake rupture scenario. In addition to this minimum number of rupture segments, multiple segments are allowed to rupture as part of a single earthquake scenario based on the assigned rules for multiple rupturing segments. Note that segments do not need to be continuous but must be within proximity of each other (e.g., about 5 km) for multiple segments to rupture in each scenario. This allowance for the joining of close but not continuous fault segments is a feature of the UCERF3 SSC that was not included in earlier versions of the UCERF SSC model.

Two fault models (FM3.1 and FM3.2) were developed for the UCERF3 SSC model, and the recommended weights for these two models are 50% each. As part of the available data for the UCERF3 model, a combined dataset for both the FM3.1 and FM3.2 identified as the "true mean" solution (*http://opensha.usc.edu/trac/wiki/UCERF3FaultSystemSolutions*) was used. This solution uses duplicate versions of each rupture whenever a key property (rake, magnitude, area, etc.) changes and retains all the variability in the UCERF3 logic tree while allowing for a quick reproduction of the mean UCERF3 results with minimum sets of rupture. With this combined UCERF3 SSC fault model, there are a total of 1,634,466 individual earthquake rupture scenarios associated with combinations of the 3412 individual fault segments for the entire California region. For each fault rupture scenario, the closest distance (rupture distance) from the site to all the fault segments associated with this rupture was measured; scenarios with closest distance of less than 300 km from each of the ten sites were included in the study. It should be noted that the 2014 USGS National Hazard Maps also were computed using the "true mean."

The individual fault segments with rupture scenario distances less than 300 km are plotted in Figure 2.2 for the Oakland site and Figure 2.3 for the Los Angeles site. As can be observed in these maps, the UCERF3 SSC model contains rupture scenarios in which multiple segments rupture together, thereby spanning a large area around each of the sites. The distance from these multiple segment ruptures can extend beyond the 300-km limit, but for some point along the fault segment the closest distance is less than 300 km. Based on this long fault-rupture length, the associated magnitude for these scenarios is large; however, their estimated rate of occurrence is generally low.

For rupture scenarios in which multiple fault segments are included—each with potentially different dip angle—a weighted-average dip angle is computed. This average dip angle is calculated based on the area-weighted dip angles for the individual fault segments relative to the total area of the entire rupture scenario (total area of all associated segments). Similarly, the average depth-to-top of rupture was calculated based on the area-weighted average of the depth-to-top of rupture of the individual fault segments associated with a particular rupture.

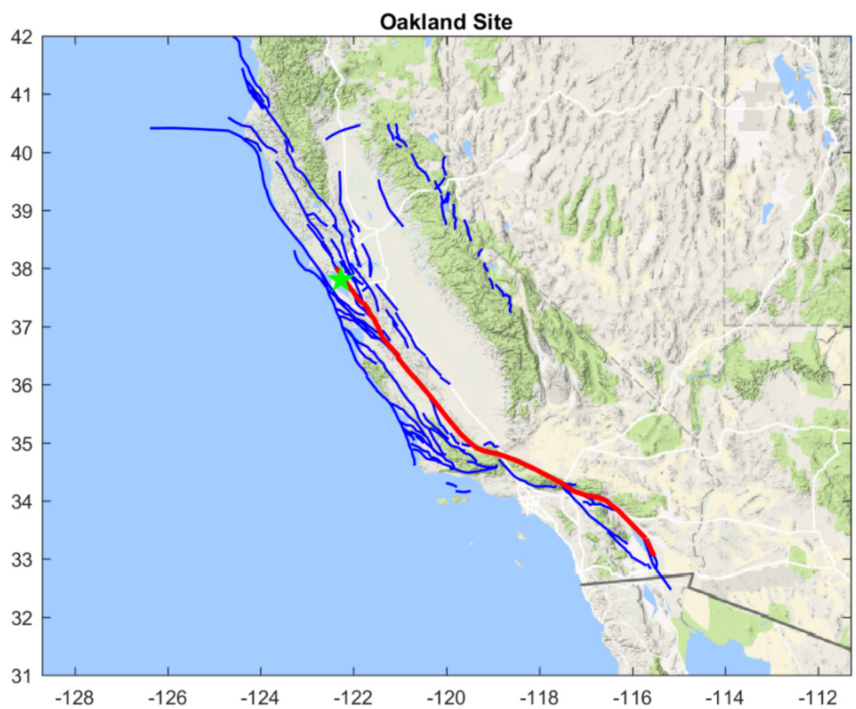

Figure 2.2 Regional map showing the fault segments (red and blue traces) associated with all rupture scenarios within a maximum distance of 300 km from the Oakland site location (star).

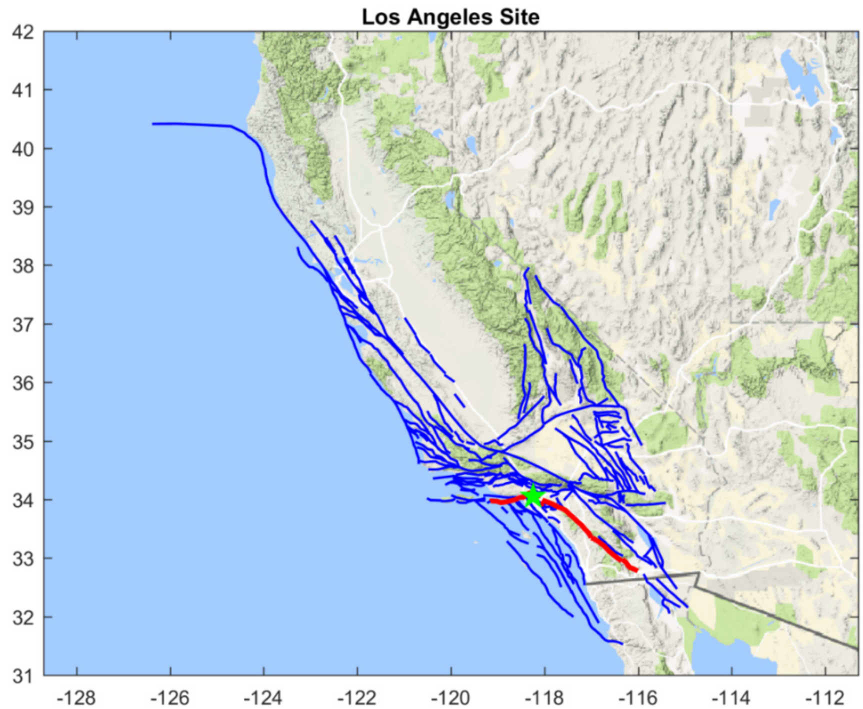

Figure 2.3 **Regional map showing the fault segments (red and blue traces) associated with all rupture scenarios within a maximum distance of 300 km from Los Angeles site location (star).**

2.2.2 Gridded Seismicity

For the gridded point sources, a standard approach in analyzing and smoothing the historical earthquake catalog was employed in the development of the UCERF3 model. For the region of California, a total of 7636 grid points is defined and provided as part of the "true mean" data files. Gridded point source locations are defined at 0.1 × 0.1° latitude and longitude intervals, and the UCERF3 SSC model also provides a weighting scheme for each defined point location for the strike–slip, reverse, and normal earthquake mechanisms. These fault mechanism weights are used with the GMPEs when estimating the ground motions from the grid point sources.

For the implementation of the gridded source model, distance corrections are computed based on the modeling of virtual faults centered at each grid point. For this distance correction, three virtual faults are considered: a vertical dipping strike–slip fault, and reverse and normal dipping faults with a dip angle of 50°. For the two dipping fault cases, both the hanging wall and footwall cases are considered with equal weights between the two cases. To account for the potential strike orientation of these virtual faults, three azimuthal orientations of perpendicular, parallel, and rotated by 45° related to the site location were considered. Note that this application of the distance correction for the gridded point sources is different than the correction implemented by the USGS [Petersen et al. 2014]. As stated by the USGS [Petersen et al. 2014], part of the technical decision for the distance correction was driven by the end result of having smooth contour ground-motion maps on a regional scale rather than the estimation for a given site location or locations.

2.3 GROUND-MOTION CHARACTERIZATION MODEL

Four equally weighted Next Generation Attenuation for the western United States (NGA-West2) GMPEs were used to predict ground motions for the PSHA study. These GMPEs are: Abrahamson et al. [2014] (referred to as ASK14), Boore et al. [2014] (referred to as BSSA14), Campbell and Bozorgnia [2014] (referred to as CB14), and Chiou and Youngs [2014] (referred to as CY14). Two V_{S30} values of 270 m/sec and 760 m/sec were assigned for the analysis. These two V_{S30} values are representative of typical "soil" and the industry adopted "reference condition" values. We note that the Idriss [2014] model was not used in this study due to the V_{S30} value of 270 m/sec being less than the minimum applicable range of 450 m/sec. For 760 m/sec, the Idriss model could be used; however, to keep the results of 270 m/sec and 760 m/sec consistent, we use the four GMPEs throughout.

For the ASK14 and CY14 models, the functional form of the models based on an "estimated V_{S30}" value was implemented in this study. Note that the differences between the estimated and measured V_{S30} flag only impact the uncertainty of each GMPE model but does not impact the median ground-motion estimates. Based on the V_{S30} values for each site, the default $Z_{1.0}$ and $Z_{2.5}$ parameter values used in this study for each GMPE are listed in Table 2.2. For the $Z_{1.0}$ value, an average value as predicted from the ASK14 and CY14 models was used in the analysis. No other basin effects were considered in the analyses. These $Z_{1.0}$ and $Z_{2.5}$ average values were used rather than the estimated site-specific values for the ten site locations because the goal of the PSHA study was to develop representative ground motions throughout California and not focus on the potential variability from any of the site-specific locations. In addition, the impact of the $Z_{1.0}$ and $Z_{2.5}$ terms on the ground-motion spectra is an intermediate to long-period effects, which falls primarily outside the spectral period range of interest. Using the default values provides a nominal representation of basin effects without being site-specific.

Because the NGA-West2 GMPEs were developed in a collaborative effort with interactions and exchange of ideas among the developers, the NGA-West2 developers indicated that additional epistemic uncertainty needed to be incorporated into the median ground-motion estimation from their GMPEs. The additional epistemic uncertainty model of Al Atik and Youngs [2014] developed as part of the NGA-West2 project was implemented for the PSHA calculations. Incorporating the Al Atik and Youngs [2014] model is consistent with the NGA-West2 ground-motion models used in this study. The Al Atik and Youngs [2014] epistemic uncertainty model is distance-independent but depends on magnitude, style-of-faulting, and spectral period. The upper and lower branches of the epistemic model were assigned weights of 0.185, and the central branch of the model was assigned a weight of 0.63 [Al Atik and Youngs 2014; Keefer and Bodily 1983].

Table 2.2 Location of selected sites for PSHA

V_{S30} m/sec	$Z_{1.0}$ km	$Z_{2.5}$ (CB14) km
270	0.475	1.983
760	0.0445	0.607

2.4 PROBABILISTIC SEISMIC HAZARD CALCULATIONS

Probabilistic seismic hazard calculations were carried out using the computer PSHA program HAZ45-HSR. This PSHA program is based on the HAZ45 computer program [Abrahamson and Gregor 2015] and follows a standard state-of-practice approach for PSHA. HAZ45-HSR was specifically developed to implement the UCERF3 source model for the California High-Speed Rail (HSR) Project. It has successfully passed the verification test cases associated with the recent PSHA Code Verification testing program [Hale et al. 2018]. Hale et al. [2018] provide a list of all participated and passed PSHA computer codes in the verification process.

A sigma truncation value of 8.0 was used for the PSHA. The minimum magnitude used in the analysis was 5.0. Mean hazard curves were computed for each of the ten site locations and two V_{S30} for the following suite of 22 spectral periods listed in Table 2.3.

Based on the computed hazard curves, ground motions and UHS were computed for a suite of 10 hazard levels defined in Table 2.4. For presentation, labeling, and discussion, the UHS were identified by the approximate return period in years of 15, 25, 50, 75, 100, 150, 250, 500, 1000, and 2500 years. Estimates of the mean magnitude, distance, and epsilon values associated with the ten levels of exceedance were also computed for all 22 spectral periods. Finally, the deaggregation of the PSHA was computed at all 22 spectral periods, and summary plots were provided for the sub-sample of spectral periods: 0.01 (PGA), 0.04, 0.1, 0.2, 0.3, 0.5, 1.0, 2.0, and 5.0 sec. The results from the hazard–deaggregation data were used in the selection of appropriate time histories for scaling.

Table 2.3 Suite of spectral periods used in the PSHA.

Period (sec)	
0.01 (PGA)	0.4
0.02	0.5
0.03	0.75
0.04	1.0
0.05	1.5
0.075	2.0
0.1	3.0
0.15	4.0
0.2	5.0
0.25	7.5
0.3	10.0

Table 2.4 Annual exceedance probabilities and return periods.

Mean annual exceedance probability	Return period (years)
6.449E-02	15.5
3.921E-02	25.5
1.980E-02	50.5
1.324E-02	75.5
9.950E-03	100.5
6.640E-03	150.6
3.990E-03	250.6
2.000E-03	500
1.000E-03	1000
4.000E-04	2500

2.5 PROBABILISTIC SEISMIC HAZARD ANALYSIS RESULTS

As an example, the results for the Oakland and Los Angeles site locations for the V_{S30} value of 760 m/sec are presented in this main section of the report. The full suite of results for all the sites is contained in the accompanying Appendix B.

2.5.1 Oakland Site Location

For the Oakland site location, the hazard curves are shown in Figure 2.4 for PGA and spectral periods of 0.2 and 1.0 sec. In these plots, individual hazard curves from the scenario fault ruptures, gridded sources, and the combined total hazard are presented. Overall, the hazard curve plots indicate that the hazard is primarily controlled by the contribution from either the fault sources and/or grid sources depending on the hazard level and spectral period. This variation is dependent on the relative location of a given site to the faults contained in the UCERF3 seismic-source model as should be expected. In addition, the results indicate an increase in the relative contribution from the fault sources over the gridded point sources for longer spectral periods and lower hazard levels.

Given the hazard curves for the full suite of 22 spectral periods, the computed UHS for the levels of the ten return periods are plotted in Figure 2.5 for the Oakland site location. The UHS values are given in Table 2.5. The mean magnitude, distance (defined in terms of rupture distance), and epsilon values are plotted in Figure 2.6–Figure 2.8 for the Oakland site location. The mean magnitude, distance, and epsilon values are also listed in Table 2.6–Table 2.8.

To assist in the selection of the appropriate time histories for scaling, deaggregation results were computed for all site locations. A representative set of deaggregation results is presented in this main report, with the complete set for all of the sites contained in Appendix B. Deaggregation plots for PGA and spectral periods of 0.2 and 1.0 sec at the returns periods of 15, 100, and 2500 years are plotted in Figure 2.9, Figure 2.10, and Figure 2.11, respectively.

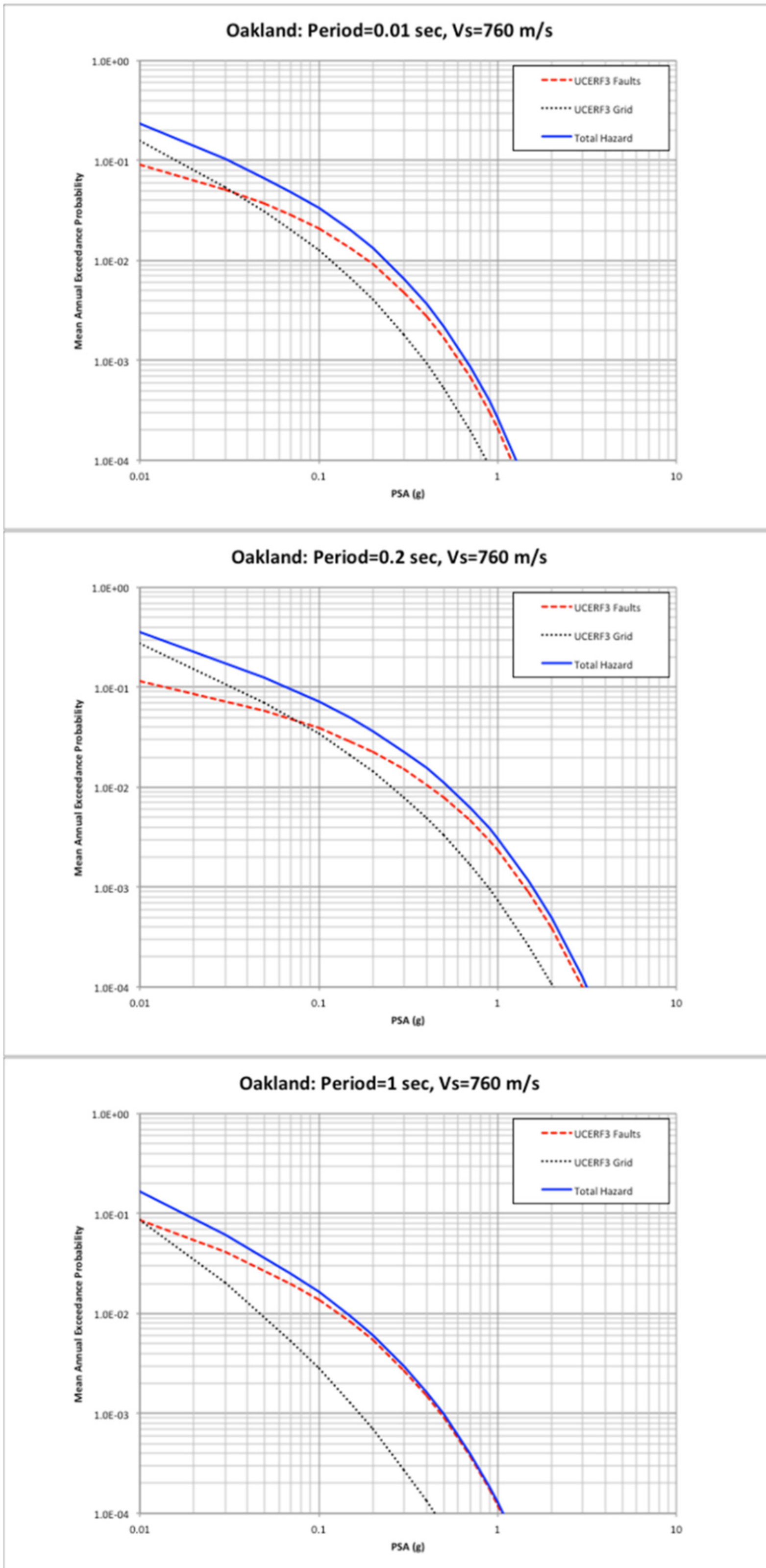

Figure 2.4 **Mean hazard curves from the gridded, faults, and all sources for (PGA, 0.2 sec, and 1.0 sec) for the Oakland site location (V_{s30} = 760 m/sec).**

Table 2.5 UHS [PSA (g)] results for the Oakland site location (V_{s30} = 760 m/sec).

Period (sec)	15-yr	25-yr	50-yr	75-yr	100-yr	150-yr	250-yr	500-yr	1000-yr	2500-yr
0.01	0.0518	0.0854	0.1512	0.1999	0.2363	0.2995	0.3847	0.5164	0.6648	0.8897
0.02	0.0525	0.0868	0.1539	0.2035	0.2413	0.3058	0.3945	0.5290	0.6849	0.9169
0.03	0.0573	0.0957	0.1696	0.2241	0.2685	0.3390	0.4394	0.5913	0.7696	1.0348
0.04	0.0647	0.1083	0.1940	0.2558	0.3089	0.3901	0.5061	0.6861	0.8943	1.1955
0.05	0.0711	0.1211	0.2175	0.2908	0.3483	0.4414	0.5717	0.7807	1.0223	1.3817
0.075	0.0921	0.1565	0.2807	0.3746	0.4502	0.5679	0.7418	1.0133	1.3178	1.8031
0.1	0.1063	0.1792	0.3210	0.4275	0.5133	0.6472	0.8427	1.1402	1.5048	2.0431
0.15	0.1166	0.1968	0.3505	0.4675	0.5595	0.7115	0.9263	1.2509	1.6460	2.2307
0.2	0.1117	0.1869	0.3331	0.4439	0.5326	0.6754	0.8808	1.1911	1.5712	2.1325
0.25	0.1020	0.1688	0.3011	0.4008	0.4810	0.6066	0.7929	1.0805	1.4190	1.9385
0.3	0.0916	0.1517	0.2677	0.3575	0.4307	0.5451	0.7148	0.9800	1.2758	1.7513
0.4	0.0737	0.1216	0.2171	0.2916	0.3513	0.4487	0.5873	0.8124	1.0711	1.4789
0.5	0.0612	0.1010	0.1805	0.2417	0.2948	0.3773	0.4999	0.6937	0.9219	1.2641
0.75	0.0400	0.0657	0.1201	0.1639	0.2007	0.2582	0.3465	0.4896	0.6563	0.9227
1	0.0282	0.0458	0.0855	0.1173	0.1450	0.1895	0.2543	0.3632	0.4936	0.6967
1.5	0.0163	0.0273	0.0506	0.0718	0.0888	0.1169	0.1601	0.2282	0.3124	0.4426
2	0.0110	0.0183	0.0353	0.0492	0.0624	0.0836	0.1144	0.1655	0.2249	0.3208
3	0.0061	0.0106	0.0211	0.0304	0.0382	0.0521	0.0724	0.1052	0.1446	0.2065
4	0.0040	0.0071	0.0144	0.0213	0.0272	0.0369	0.0523	0.0763	0.1052	0.1510
5	0.0028	0.0051	0.0107	0.0158	0.0206	0.0284	0.0398	0.0594	0.0823	0.1184
7.5	0.0015	0.0028	0.0060	0.0091	0.0116	0.0161	0.0233	0.0347	0.0493	0.0719
10	0.0009	0.0017	0.0039	0.0059	0.0077	0.0106	0.0150	0.0231	0.0325	0.0479

Table 2.6 Mean magnitude values for the Oakland site location (V_{s30} = 760 m/sec).

Period (sec)	15-yr	25-yr	50-yr	75-yr	100-yr	150-yr	250-yr	500-yr	1000-yr	2500-yr
0.01	6.32	6.45	6.62	6.69	6.72	6.78	6.81	6.85	6.88	6.90
0.02	6.31	6.45	6.62	6.68	6.72	6.77	6.82	6.85	6.88	6.90
0.03	6.31	6.45	6.60	6.67	6.71	6.76	6.81	6.84	6.87	6.90
0.04	6.31	6.44	6.60	6.67	6.71	6.76	6.80	6.84	6.87	6.89
0.05	6.28	6.43	6.59	6.66	6.70	6.75	6.79	6.83	6.85	6.88
0.075	6.28	6.41	6.56	6.63	6.67	6.71	6.76	6.79	6.82	6.84
0.1	6.27	6.40	6.54	6.61	6.65	6.69	6.74	6.77	6.80	6.82
0.15	6.28	6.41	6.57	6.63	6.67	6.72	6.77	6.81	6.84	6.86
0.2	6.30	6.44	6.60	6.68	6.72	6.77	6.82	6.86	6.89	6.92
0.25	6.33	6.47	6.63	6.71	6.76	6.80	6.85	6.90	6.93	6.97
0.3	6.34	6.49	6.65	6.74	6.79	6.84	6.89	6.94	6.97	7.01
0.4	6.38	6.53	6.71	6.80	6.85	6.90	6.96	7.01	7.04	7.07
0.5	6.41	6.57	6.75	6.84	6.89	6.95	7.01	7.06	7.09	7.12
0.75	6.45	6.63	6.82	6.91	6.97	7.02	7.07	7.13	7.15	7.18
1	6.53	6.66	6.87	6.96	7.02	7.08	7.12	7.17	7.20	7.22
1.5	6.57	6.76	6.93	7.06	7.11	7.16	7.21	7.25	7.27	7.29
2	6.66	6.78	7.00	7.08	7.15	7.21	7.25	7.30	7.32	7.34
3	6.72	6.90	7.09	7.18	7.22	7.29	7.33	7.37	7.40	7.41
4	6.76	6.95	7.12	7.23	7.28	7.33	7.38	7.43	7.45	7.49
5	6.81	6.97	7.16	7.24	7.31	7.37	7.41	7.47	7.50	7.53
7.5	6.84	7.03	7.22	7.31	7.35	7.41	7.48	7.55	7.60	7.65
10	6.86	7.04	7.24	7.33	7.39	7.45	7.50	7.58	7.64	7.70

Table 2.7 Mean rupture distance (km) values for the Oakland site location (V_{s30} = 760 m/sec).

Period (sec)	15-yr	25-yr	50-yr	75-yr	100-yr	150-yr	250-yr	500-yr	1000-yr	2500-yr
0.01	31.94	25.04	18.64	16.30	15.17	13.22	11.59	9.98	8.90	7.87
0.02	31.86	24.93	18.70	16.29	15.12	13.19	11.51	9.98	8.79	7.79
0.03	32.00	24.76	18.82	16.53	15.11	13.32	11.59	10.04	8.80	7.79
0.04	31.83	24.85	18.81	16.66	15.01	13.31	11.64	9.99	8.80	7.93
0.05	33.18	25.06	19.01	16.51	15.19	13.48	11.88	10.13	8.93	7.98
0.075	31.96	24.61	19.02	16.58	15.20	13.65	11.91	10.26	9.26	8.15
0.1	31.41	24.67	18.90	16.53	15.15	13.61	11.93	10.48	9.14	8.15
0.15	31.91	24.62	18.94	16.48	15.19	13.41	11.84	10.41	9.13	8.15
0.2	32.55	25.14	19.17	16.75	15.41	13.70	11.95	10.49	9.21	8.22
0.25	33.25	25.95	19.47	16.99	15.54	13.97	12.20	10.61	9.41	8.32
0.3	35.39	26.58	20.32	17.56	15.98	14.28	12.40	10.70	9.67	8.49
0.4	39.28	28.90	21.31	18.34	16.77	14.77	12.98	11.07	9.79	8.58
0.5	41.48	30.18	22.39	19.47	17.40	15.42	13.30	11.36	10.01	8.95
0.75	53.35	35.98	24.87	20.87	18.67	16.66	14.27	12.04	10.57	9.16
1	50.05	39.57	25.97	21.94	19.45	16.95	14.77	12.39	10.77	9.35
1.5	61.46	43.37	31.09	23.46	21.14	18.38	15.58	13.28	11.54	10.07
2	60.53	50.13	31.63	27.20	23.02	19.11	16.44	13.81	12.25	10.69
3	66.69	49.43	33.01	26.46	23.95	19.79	16.91	14.58	12.93	11.42
4	70.68	51.64	36.61	27.86	24.42	21.15	17.75	15.44	13.93	12.48
5	70.32	53.72	36.75	30.63	25.22	21.62	19.04	16.30	14.87	13.70
7.5	78.31	60.96	43.25	35.39	31.90	27.77	23.11	20.28	18.40	17.26
10	80.66	65.56	48.35	40.18	35.75	31.13	27.87	23.41	21.35	19.81

Table 2.8 Mean epsilon values for the Oakland site location (V_{s30} = 760 m/sec).

Period (sec)	15-yr	25-yr	50-yr	75-yr	100-yr	150-yr	250-yr	500-yr	1000-yr	2500-yr
0.01	-0.719	-0.448	-0.073	0.133	0.254	0.464	0.695	1.002	1.291	1.664
0.02	-0.72	-0.449	-0.076	0.127	0.25	0.457	0.692	0.991	1.291	1.654
0.03	-0.707	-0.428	-0.067	0.128	0.265	0.459	0.692	0.98	1.274	1.637
0.04	-0.692	-0.418	-0.048	0.139	0.288	0.475	0.702	0.997	1.282	1.602
0.05	-0.692	-0.401	-0.036	0.169	0.3	0.488	0.703	0.999	1.281	1.619
0.075	-0.63	-0.343	0.018	0.22	0.357	0.536	0.767	1.061	1.317	1.676
0.1	-0.597	-0.318	0.048	0.249	0.387	0.568	0.797	1.078	1.383	1.721
0.15	-0.614	-0.332	0.023	0.225	0.354	0.549	0.778	1.055	1.353	1.693
0.2	-0.629	-0.359	-0.004	0.195	0.328	0.517	0.747	1.024	1.327	1.675
0.25	-0.618	-0.366	-0.012	0.182	0.313	0.489	0.72	1.012	1.301	1.659
0.3	-0.594	-0.346	-0.019	0.176	0.311	0.49	0.722	1.019	1.283	1.646
0.4	-0.573	-0.35	-0.03	0.161	0.286	0.47	0.686	0.985	1.264	1.631
0.5	-0.531	-0.323	-0.025	0.148	0.287	0.464	0.693	0.986	1.274	1.598
0.75	-0.491	-0.314	-0.035	0.143	0.273	0.439	0.668	0.972	1.249	1.617
1	-0.483	-0.344	-0.069	0.099	0.231	0.412	0.629	0.943	1.246	1.604
1.5	-0.523	-0.376	-0.147	0.048	0.173	0.358	0.607	0.911	1.226	1.587
2	-0.572	-0.451	-0.196	-0.036	0.115	0.322	0.568	0.902	1.194	1.577
3	-0.68	-0.537	-0.286	-0.103	0.025	0.25	0.517	0.854	1.167	1.539
4	-0.799	-0.645	-0.4	-0.199	-0.051	0.156	0.455	0.802	1.124	1.507
5	-0.865	-0.711	-0.447	-0.265	-0.095	0.13	0.388	0.76	1.077	1.444
7.5	-0.992	-0.816	-0.507	-0.299	-0.163	0.05	0.343	0.675	1.013	1.372
10	-1.098	-0.914	-0.584	-0.362	-0.204	0.009	0.24	0.609	0.913	1.28

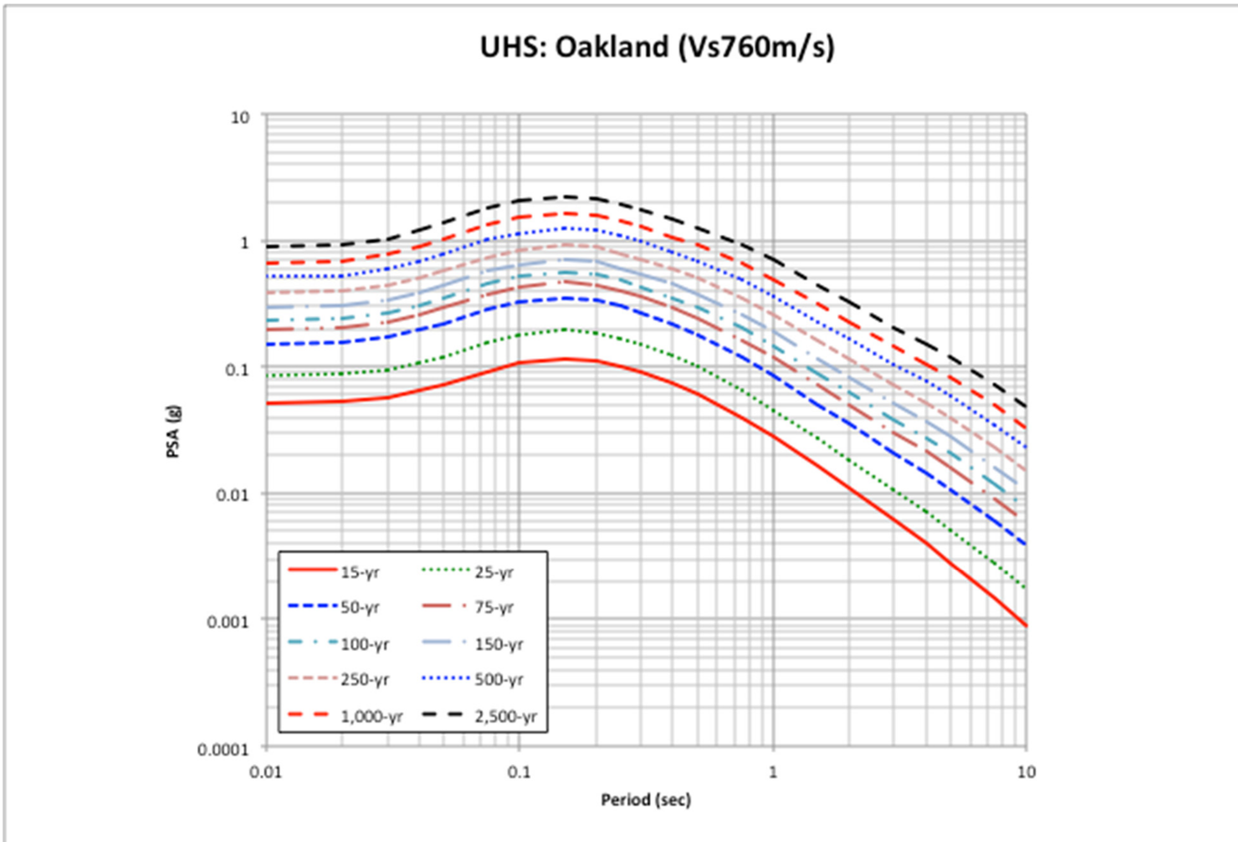

Figure 2.5 UHS for the Oakland site location (V_{s30} = 760 m/sec).

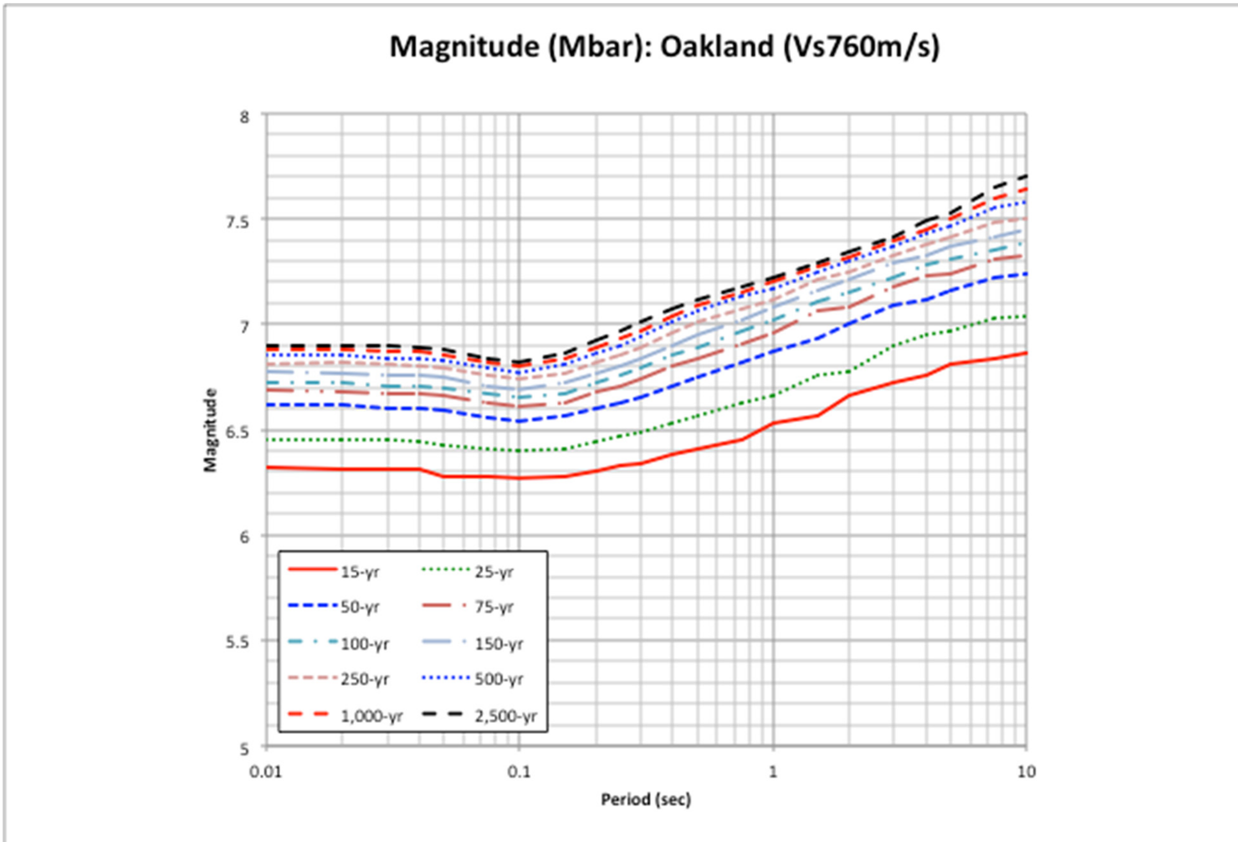

Figure 2.6 Mean magnitude results at the Oakland site location (V_{s30} = 760 m/sec).

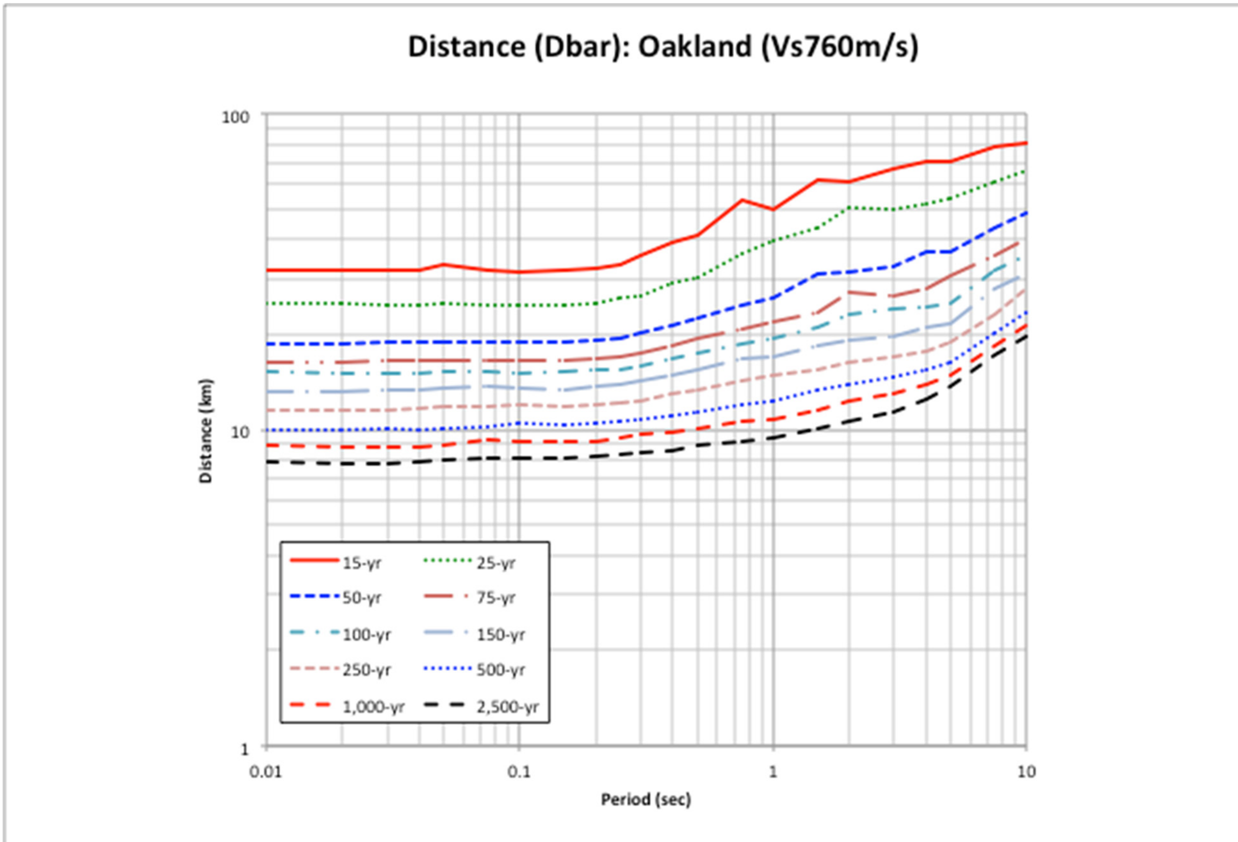

Figure 2.7 **Mean distance (rupture distance) results at the Oakland site location (V_{s30} = 760 m/sec).**

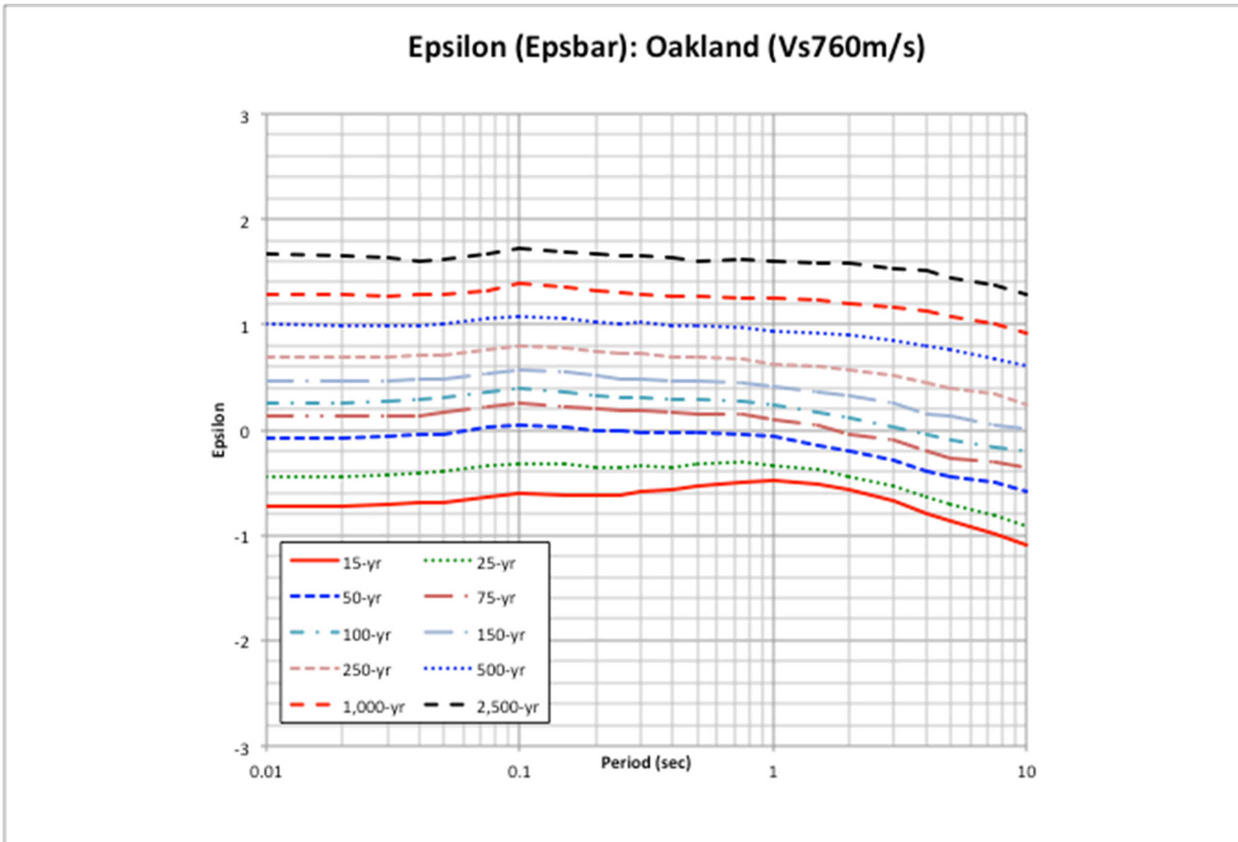

Figure 2.8 Mean epsilon results at the Oakland site location (V_{s30} = 760 m/sec).

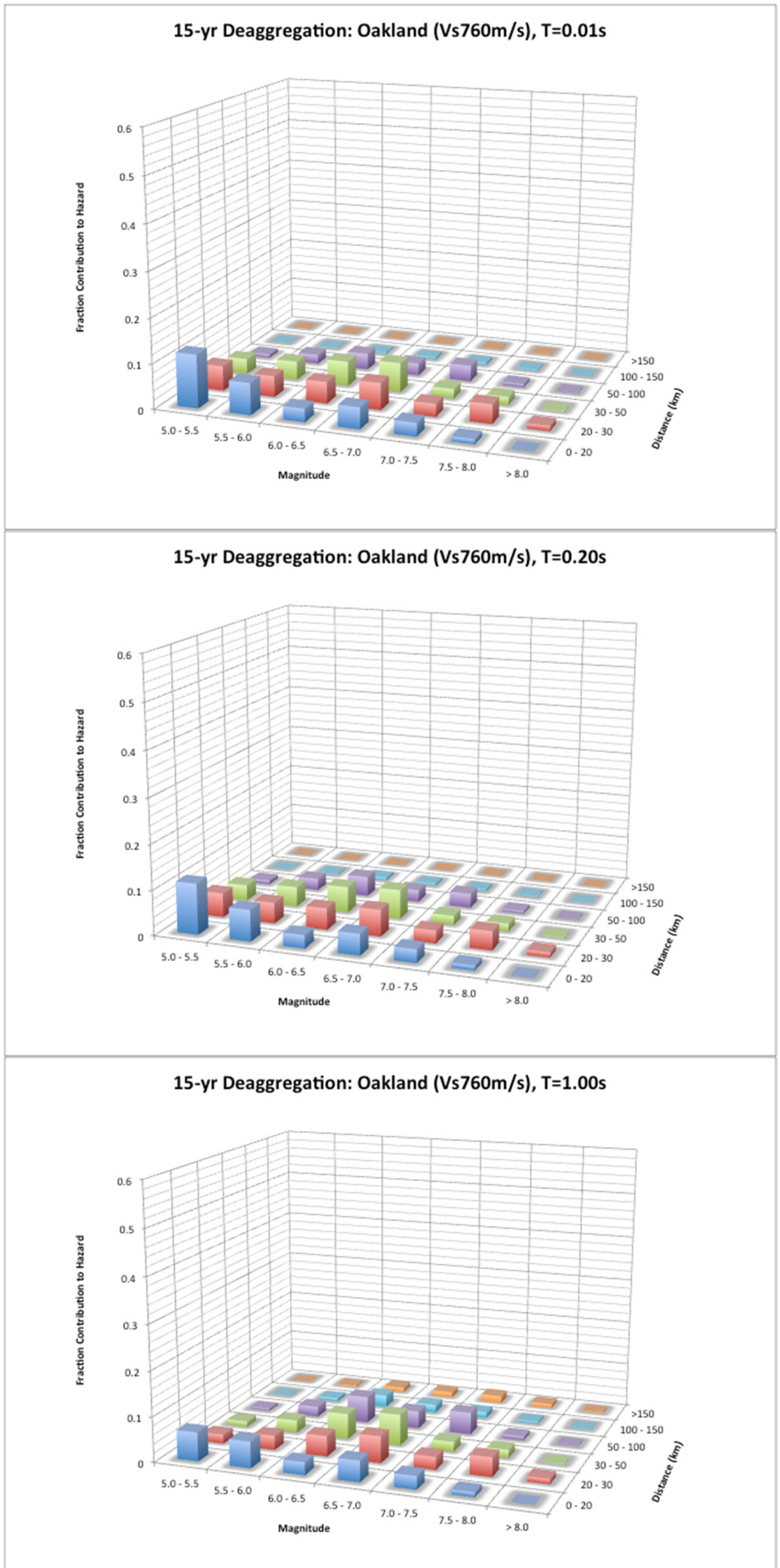

Figure 2.9 **Deaggregation for (PGA, 0.2 sec, and 1.0 sec) at the 15-year return period hazard level for the Oakland site location (V_{s30} = 760 m/sec).**

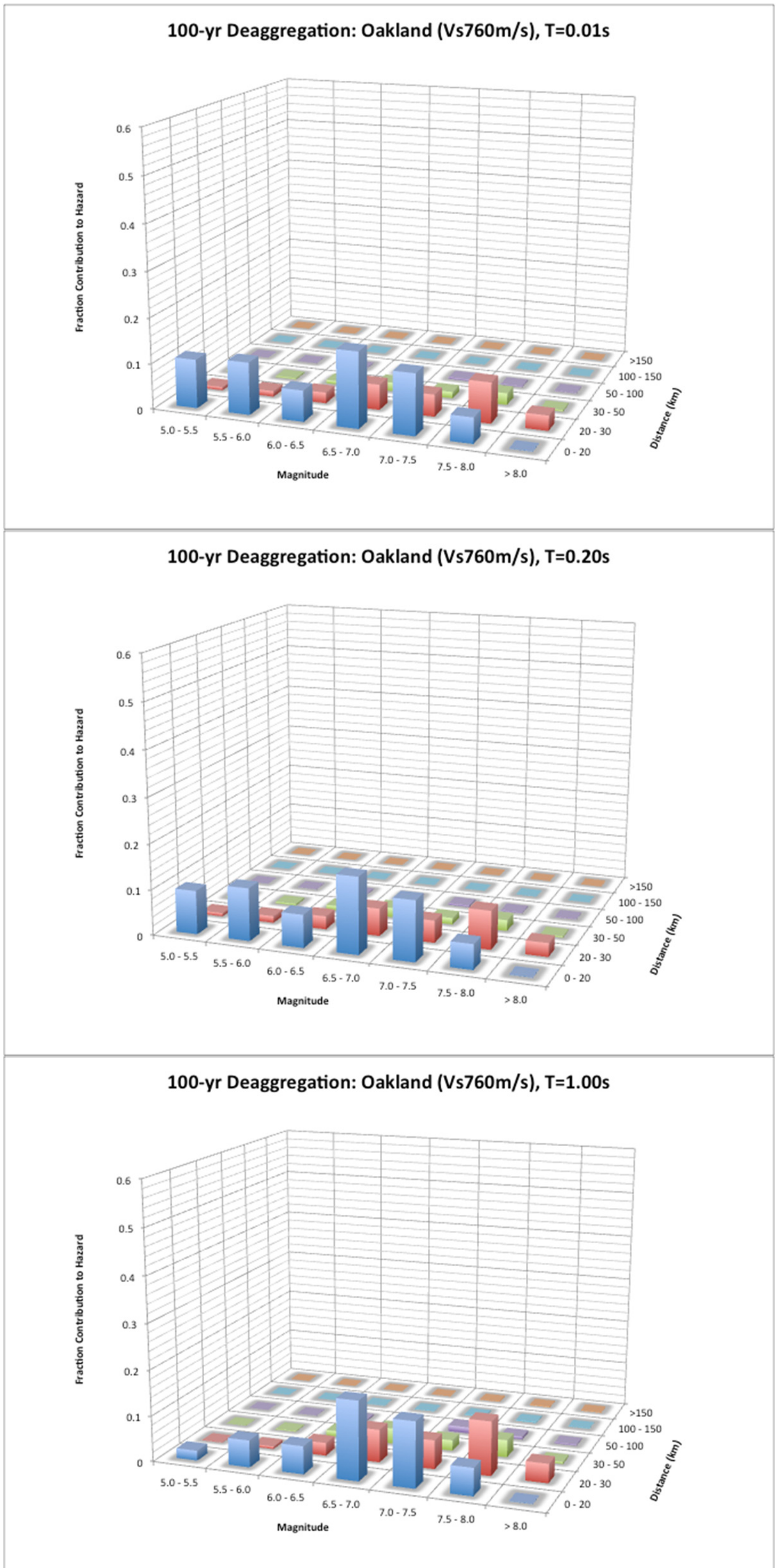

Figure 2.10 Deaggregation for (PGA, 0.2 sec, and 1.0 sec) at the 100-year return period hazard level for the Oakland site location (V_{s30} = 760 m/sec).

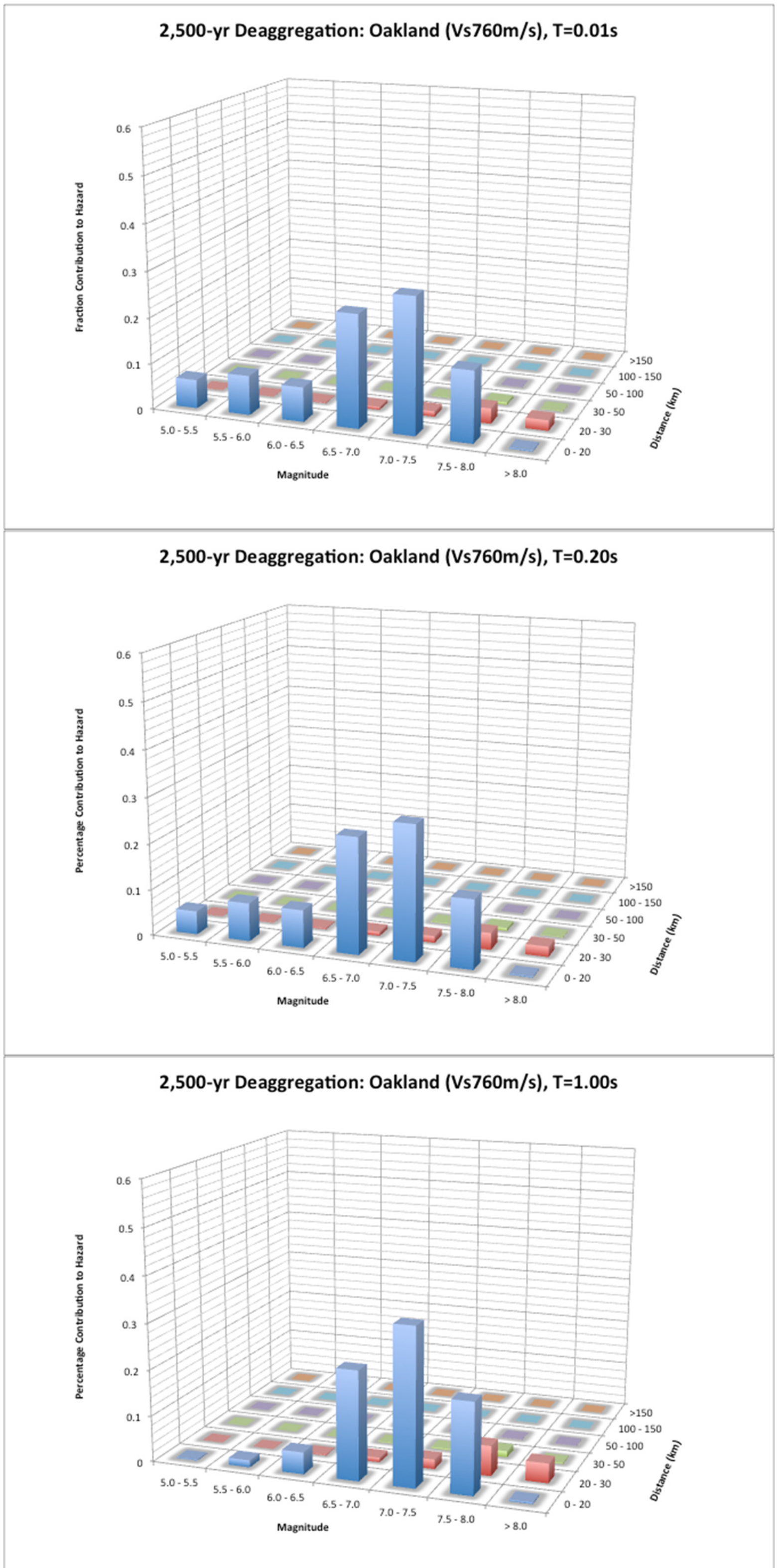

Figure 2.11 Deaggregation for (PGA, 0.2 sec, and 1.0 sec) at the 2500-year return period hazard level for the Oakland site location (V_{s30} = 760 m/sec).

2.5.2 Los Angeles Site Location

For the Los Angeles site location, the hazard curves are shown in Figure 2.12 for PGA and spectral periods of 0.2 and 1.0 sec. Similar to the results for the Oakland site location, individual hazard curves from the scenario fault ruptures, gridded sources, and the combined total hazard are presented. The similar observation of the contribution to the total hazard from both the fault sources and grid sources that were observed for the Oakland site are observed for the Los Angeles site. This variation is dependent on the relative location of a given site to the faults contained in the UCERF3 seismic-source model as should be expected. In addition, the results indicate an increase in the relative contribution from the fault sources over the gridded point sources for longer spectral periods and lower hazard levels.

Given the hazard curves for the full suite of 22 spectral periods, the computed UHS for the levels of ten return periods are plotted in Figure 2.13 for the Los Angeles site location. The UHS values are given in Table 2.9. The mean magnitude, distance (defined based on rupture distance), and epsilon values are plotted in Figure 2.14–Figure 2.16 for the Los Angeles site location. The mean magnitude, distance, and epsilon values are also listed in Table 2.10–Table 2.12.

To assist in the selection of the appropriate time histories for scaling, deaggregation results were computed for all site locations. A representative set is presented in this main report, with the complete set for all of the sites contained in Appendix B. Deaggregation plots for PGA and spectral periods of 0.2 and 1.0 sec at the returns periods of 15, 100, and 2500 years are plotted in Figure 2.17, Figure 2.18, and Figure 2.19, respectively.

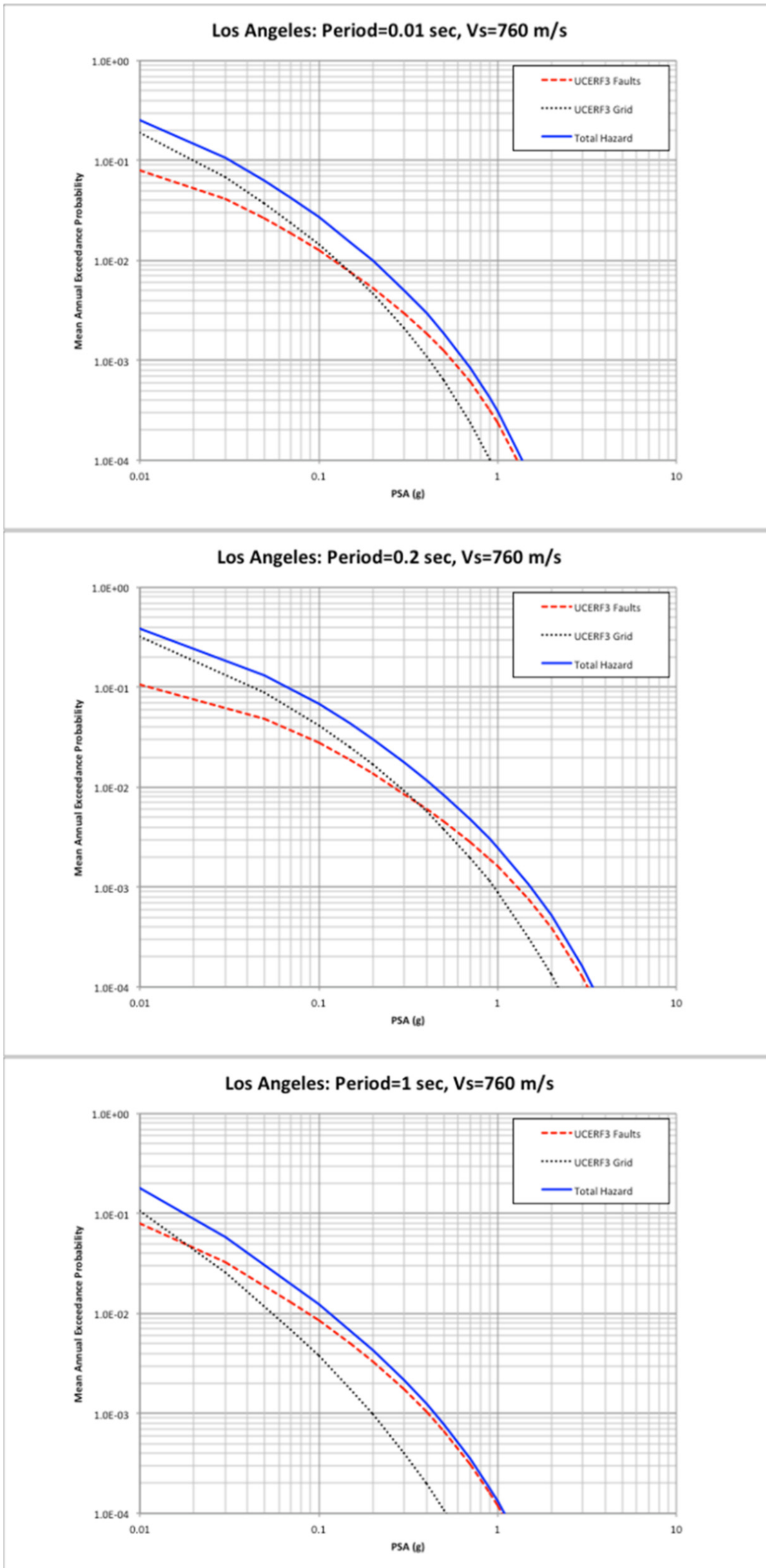

Figure 2.12 Mean hazard curves from the gridded, faults, and all sources for (PGA, 0.2 sec, and 1.0 sec) for the Los Angeles site location (V_{s30} = 760 m/sec).

Table 2.9 UHS PSA (g) results for the Los Angeles site location (V_{s30} = 760 m/sec).

Period (sec)	15-yr	25-yr	50-yr	75-yr	100-yr	150-yr	250-yr	500-yr	1000-yr	2500-yr
0.01	0.0487	0.0744	0.1244	0.1646	0.1987	0.2536	0.3396	0.4832	0.6515	0.9167
0.02	0.0494	0.0755	0.1266	0.1677	0.2025	0.2591	0.3476	0.4963	0.6713	0.9447
0.03	0.0539	0.0827	0.1400	0.1856	0.2237	0.2887	0.3880	0.5519	0.7531	1.0606
0.04	0.0607	0.0939	0.1596	0.2116	0.2553	0.3300	0.4443	0.6344	0.8687	1.2194
0.05	0.0668	0.1053	0.1796	0.2383	0.2894	0.3737	0.5045	0.7234	0.9919	1.4033
0.075	0.0861	0.1354	0.2318	0.3098	0.3752	0.4856	0.6536	0.9407	1.2774	1.8291
0.1	0.1004	0.1562	0.2661	0.3546	0.4299	0.5542	0.7478	1.0690	1.4676	2.0845
0.15	0.1099	0.1705	0.2906	0.3865	0.4682	0.6044	0.8176	1.1702	1.6142	2.2933
0.2	0.1054	0.1623	0.2747	0.3653	0.4426	0.5714	0.7738	1.1117	1.5391	2.1941
0.25	0.0961	0.1474	0.2474	0.3287	0.3986	0.5149	0.6975	1.0079	1.3838	1.9997
0.3	0.0865	0.1324	0.2223	0.2951	0.3564	0.4611	0.6228	0.9060	1.2425	1.8012
0.4	0.0701	0.1074	0.1799	0.2377	0.2883	0.3733	0.5073	0.7386	1.0288	1.5000
0.5	0.0586	0.0887	0.1495	0.1981	0.2391	0.3109	0.4230	0.6169	0.8664	1.2590
0.75	0.0376	0.0588	0.0997	0.1324	0.1612	0.2102	0.2883	0.4264	0.6017	0.8991
1	0.0270	0.0408	0.0702	0.0940	0.1146	0.1510	0.2082	0.3107	0.4424	0.6611
1.5	0.0156	0.0241	0.0414	0.0560	0.0694	0.0914	0.1264	0.1893	0.2686	0.4042
2	0.0107	0.0162	0.0287	0.0387	0.0476	0.0638	0.0889	0.1324	0.1887	0.2810
3	0.0059	0.0094	0.0167	0.0231	0.0288	0.0383	0.0539	0.0802	0.1134	0.1691
4	0.0038	0.0062	0.0113	0.0158	0.0200	0.0270	0.0376	0.0565	0.0795	0.1170
5	0.0027	0.0044	0.0083	0.0117	0.0148	0.0205	0.0290	0.0431	0.0612	0.0905
7.5	0.0014	0.0024	0.0047	0.0068	0.0087	0.0119	0.0172	0.0264	0.0372	0.0555
10	0.0009	0.0015	0.0030	0.0044	0.0058	0.0081	0.0116	0.0179	0.0256	0.0377

Table 2.10 Mean magnitude values for the Los Angeles site location (V_{s30} = 760 m/sec).

Period (sec)	15-yr	25-yr	50-yr	75-yr	100-yr	150-yr	250-yr	500-yr	1000-yr	2500-yr
0.01	6.21	6.30	6.40	6.45	6.48	6.52	6.57	6.63	6.70	6.77
0.02	6.21	6.30	6.40	6.44	6.47	6.51	6.56	6.64	6.70	6.77
0.03	6.20	6.29	6.39	6.44	6.46	6.50	6.55	6.62	6.69	6.76
0.04	6.20	6.29	6.39	6.43	6.45	6.50	6.55	6.62	6.68	6.75
0.05	6.18	6.28	6.37	6.41	6.44	6.49	6.54	6.61	6.67	6.73
0.075	6.16	6.25	6.34	6.38	6.42	6.46	6.51	6.58	6.63	6.70
0.1	6.15	6.24	6.32	6.37	6.40	6.44	6.49	6.56	6.62	6.70
0.15	6.16	6.24	6.34	6.38	6.42	6.46	6.52	6.59	6.66	6.72
0.2	6.19	6.27	6.38	6.43	6.47	6.51	6.57	6.64	6.70	6.77
0.25	6.22	6.32	6.42	6.47	6.51	6.55	6.61	6.68	6.74	6.81
0.3	6.24	6.34	6.45	6.51	6.54	6.59	6.65	6.71	6.77	6.84
0.4	6.29	6.40	6.52	6.58	6.62	6.67	6.72	6.79	6.83	6.90
0.5	6.34	6.44	6.58	6.65	6.68	6.73	6.78	6.83	6.88	6.93
0.75	6.37	6.52	6.67	6.73	6.78	6.83	6.87	6.92	6.95	6.99
1	6.46	6.57	6.74	6.80	6.84	6.90	6.94	6.97	7.00	7.03
1.5	6.53	6.67	6.82	6.90	6.98	7.02	7.06	7.09	7.10	7.13
2	6.61	6.71	6.92	6.98	7.02	7.09	7.14	7.16	7.18	7.20
3	6.69	6.85	7.02	7.12	7.18	7.22	7.26	7.28	7.29	7.30
4	6.73	6.89	7.09	7.18	7.26	7.31	7.35	7.38	7.39	7.41
5	6.77	6.93	7.14	7.23	7.28	7.37	7.42	7.45	7.47	7.49
7.5	6.81	6.99	7.21	7.33	7.39	7.45	7.52	7.59	7.62	7.66
10	6.84	7.01	7.25	7.35	7.42	7.49	7.56	7.63	7.69	7.73

Table 2.11 **Mean rupture distance (km) values for the Los Angeles site location (V_{s30} = 760 m/sec).**

Period (sec)	15-yr	25-yr	50-yr	75-yr	100-yr	150-yr	250-yr	500-yr	1000-yr	2500-yr
0.01	38.42	31.32	23.96	20.02	17.50	15.04	12.05	9.37	7.96	6.81
0.02	38.18	31.30	23.82	19.93	17.49	14.94	11.96	9.25	7.85	6.75
0.03	38.20	31.37	23.64	19.86	17.71	14.72	11.83	9.40	7.83	6.78
0.04	38.25	31.13	23.57	19.94	17.85	14.83	11.96	9.49	7.87	6.91
0.05	39.19	31.09	23.65	20.23	17.72	14.92	11.95	9.48	7.93	6.94
0.075	38.33	30.92	23.58	19.77	17.54	14.73	12.17	9.58	8.33	7.10
0.1	37.15	30.49	23.40	19.69	17.38	14.83	12.05	9.72	8.19	7.15
0.15	37.82	30.84	23.23	19.59	17.39	14.83	12.02	9.77	8.12	7.12
0.2	38.57	31.44	23.94	20.15	17.84	15.22	12.36	9.85	8.21	7.17
0.25	40.08	32.46	24.90	20.87	18.35	15.56	12.64	9.94	8.47	7.13
0.3	42.60	34.09	25.83	21.68	19.37	16.27	13.34	10.26	8.74	7.29
0.4	46.62	36.63	27.75	23.75	20.87	17.64	14.19	10.97	8.94	7.39
0.5	49.11	40.01	29.47	25.07	22.71	18.92	15.27	11.86	9.44	7.86
0.75	62.79	45.40	33.39	28.77	25.34	21.46	17.32	13.10	10.52	8.14
1	60.38	50.06	35.65	30.42	27.23	22.63	18.42	13.92	10.92	8.57
1.5	70.78	57.56	43.16	36.59	30.57	26.16	21.49	16.21	12.89	9.71
2	70.77	62.76	44.62	39.33	35.77	29.30	23.52	18.36	14.43	11.21
3	78.38	64.15	50.32	41.80	36.93	32.38	26.48	21.24	17.28	13.29
4	82.00	68.88	52.86	45.86	39.29	34.50	29.77	24.21	20.30	16.41
5	82.61	70.56	54.47	47.35	43.30	36.14	31.35	27.00	23.04	19.18
7.5	90.89	78.32	62.50	53.95	49.37	44.62	39.48	34.32	31.46	28.22
10	93.91	83.41	67.43	59.95	54.67	48.87	44.13	39.48	36.26	33.73

Table 2.12 Mean epsilon values for the Los Angeles site location (V_{s30} = 760 m/sec).

Period (sec)	15-yr	25-yr	50-yr	75-yr	100-yr	150-yr	250-yr	500-yr	1000-yr	2500-yr
0.01	-0.454	-0.29	-0.092	0.031	0.118	0.234	0.406	0.67	0.95	1.332
0.02	-0.451	-0.291	-0.093	0.027	0.113	0.229	0.4	0.664	0.943	1.324
0.03	-0.439	-0.277	-0.073	0.044	0.123	0.246	0.412	0.661	0.941	1.299
0.04	-0.428	-0.258	-0.054	0.06	0.138	0.261	0.425	0.672	0.948	1.287
0.05	-0.433	-0.235	-0.03	0.081	0.167	0.285	0.448	0.693	0.964	1.309
0.075	-0.387	-0.193	0.016	0.139	0.22	0.342	0.504	0.757	1.014	1.377
0.1	-0.339	-0.164	0.04	0.16	0.244	0.363	0.531	0.779	1.057	1.41
0.15	-0.359	-0.184	0.021	0.134	0.213	0.329	0.496	0.74	1.021	1.372
0.2	-0.366	-0.199	-0.005	0.106	0.185	0.299	0.461	0.704	0.985	1.337
0.25	-0.359	-0.195	-0.014	0.097	0.175	0.286	0.444	0.689	0.95	1.33
0.3	-0.345	-0.179	0.005	0.112	0.182	0.291	0.44	0.683	0.934	1.301
0.4	-0.316	-0.152	0.019	0.112	0.184	0.286	0.43	0.659	0.921	1.29
0.5	-0.264	-0.13	0.046	0.138	0.2	0.304	0.443	0.663	0.922	1.257
0.75	-0.277	-0.087	0.072	0.154	0.219	0.315	0.45	0.667	0.909	1.269
1	-0.219	-0.109	0.053	0.134	0.194	0.294	0.432	0.654	0.907	1.252
1.5	-0.273	-0.147	0.008	0.094	0.172	0.278	0.428	0.667	0.914	1.269
2	-0.275	-0.199	-0.027	0.059	0.129	0.258	0.43	0.675	0.938	1.273
3	-0.382	-0.242	-0.111	-0.008	0.08	0.212	0.416	0.683	0.943	1.279
4	-0.486	-0.356	-0.202	-0.095	0.006	0.164	0.37	0.678	0.953	1.282
5	-0.529	-0.411	-0.262	-0.152	-0.053	0.129	0.363	0.654	0.954	1.291
7.5	-0.68	-0.533	-0.366	-0.237	-0.127	0.035	0.28	0.62	0.91	1.3
10	-0.78	-0.65	-0.461	-0.328	-0.213	-0.032	0.195	0.536	0.865	1.234

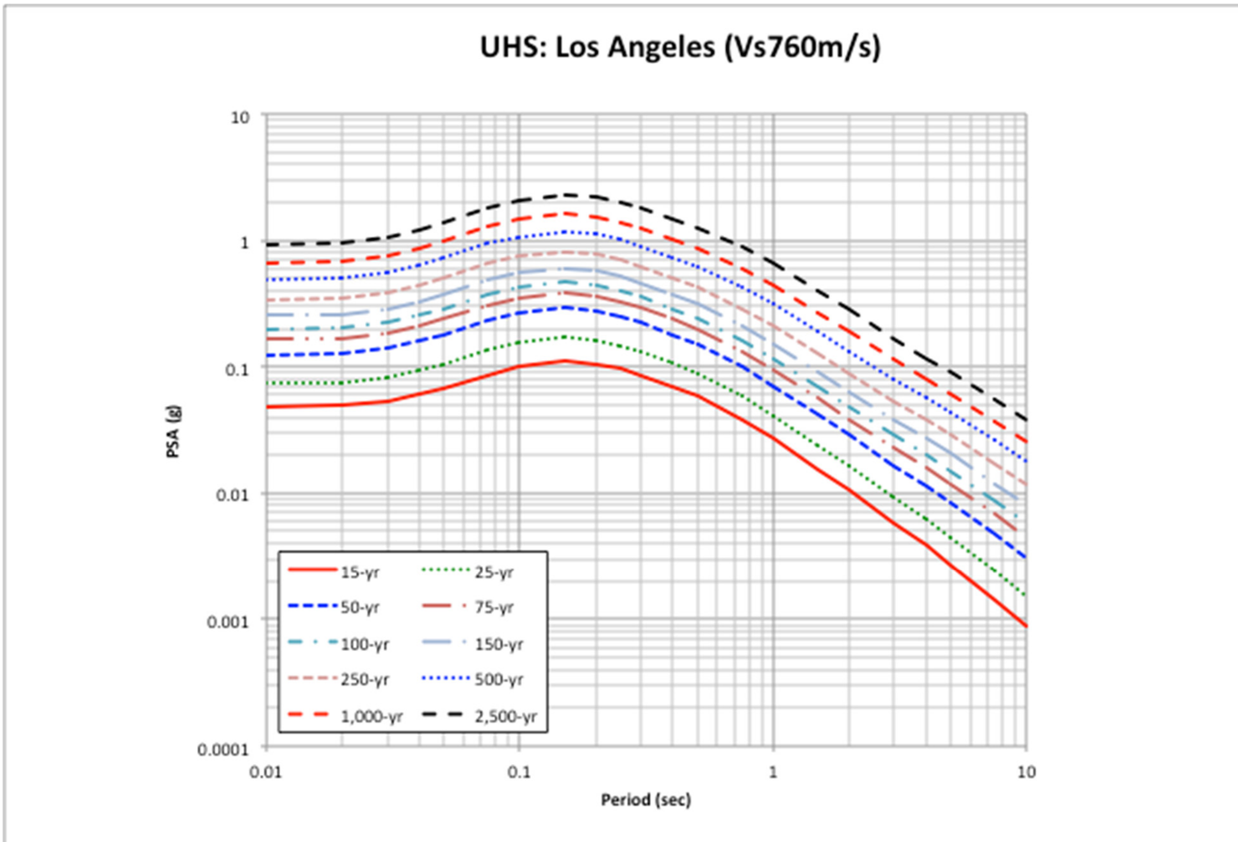

Figure 2.13 UHS for the Los Angeles site location (Vs_{30} = 760 m/sec).

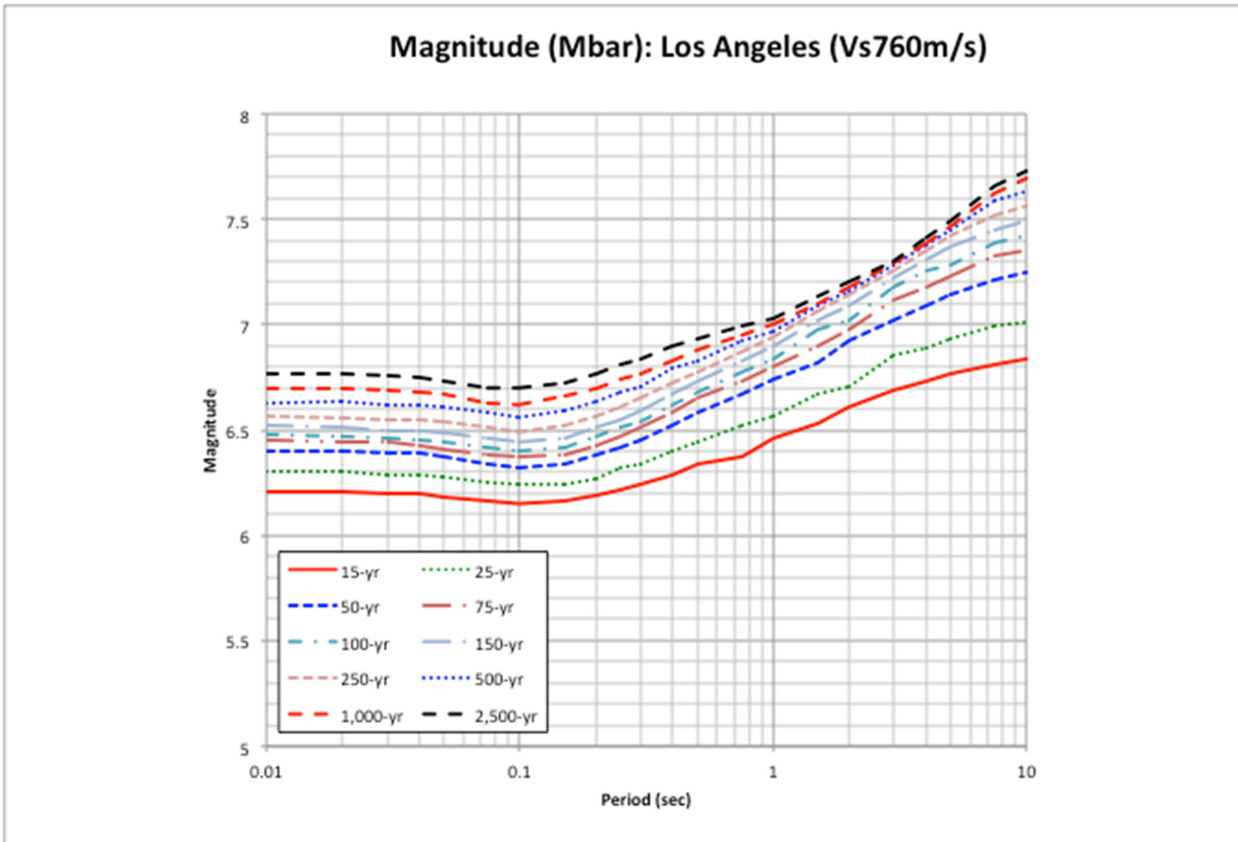

Figure 2.14 **Mean magnitude results at the Los Angeles site location (V_{s30} = 760 m/sec).**

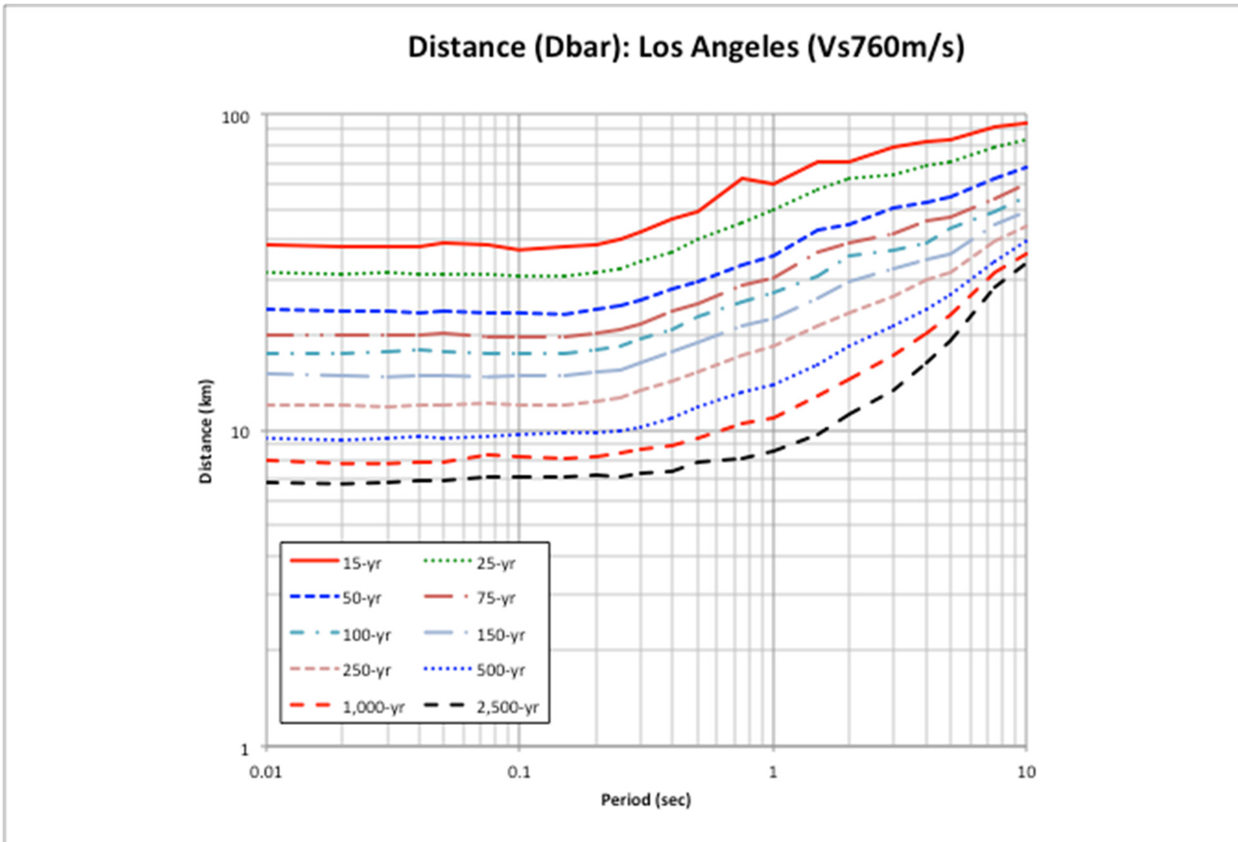

Figure 2.15 Mean distance results at the Los Angeles site location (V_{s30} = 760 m/sec).

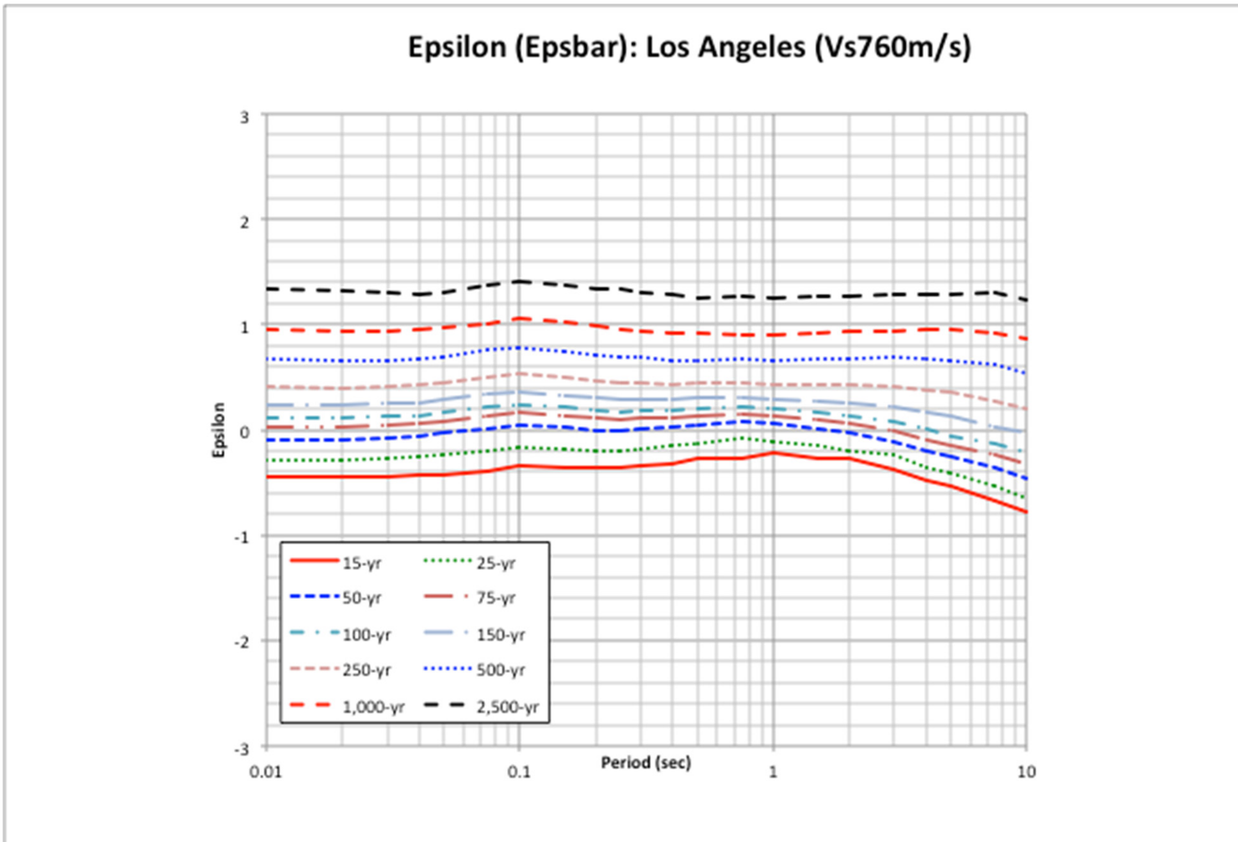

Figure 2.16 Mean epsilon results at the Los Angeles site location (V_{s30} = 760 m/sec).

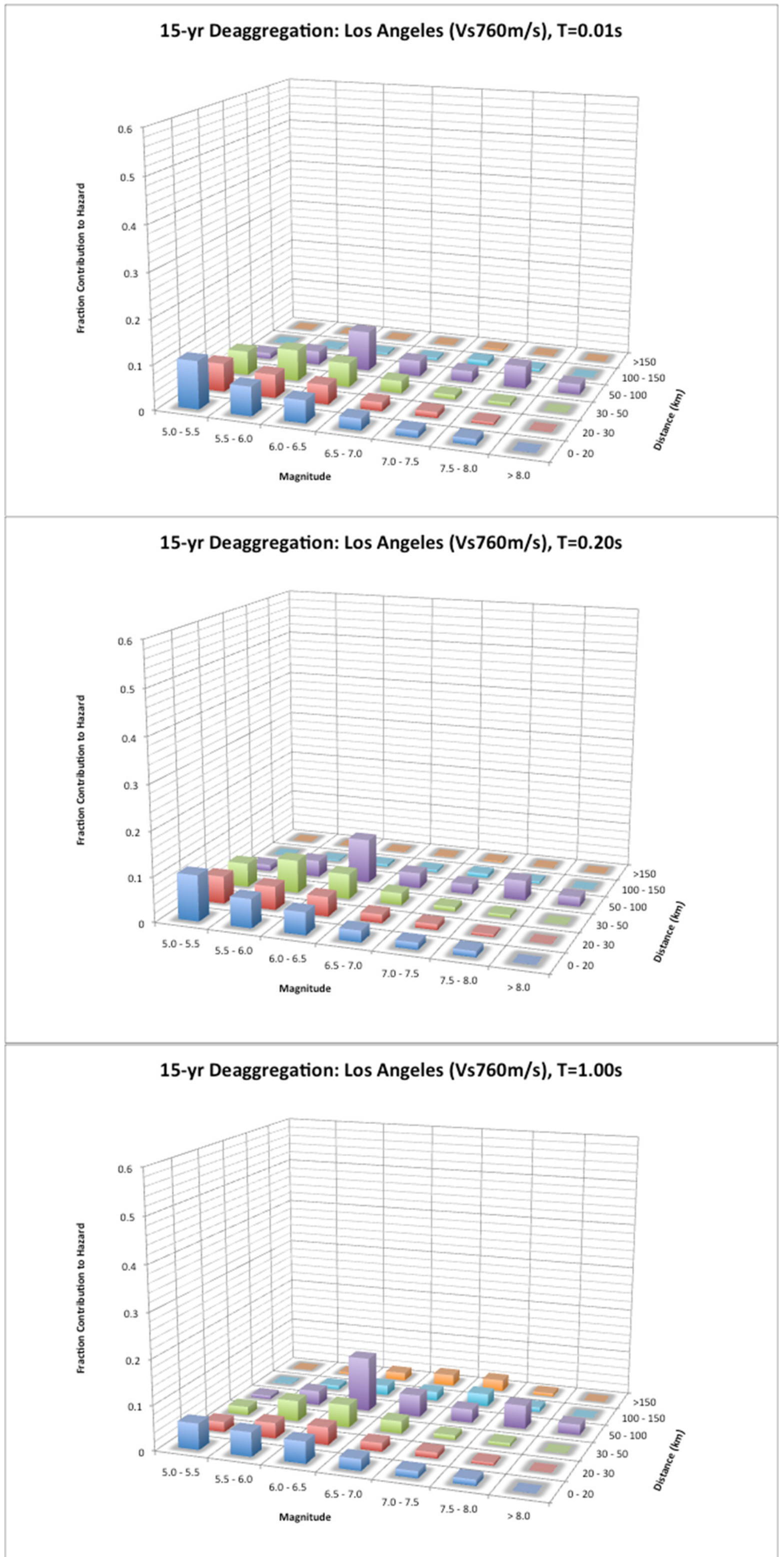

Figure 2.17 Deaggregation for (PGA, 0.2 sec, and 1.0 sec) at the 15-year return period hazard level for the Los Angeles site location (V_{s30} = 760 m/sec).

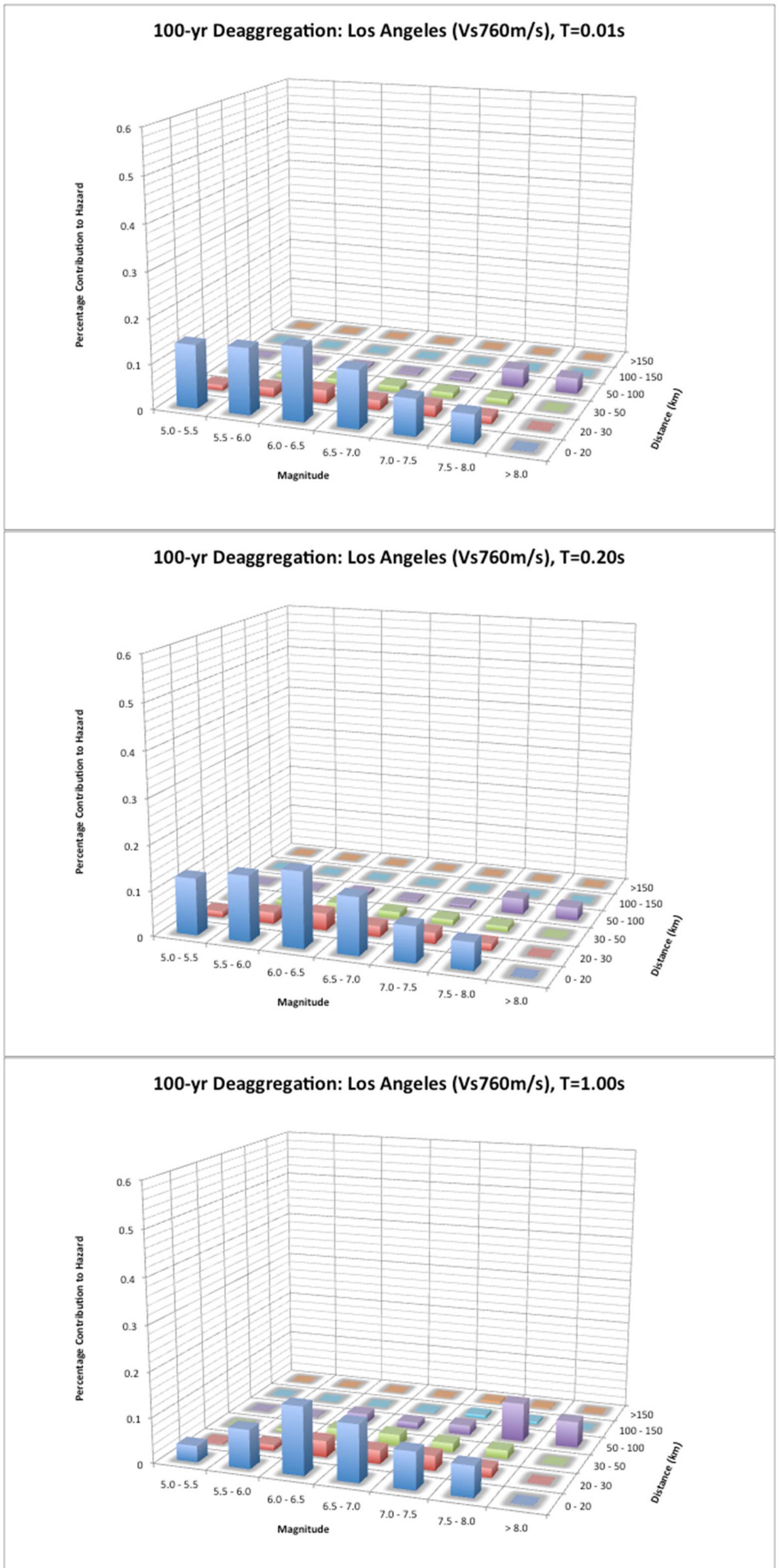

Figure 2.18 **Deaggregation for (PGA, 0.2 sec, and 1.0 sec) at the 100-year return period hazard level for the Los Angeles site location (V_{s30} = 760 m/sec).**

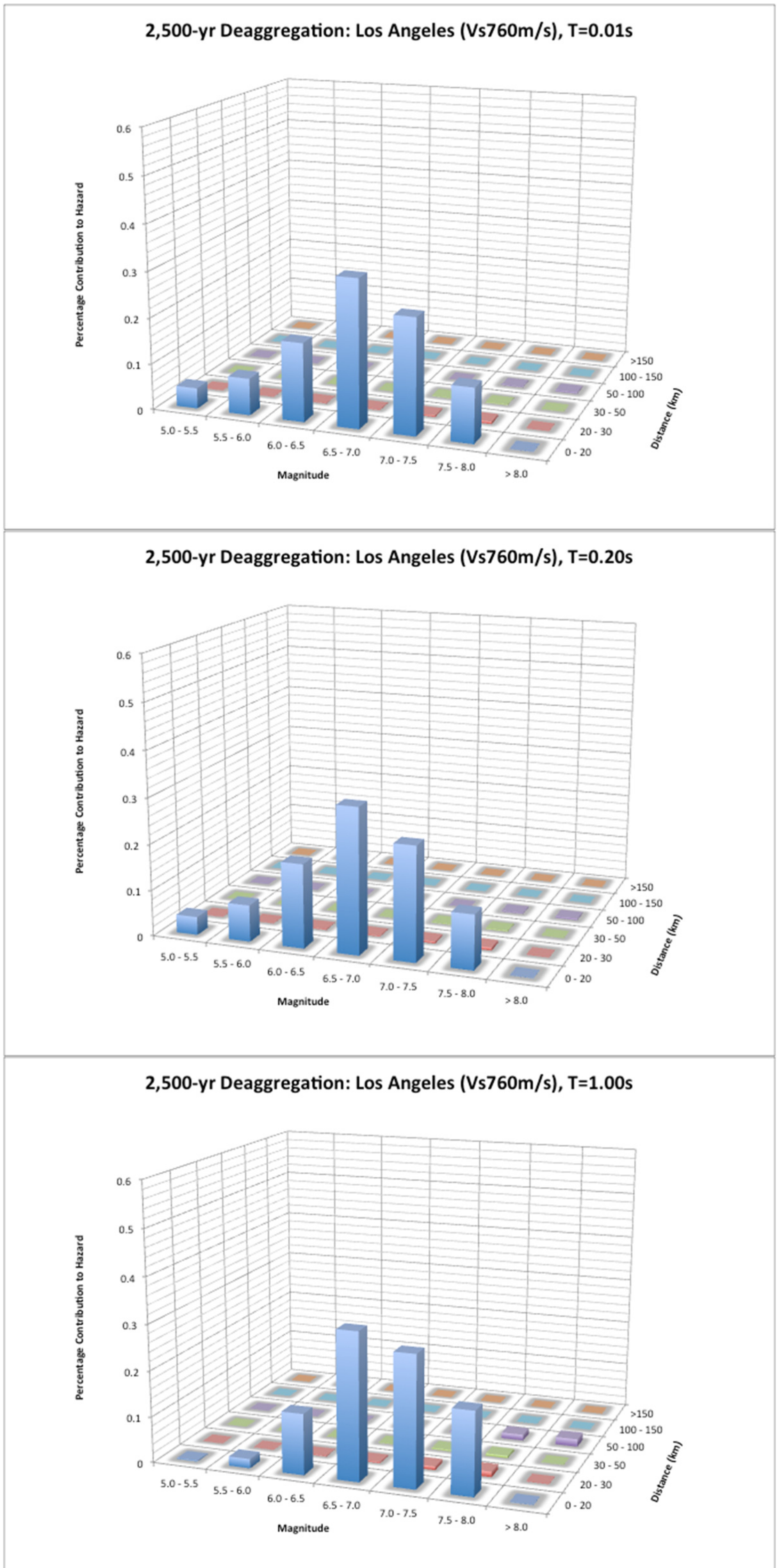

Figure 2.19 Deaggregation for (PGA, 0.2 sec, and 1.0 sec) at the 2500-year return period hazard level for the Los Angeles site location (V_{s30} = 760 m/sec).

3 Ground-Motion Selection and Modification for the Uniform Hazard Spectrum-Based Records

The process used in the selection and scaling the ground motions is like that used in engineering practice for building design and assessment. The ground motions used in this project are intended to span the expected seismic hazard at the sites for a wide range of return periods such that a probabilistic relationship between structural response and hazard level can be developed by other working groups in the project. A suite of 40 ground-motion horizontal component pairs was selected for each case that is a combination of site, soil class, and return period, as well as spectral shape. The methodology described in the next section was applied for each suite of ground motions. Even though some of these cases may have similar spectral shapes, there may be differences in the deaggregation of hazard—magnitude and distance characteristics of scenarios that control the hazard—resulting in a different record selection.

In the following sections, the methodology of ground-motion selection and modification is explained, followed by the selected and scaled motions for two sites: Oakland and Los Angeles sites. The selected and scaled ground motions for all ten sites, as well as the target spectra, are documented in Appendix A of this report.

3.1 METHODOLOGY

The RotD50 component of the UHS with 5% damping—developed through PSHA process explained in previous sections—was used as the target spectrum for selection and modification because ground-motion models use this component. RotD50 is the statistical median spectrum-resultant over all possible rotations of the two horizontal components of ground motion.

The building code prescribes the use of the maximum component for both the target spectrum and the ground-motion pairs. While this practice may yield conservative results, it does not necessarily have the consistency required in the probabilistic analysis that is within the scope of this project. Additionally, the results of our PEER–CEA Project will be used to develop fragility modification functions for a given hazard level (e.g., at a spectral ordinate); thus, the exact absolute value of the input motion can be adjusted for the end-users (e.g., financial loss modelers).

Damping at 5% was used in the process as it is consistent with ground-motion models in NGA-West2. Since the analyses being performed use the ground motions through nonlinear response history analysis (i.e., time-history analysis), different energy-dissipation mechanisms are explicitly modeled, such as hysteretic energy dissipation. Thus, the choice of 5% damping in the ground-motion selection and scaling does not impose any limitations on the use of the ground motions.

The period range to be used for selection and scaling was determined in collaboration with the simulation working group. The simulation working group provided a range for the fundamental period of the type of structure under consideration to be between 0.1 and 1.0 sec. To account for period lengthening during inelastic response, the period range for ground-motion selection and scaling was extended to be between 0.1 and 2.0 sec. This method is consistent with what is required by the building code.

Sample target spectra for the ten sites—the UHS for a 500-year return period at a V_{s30} of 760 m/sec—is shown in Figure 3.1. As the figure demonstrates, Sacramento has the lowest spectral values, with Bakersfield and San Diego having moderate spectral demands. The remaining sites in Northern and Southern California have comparable spectral accelerations, with different controlling events.

In addition to the UHS, the hazard-deaggregation data obtained from the PSHA—magnitude and distance contributions to the hazard—was used to set the initial search criteria for the ground-motion records. The deaggregation data is used to determine the magnitude and distance ranges for the controlling events. An example of deaggregation data is shown in Figure 3.2. This deaggregation is for the Oakland site with a 500-year return period, V_{s30} = 760 m/sec, and T = 0.10 sec. The deaggregation data was evaluated at a range of periods to determine the most appropriate search criteria (0.01–2.0 sec).

In the ground-motion selection process, the severity of the level of the ground motion is included by having multiple UHS associated with multiple return periods. A typical example where additional variability has also been included is shown in Figure 3.3.

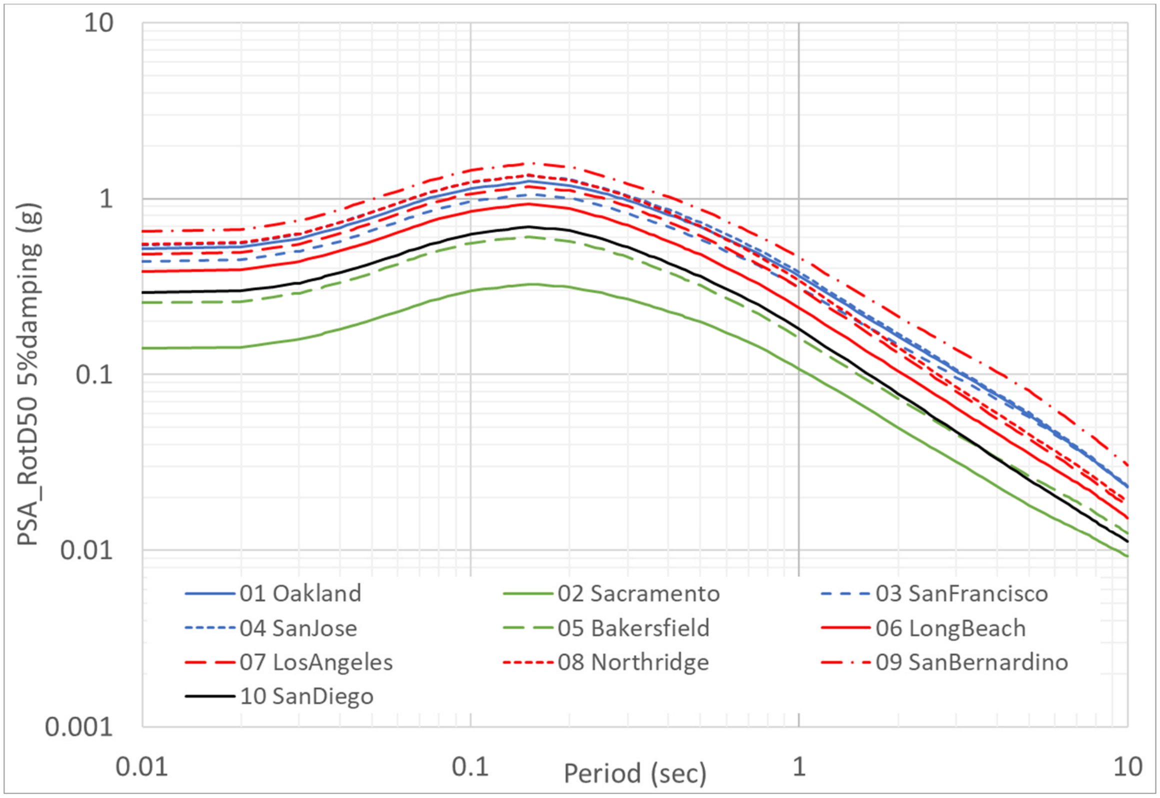

Figure 3.1 Sample target spectra.

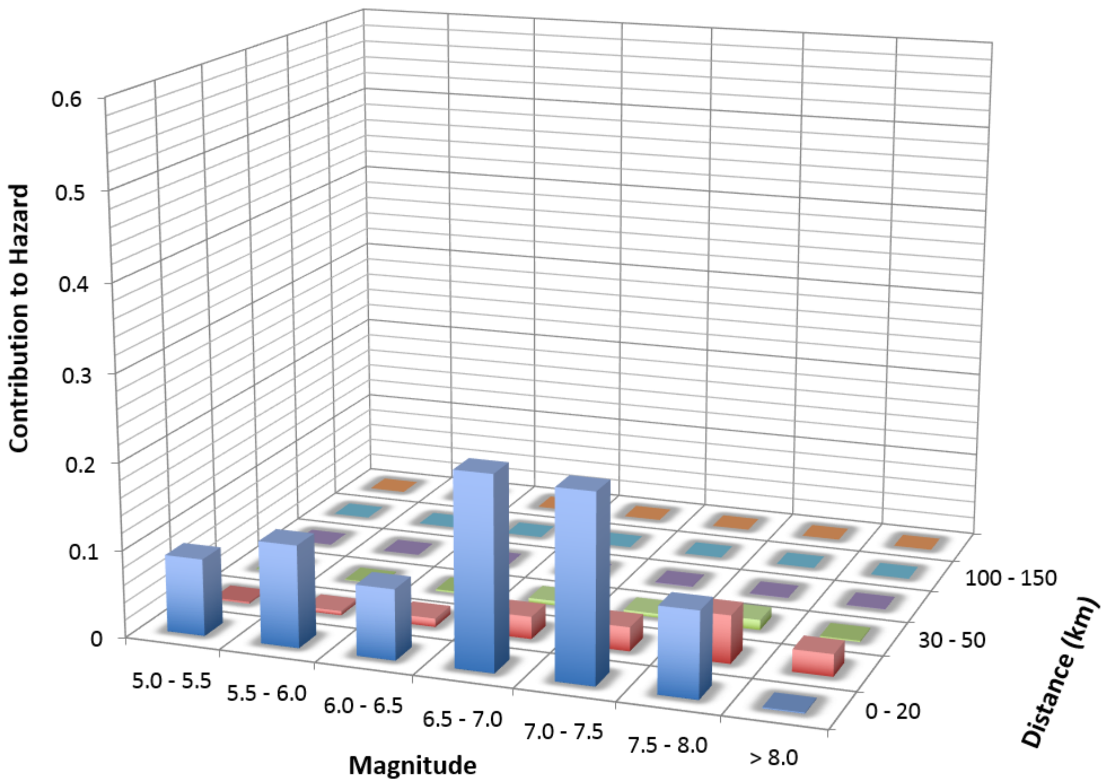

Figure 3.2 **Sample hazard deaggregation, Oakland, 500-year return period, V_{s30} = 760 m/sec, T = 0.1 sec.**

The ground-motion records were selected from the PEER NGA-West2 Ground-Motion Database (*https://ngawest2.berkeley.edu/site*). The record selection is a multi-step process using both record metadata (magnitude, distance, site class, event, and site characteristics), spectral shape (5% damped elastic spectrum), and significant-duration data. The following steps outline the selection process, which was repeated for each case. These steps follow the same methodology implemented in the PEER NGA ground-motion portal. The process was implemented using Microsoft Access to improve the efficiency in implementing the process for 200 ground-motion sets.

1. From the deaggregation data in the period range of interest (0.01–2 sec), determine combinations of magnitude and distance ranges of the controlling events to be used for the ground motions. For the case shown above, there are two magnitude-distance pairs to be used in the search: **M**5–8/D0-20 km and **M**6.5–8.5/D20–30 km. The magnitude range was selected to be wide enough to consider the smaller, more frequent events, that are shown by the deaggregation to affect the hazard at the site. The deaggregation data from other periods, such as 0.5, 1, and 2 sec, were also evaluated to determine all relevant magnitude–distance ranges. It is noted that the deaggregation was used as a tool to shed light on the selection process of recordings. Even though the distance metric in the deaggregation data is the closest rupture distance, the Joyner-Boore distance (R_{jb}) metric was used in the ground-motion selection because

this is the metric used by the selection tool. The R_{jb} distance ranges used meet the distance criteria.

2. Site class search criteria: For the case of V_{s30} = 270 m/sec, select stations with a V_{s30} range of 180–540 m/sec. For the case of V_{s30} = 760 m/sec, stations with a V_{s30} range of 360–1200/sec were selected.
3. Select all ground-motion records that meet the magnitude–distance combinations from the deaggregation and the site-class range. Because there are no restrictions on the style of faulting, they are all present in the selection. When possible, preference was given to records from California.
4. For each record in the initial selection, compute the scale factor (SF_{MSEmin}) that would yield the minimum mean squared error (MSE) between the individual-record RotD50 spectrum and the target UHS spectrum.
5. Records whose MSE-min scale factor was less than 1/4 or greater than 4 were removed from the selection. This range is what is used in practice for ground-motion selection and scaling.
6. All remaining records were scaled by the MSE-min scale factor (SF_{MSEmin}).
7. The MSE was computed for each scaled record. The MSE is a measure of spectral shape. The lower the MSE, the closer the spectral shape is to the target spectrum.
8. The records were sorted in order of MSE.
9. Further selection was based on spectral shape: Starting from the records with the lowest MSE, individual records were selected in order of MSE. One additional criterion was considered in selecting the 40 record pairs with the lowest MSE: No more than 5 records from the same event were used.
10. Once a set of records that met the above criteria was selected, the average of the RotD50 response spectra of the ground-motion suite was computed.
11. An additional scale factor that minimizes the MSE between this average and the target spectrum was computed. This scale factor, typically close to 1.0, was applied to the entire suite. As a result, the total scale factor for the individual record was set equal to the record-specific MSE-min scale factor (Step 6) multiplied by the MSE-min scale factor of the suite.

For the Oakland site, the spectra for a sample ground-motion suite with V_{s30} = 270 m/sec and a 100-year return period is shown in Figure 3.3. In addition to the 40 scaled response spectra, the figure shows the target UHS spectrum (black) and the average of the scaled ground-motion suite (red). The data in this figure highlight two important characteristics of the ground-motion suites: (a) while the average of the spectra at each period matches closely to the target spectrum, the individual spectra do not. Because the frequency content of each record was not modified (amplitude scaling only), each record has its own characteristic energy content across the period range; and (b) the large number of records have maintained their original spectral shape leading to noticeable record-to-record and period-to-period dispersion.

Because the UHS already accounts for some variability in ground motions, there is no analytical method to estimate the required variability in the records. Figure 3.4. shows the coefficient of variability (COV), defined as the ratio of the standard deviation to the mean—for all 200 ground-motion suites—in the period range of interest. As the figure shows, the natural variability within and between records leads to a constant variation in the period range of interest. As a result, the observed variability in each ground-motion suite, when combined with that of other return-period suites at a site, results in wide overall dispersion of period-PSA combinations, thus reducing the expectations of bias.

The suite average is shown in Figure 3.5 for a series of return periods for a single site and soil class for the Oakland site with V_{s30} = 270 m/sec. These two figures show that a total of 40 records is able to provide a ground-motion suite that captures the average target spectrum and also represents significant record-to-record and period-to-period variability, which is desired in nonlinear response-history analysis. The individual-record spectra, V_{s30} = 270 m/sec, show the large variability in spectral amplitudes represented by the wide range of return periods; see Figure 3.6.

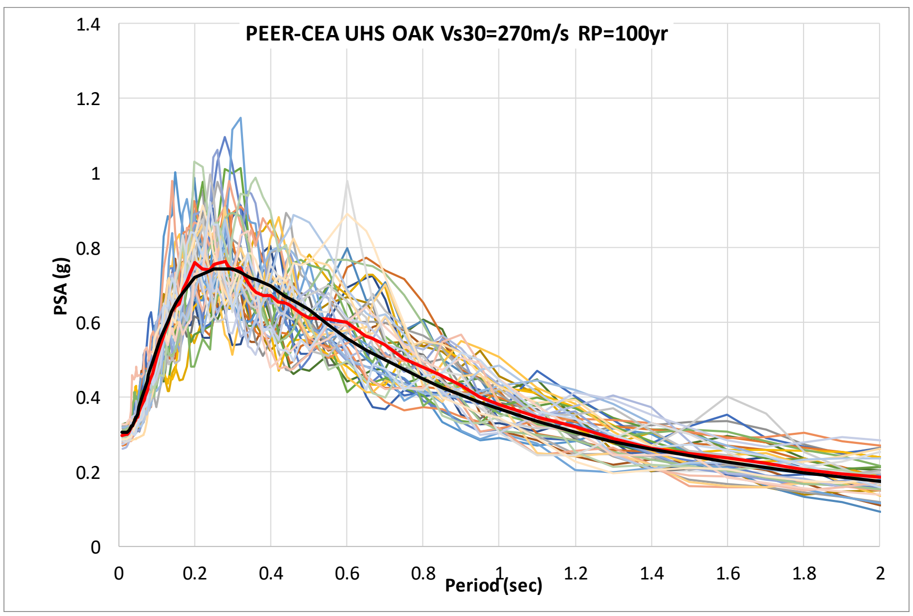

Figure 3.3 **Ground-motion suite, Oakland V_{s30} = 270 m/sec, 100-year return period (RotD50, 5% damping).**

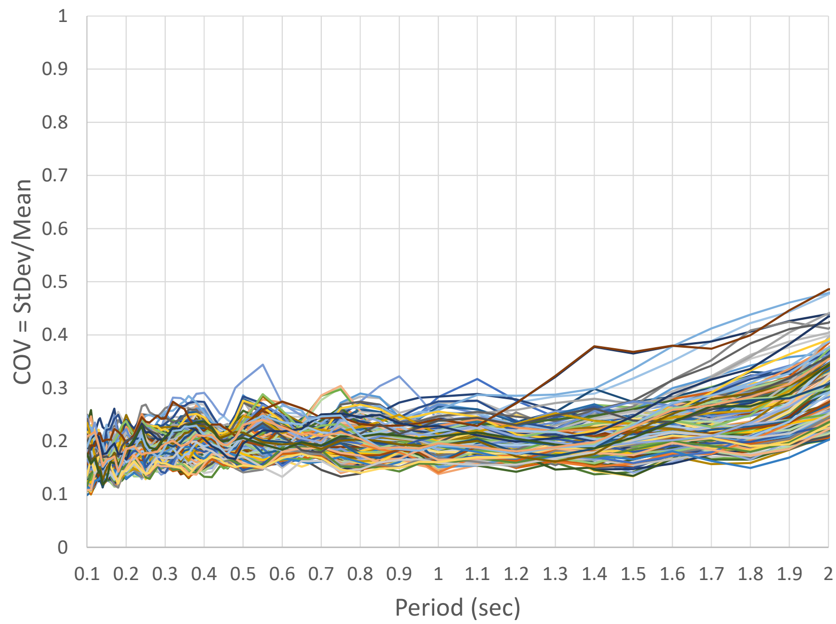

Figure 3.4 Coefficient of variation for all 200 ground-motion suites.

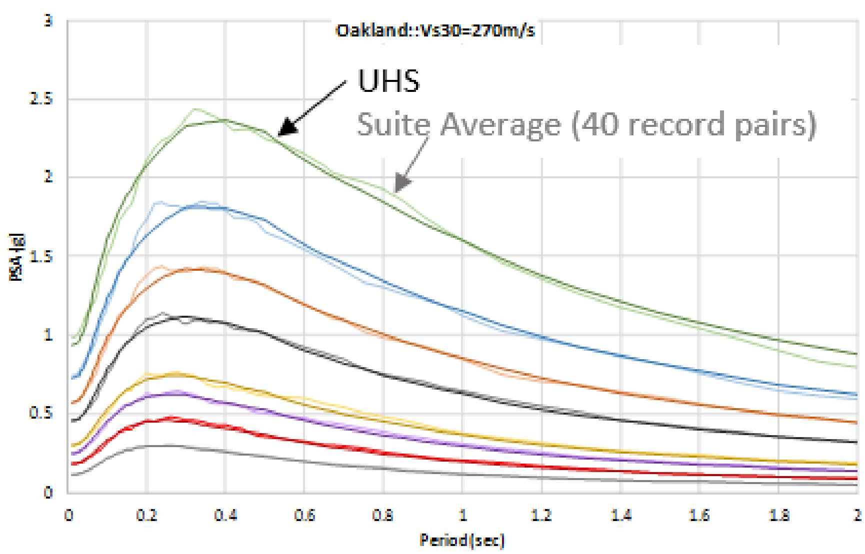

Figure 3.5 Ground-motion suite average and target UHS spectra for different return periods, Oakland V_{s30} = 270 m/sec.

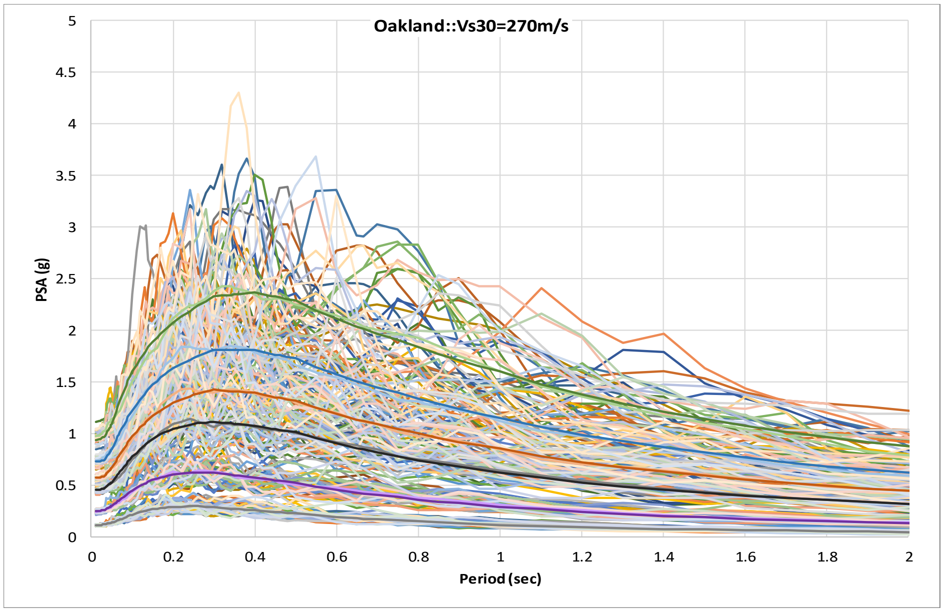

Figure 3.6 **Ground-motion records suites for different return periods, Oakland V_{s30} = 270 m/sec.**

3.2 GROUND-MOTION SUITES

For each of the ten sites, two soil classes were considered. For each site and soil class, the UHS target spectra were computed for 10 return periods. A suite of 40 ground motions was developed for each return period, resulting in 200 ground-motion suites of 40 records each. Two individual sites will be shown in this section. All 10 sites are shown in Appendix A.1. The target spectra for these ground-motion suites are given in Appendix A.3.

The deaggregation results for each hazard level (return period), site, and soil class were evaluated to determine the search criteria for the ground-motion suite. Because deaggregation is performed at each period, multiple deaggregation plots were considered for each case, using the one for T = 0.3 sec as the main plot since it was considered to represent the middle of the period range of interest (0.01–2.0 sec). To simplify the search criteria, the same magnitude and distance range were used for a single site. This simplification is consistent with the observed deaggregation for the different cases. The search criteria are shown in Table 3.1.

In the following sections, the results for two sites—the Oakland and Los Angeles sites—are presented. The selected and scaled motions for all ten sites are documented in Appendix A.1 of this report, using the same format as was done for Oakland and Los Angeles sites.

Table 3.1 Ground-motion suite search criteria.

Site label	Site V_{s30} (m/sec)	Vs_{30} range	Mag1Rrnge	JBdist1range	Mag2range	JBDist2range
01 Oakland	270	180,540	5,7.5	0,20	6,9	20,50
01 Oakland	760	360,1200	5,7.5	0,20	6,9	20,50
02 Sacramento	270	180,540	5,6.5	15,50	5.5,8	50,150
02 Sacramento	760	360,1200	5,6.5	15,50	5.5,8	50,150
03 SanFrancisco	270	180,540	5,9	0,20	6,7.5	20,50
03 SanFrancisco	760	360,1200	5,9	0,20	6,7.5	20,50
04 SanJose	270	180,540	5,9	0,20	6,7.5	20,30
04 SanJose	760	360,1200	5,9	0,20	6,7.5	20,30
05 Bakersfield	270	180,540	5,7	0,50	7,9	50,100
05 Bakersfield	760	360,1200	5,7	0,50	7,9	50,100
06 LongBeach	270	180,540	5,8	0,20	6,8	20,50
06 LongBeach	760	360,1200	5,8	0,20	6,8	20,50
07 LosAngeles	270	180,540	5,8	0,20	6,8	20,50
07 LosAngeles	760	360,1200	5,8	0,20	6,8	20,50
08 Northridge	270	180,540	5,8	0,20	6,9	20,50
08 Northridge	760	360,1200	5,8	0,20	6,9	20,50
09 SanBernardino (*)	270	180,540	5,9	0,20	*	*
09 SanBernardino (*)	760	360,1200	5,9	0,20	*	*
10 SanDiego	270	180,540	5,8	0,20	5,7.5	20,100
10 SanDiego	760	360,1200	5,8	0,20	5,7.5	20,100

*The San Bernardino site had a single Magnitude-Distance Range criterion

3.2.1 Oakland Site

The list of 50 records for the Oakland site, V_{s30} = 270 m/sec, return period = 500 years, is shown in Table 3.2. The scale factor for each record is also given in the table. The suite shown contains more than 40 records per return period. Extra records were selected so that further selection based on duration can be performed. Table 3.3 presents the data for V_{s30} = 760 m/sec.

The 5%-damped RotD50 component response spectra for the ground-motion suites for the Oakland Site are shown in Figure 3.7 and Figure 3.8, for the two different soil classes. The suite average and target spectrum for each return period are also shown in the plot. These two quantities are shown in a separate set of figures in Figure 3.9 and Figure 3.10. As the figures show, the suite average matches the target spectrum in the period range of interest for all cases.

A complete list of record-metadata for the records selected for the Oakland site is given in Table 3.4 and Table 3.5 for the different soil classes. In these tables, RSN stands for Records Sequence Number, which is a unique record number in the NGA-West2 database; JB stands for Joyner and Boore distance metric; Sig Duration is the significant duration as duration between 5% and 75% of the Arias Intensity; and SF is the scale factor used for each recording.

Table 3.2 Ground-motion suite metadata and scale factors, Oakland, V_{s30} = 270 m/sec, 500-year return period.

Site label	Site Vs_{30} (m/sec)	Return period (yr)	RSN	EQ name	Station name	EQ year	EQ mag	JB dist (km)	Station V_{s30} (m/sec)	Sig duration (sec)	SF
01 Oakland	270	500	6	Imperial Valley-02	El Centro Array #9	1940	6.95	6	213.44	14.7	2.46
01 Oakland	270	500	15	Kern County	Taft Lincoln School	1952	7.36	38	385.43	10.4	3.79
01 Oakland	270	500	161	Imperial Valley-06	Brawley Airport	1979	6.53	9	208.71	4	3.11
01 Oakland	270	500	179	Imperial Valley-06	El Centro Array #4	1979	6.53	5	208.91	3	1.61
01 Oakland	270	500	185	Imperial Valley-06	Holtville Post Office	1979	6.53	5	202.89	4.7	2.48
01 Oakland	270	500	292	Irpinia, Italy-01	Sturno (STN)	1980	6.9	7	382	6.5	2.01
01 Oakland	270	500	313	Corinth, Greece	Corinth	1981	6.6	10	361.4	5.2	2.54
01 Oakland	270	500	316	Westmorland	Parachute Test Site	1981	5.9	17	348.69	5.9	3
01 Oakland	270	500	568	San Salvador	Geotech Investig Center	1986	5.8	2	489.34	1.1	1.1
01 Oakland	270	500	721	Superstition Hills-02	El Centro Imp. Co. Cent	1987	6.54	18	192.05	8.1	2.12
01 Oakland	270	500	728	Superstition Hills-02	Westmorland Fire Sta	1987	6.54	13	193.67	10.9	2.58
01 Oakland	270	500	764	Loma Prieta	Gilroy - Historic Bldg.	1989	6.93	10	308.55	3.6	2.42
01 Oakland	270	500	766	Loma Prieta	Gilroy Array #2	1989	6.93	10	270.84	2.3	1.71
01 Oakland	270	500	768	Loma Prieta	Gilroy Array #4	1989	6.93	14	221.78	4.5	2.07
01 Oakland	270	500	787	Loma Prieta	Palo Alto - SLAC Lab	1989	6.93	31	425.3	4.5	2.56
01 Oakland	270	500	803	Loma Prieta	Saratoga - W Valley Coll.	1989	6.93	8	347.9	4.1	1.98
01 Oakland	270	500	806	Loma Prieta	Sunnyvale - Colton Ave.	1989	6.93	24	267.71	9.8	2.9
01 Oakland	270	500	850	Landers	Desert Hot Springs	1992	7.28	22	359	21.7	3.8
01 Oakland	270	500	949	Northridge-01	Arleta - Nordhoff Fire Sta	1994	6.69	3	297.71	6	1.99
01 Oakland	270	500	959	Northridge-01	Canoga Park - Topanga Can	1994	6.69	0	267.49	6.4	1.56
01 Oakland	270	500	963	Northridge-01	Castaic - Old Ridge Route	1994	6.69	20	450.28	5.1	1.23
01 Oakland	270	500	986	Northridge-01	LA - Brentwood VA Hospital	1994	6.69	13	416.58	6	3.38
01 Oakland	270	500	988	Northridge-01	LA - Century City CC North	1994	6.69	16	277.98	7.1	2.58
01 Oakland	270	500	1044	Northridge-01	Newhall - Fire Sta	1994	6.69	3	269.14	2.8	0.91
01 Oakland	270	500	1048	Northridge-01	Northridge - 17645 Saticoy St	1994	6.69	0	280.86	5.9	1.39
01 Oakland	270	500	1063	Northridge-01	Rinaldi Receiving Sta	1994	6.69	0	282.25	3.9	0.82
01 Oakland	270	500	1082	Northridge-01	Sun Valley - Roscoe Blvd	1994	6.69	6	320.93	5.8	1.79
01 Oakland	270	500	1083	Northridge-01	Sunland - Mt Gleason Ave	1994	6.69	12	402.16	6	3.96
01 Oakland	270	500	1085	Northridge-01	Sylmar - Converter Sta East	1994	6.69	0	370.52	3.6	0.98
01 Oakland	270	500	1086	Northridge-01	Sylmar - Olive View Med FF	1994	6.69	2	440.54	2.5	0.93
01 Oakland	270	500	1119	Kobe, Japan	Takarazuka	1995	6.9	0	312	2.1	0.94
01 Oakland	270	500	1208	Chi-Chi, Taiwan	CHY046	1999	7.62	24	442.15	19.1	3.46
01 Oakland	270	500	3751	Cape Mendocino	South Bay Union School	1992	7.01	33	459.04	7.8	3.39

Site label	Site Vs_{30} (m/sec)	Return period (yr)	RSN	EQ name	Station name	EQ year	EQ mag	JB dist (km)	Station V_{s30} (m/sec)	Sig duration (sec)	SF
01 Oakland	270	500	4117	Parkfield-02, CA	Parkfield - Fault Zone 15	2004	6	1	307.59	4.1	2.95
01 Oakland	270	500	4457	Montenegro, Yugo.	Ulcinj - Hotel Albatros	1979	7.1	2	410.35	7.7	2.74
01 Oakland	270	500	4860	Chuetsu-oki	Sanjo Shinbori	2007	6.8	16	278.12	10.5	2.05
01 Oakland	270	500	4863	Chuetsu-oki	Nagaoka	2007	6.8	4	514.3	9.5	1.8
01 Oakland	270	500	4894	Chuetsu-oki	Kashiwazaki NPP, Unit 1: ground surface	2007	6.8	0	329	5.7	0.64
01 Oakland	270	500	5774	Iwate	Nakashinden Town	2008	6.9	29	276.3	11	3.21
01 Oakland	270	500	5823	El Mayor-Cucapah	Chihuahua	2010	7.2	18	242.05	25.1	2.49
01 Oakland	270	500	5975	El Mayor-Cucapah	Calexico Fire Station	2010	7.2	19	231.23	18.6	2.13
01 Oakland	270	500	6890	Darfield, New Zealand	Christchurch Cashmere High School	2010	7	18	204	8.7	2.4
01 Oakland	270	500	6911	Darfield, New Zealand	HORC	2010	7	7	326.01	6.7	1.25
01 Oakland	270	500	6953	Darfield, New Zealand	Pages Road Pumping Station	2010	7	25	206	11.2	2.63
01 Oakland	270	500	6969	Darfield, New Zealand	Styx Mill Transfer Station	2010	7	21	247.5	12.2	3.22
01 Oakland	270	500	8063	Christchurch, New Zealand	Christchurch Botanical Gardens	2011	6.2	6	187	3.8	1.26
01 Oakland	270	500	8130	Christchurch, New Zealand	Shirley Library	2011	6.2	6	207	4.3	1.55
01 Oakland	270	500	8134	Christchurch, New Zealand	Styx Mill Transfer Station	2011	6.2	11	247.5	5.6	3.44
01 Oakland	270	500	8161	El Mayor-Cucapah	El Centro Array #12	2010	7.2	10	196.88	13.2	1.69
01 Oakland	270	500	8606	El Mayor-Cucapah	Westside Elementary School	2010	7.2	10	242	9.3	2.13

Table 3.3 Ground-motion suite metadata and scale factors, Oakland, V_{s30} = 760 m/sec, return period = 500 years.

Site label	Site Vs_{30} (m/sec)	Return period (yr)	RSN	EQ name	Station name	EQ year	EQ mag	JB dist (km)	Station V_{s30} (m/sec)	Sig duration (sec)	SF
01 Oakland	760	500	1	Helena, Montana-01	Carroll College	1935	6	2	593.35	1.2	3.45
01 Oakland	760	500	139	Tabas, Iran	Dayhook	1978	7.35	0	471.53	6.7	1.4
01 Oakland	760	500	156	Norcia, Italy	Cascia	1979	5.9	1	585.04	2.5	2.93
01 Oakland	760	500	230	Mammoth Lakes-01	Convict Creek	1980	6.06	1	382.12	6.9	1.15
01 Oakland	760	500	233	Mammoth Lakes-02	Convict Creek	1980	5.69	3	382.12	2.6	2.82
01 Oakland	760	500	236	Mammoth Lakes-03	Convict Creek	1980	5.91	3	382.12	2.4	2.26
01 Oakland	760	500	408	Coalinga-05	Oil Fields Fire Station - FF	1983	5.77	6	474.15	3.6	2.61
01 Oakland	760	500	409	Coalinga-05	Oil Fields Fire Station - Pad	1983	5.77	6	474.15	3.6	2.44
01 Oakland	760	500	410	Coalinga-05	Palmer Ave	1983	5.77	8	458.09	1.8	1.89
01 Oakland	760	500	589	Whittier Narrows-01	Alhambra - Fremont School	1987	5.99	2	549.75	2.1	1.56
01 Oakland	760	500	632	Whittier Narrows-01	LA - Cypress Ave	1987	5.99	9	366.71	3	3.61
01 Oakland	760	500	675	Whittier Narrows-01	Pasadena - CIT Athenaeum	1987	5.99	4	415.13	3	3.53
01 Oakland	760	500	691	Whittier Narrows-01	San Marino - SW Academy	1987	5.99	2	379.43	2.9	2.88
01 Oakland	760	500	763	Loma Prieta	Gilroy - Gavilan Coll.	1989	6.93	9	729.65	1.5	1.43
01 Oakland	760	500	801	Loma Prieta	San Jose - Santa Teresa Hills	1989	6.93	14	671.77	6.3	1.66
01 Oakland	760	500	1006	Northridge-01	LA - UCLA Grounds	1994	6.69	14	398.42	5.5	1.42
01 Oakland	760	500	1078	Northridge-01	Santa Susana Ground	1994	6.69	2	715.12	4.1	1.72
01 Oakland	760	500	1281	Chi-Chi, Taiwan	HWA032	1999	7.62	43	573.04	8.3	3.48
01 Oakland	760	500	1631	Upland	Pomona - 4th & Locust FF	1990	5.63	7	384.44	2.5	2.75
01 Oakland	760	500	1633	Manjil, Iran	Abbar	1990	7.37	13	723.95	9	0.85
01 Oakland	760	500	2619	Chi-Chi, Taiwan-03	TCU067	1999	6.2	28	433.63	5.2	3.03
01 Oakland	760	500	2628	Chi-Chi, Taiwan-03	TCU078	1999	6.2	0	443.04	2.2	1.13
01 Oakland	760	500	3472	Chi-Chi, Taiwan-06	TCU076	1999	6.3	24	614.98	7.7	3.8
01 Oakland	760	500	3943	Tottori, Japan	SMN015	2000	6.61	9	616.55	3.5	2.26
01 Oakland	760	500	3979	San Simeon, CA	Cambria - Hwy 1 Caltrans Bridge	2003	6.52	7	362.42	6.3	2.81
01 Oakland	760	500	4031	San Simeon, CA	Templeton - 1-story Hospital	2003	6.52	5	410.66	3.1	1.09
01 Oakland	760	500	4096	Parkfield-02, CA	Bear Valley Ranch, Parkfield, CA, USA	2004	6	3	527.95	2.3	3.27
01 Oakland	760	500	4132	Parkfield-02, CA	Parkfield - Vineyard Cany 2E	2004	6	4	467.76	2.7	1.91
01 Oakland	760	500	4213	Niigata, Japan	NIG023	2004	6.63	25	654.76	1.9	1.5
01 Oakland	760	500	4218	Niigata, Japan	NIG028	2004	6.63	0	430.71	3.5	0.81
01 Oakland	760	500	4228	Niigata, Japan	NIGH11	2004	6.63	6	375	3.1	0.95
01 Oakland	760	500	4442	Friuli (aftershock 13), Italy	San Rocco	1976	5.9	-999	649.67	2	2.73
01 Oakland	760	500	4480	L'Aquila, Italy	L'Aquila - V. Aterno - Centro Valle	2009	6.3	0	475	4.4	0.91
01 Oakland	760	500	4869	Chuetsu-oki	Kawaguchi	2007	6.8	24	640.14	8.7	2.81

Site label	Site Vs_{30} (m/sec)	Return period (yr)	RSN	EQ name	Station name	EQ year	EQ mag	JB dist (km)	Station V_{s30} (m/sec)	Sig duration (sec)	SF
01 Oakland	760	500	4882	Chuetsu-oki	Ojiya City	2007	6.8	16	430.16	7.1	1.71
01 Oakland	760	500	5274	Chuetsu-oki	NIG028	2007	6.8	15	430.71	11.1	3.35
01 Oakland	760	500	5275	Chuetsu-oki	NIGH01	2007	6.8	16	480.4	10.9	3.32
01 Oakland	760	500	5478	Iwate	AKT023	2008	6.9	12	555.96	6.7	1.25
01 Oakland	760	500	5618	Iwate	IWT010	2008	6.9	16	825.83	8.5	1.62
01 Oakland	760	500	5623	Iwate	IWT015	2008	6.9	17	567.45	6.2	2.59
01 Oakland	760	500	5656	Iwate	IWTH24	2008	6.9	3	486.41	8	1
01 Oakland	760	500	5657	Iwate	IWTH25	2008	6.9	0	506.44	6.9	0.38
01 Oakland	760	500	5678	Iwate	MYGH02	2008	6.9	5	398.59	3.7	1.97
01 Oakland	760	500	5773	Iwate	Miyagi Great Village	2008	6.9	41	531.25	8.9	2.62
01 Oakland	760	500	5775	Iwate	Tamati Ono	2008	6.9	29	561.59	8	2.05
01 Oakland	760	500	5776	Iwate	Kami, Miyagi Miyazaki City	2008	6.9	25	477.55	7.6	3.25
01 Oakland	760	500	5809	Iwate	Minase Yuzawa	2008	6.9	17	655.45	7.6	2.08
01 Oakland	760	500	5813	Iwate	Mizusawaku Interior O ganecho	2008	6.9	8	413.04	11.8	1.52
01 Oakland	760	500	6878	Joshua Tree, CA	North Palm Springs Fire Sta #36	1992	6.1	21	367.84	4.5	3.14
01 Oakland	760	500	6928	Darfield, New Zealand	LPCC	2010	7	25	649.67	7.5	1.85

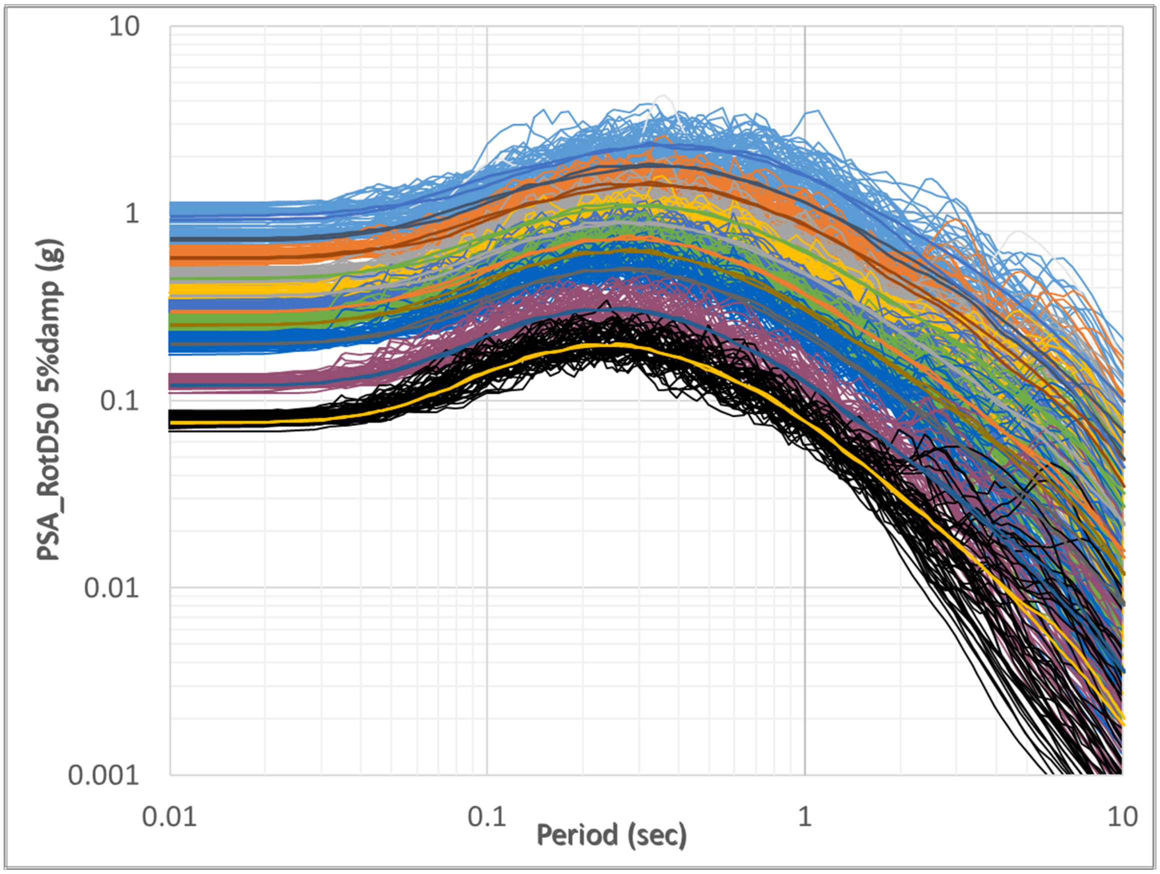

Figure 3.7 **Ground- motion suites, Oakland, V_{s30} = 270 m/sec.**

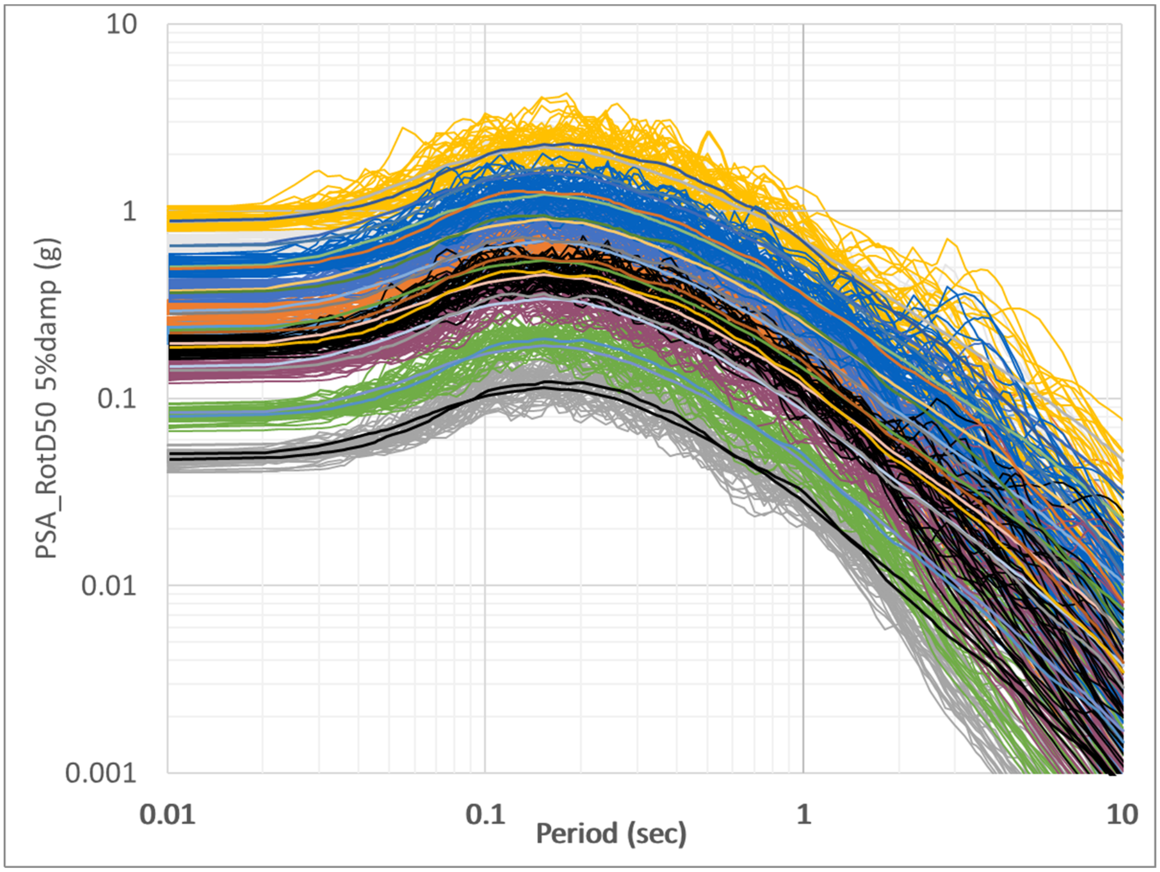

Figure 3.8 Ground-motion suites, Oakland, V_{s30}= 760 m/sec.

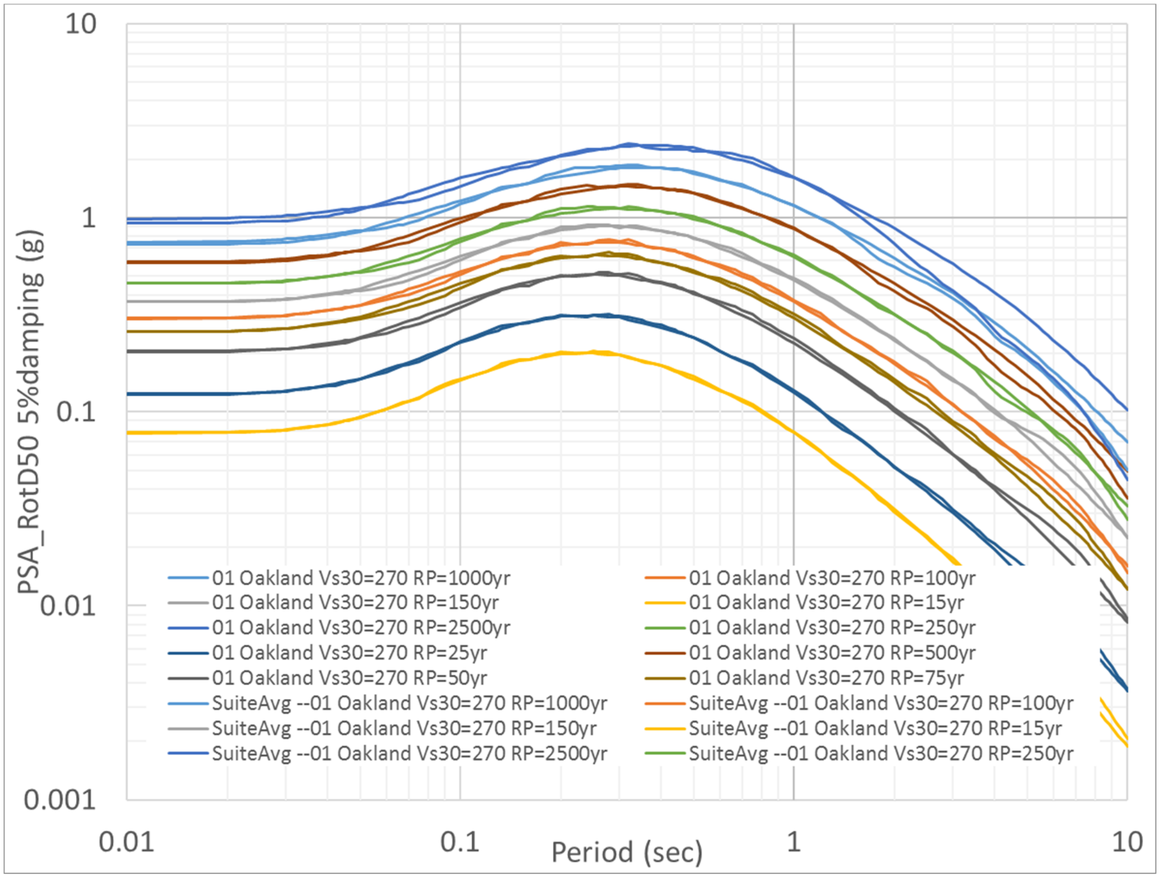

Figure 3.9 Suite average and target spectra for Oakland site, V_{s30}= 270 m/sec.

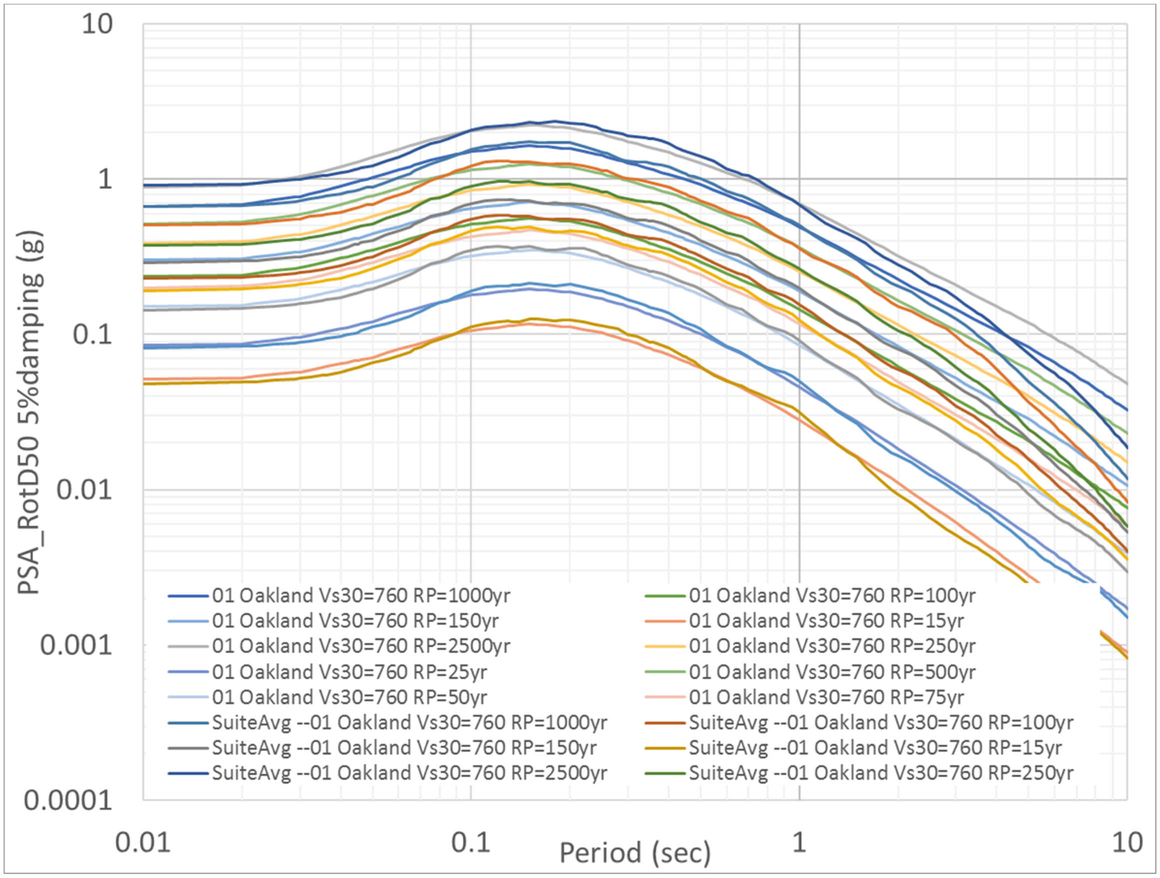

Figure 3.10 Suite average and target spectra for Oakland site, V_{s30}= 760 m/sec.

Table 3.4 List of record metadata, Oakland, V_{s30} = 270 m/sec.

RSN	EQ name	Station name	EQ year	EQ mag	JB dist (km)	Station V_{s30} (m/sec)	Sig duration (sec)
6	Imperial Valley-02	El Centro Array #9	1940	6.95	6	213.44	14.7
15	Kern County	Taft Lincoln School	1952	7.36	38	385.43	10.4
21	Imperial Valley-05	El Centro Array #9	1955	5.4	14	213.44	8
57	San Fernando	Castaic - Old Ridge Route	1971	6.61	19	450.28	6.2
95	Managua, Nicaragua-01	Managua, ESSO	1972	6.24	4	288.77	4.6
96	Managua, Nicaragua-02	Managua, ESSO	1972	5.2	4	288.77	2.5
130	Friuli, Italy-02	Buia	1976	5.91	11	310.68	4.5
136	Santa Barbara	Santa Barbara Courthouse	1978	5.92	0	514.99	2.8
139	Tabas, Iran	Dayhook	1978	7.35	0	471.53	6.7
147	Coyote Lake	Gilroy Array #2	1979	5.74	8	270.84	1.4
149	Coyote Lake	Gilroy Array #4	1979	5.74	5	221.78	4.8
154	Coyote Lake	San Juan Bautista, 24 Polk St	1979	5.74	19	335.5	6.1
161	Imperial Valley-06	Brawley Airport	1979	6.53	9	208.71	4
162	Imperial Valley-06	Calexico Fire Station	1979	6.53	10	231.23	6.4
164	Imperial Valley-06	Cerro Prieto	1979	6.53	15	471.53	18.1
165	Imperial Valley-06	Chihuahua	1979	6.53	7	242.05	12.9
169	Imperial Valley-06	Delta	1979	6.53	22	242.05	23.4
170	Imperial Valley-06	EC County Center FF	1979	6.53	7	192.05	4.2
171	Imperial Valley-06	El Centro - Meloland Geot. Array	1979	6.53	0	264.57	2.2
175	Imperial Valley-06	El Centro Array #12	1979	6.53	18	196.88	9.7
179	Imperial Valley-06	El Centro Array #4	1979	6.53	5	208.91	3
180	Imperial Valley-06	El Centro Array #5	1979	6.53	2	205.63	3.7
182	Imperial Valley-06	El Centro Array #7	1979	6.53	1	210.51	1.9
184	Imperial Valley-06	El Centro Differential Array	1979	6.53	5	202.26	3.3
185	Imperial Valley-06	Holtville Post Office	1979	6.53	5	202.89	4.7
186	Imperial Valley-06	Niland Fire Station	1979	6.53	36	212	10.1
233	Mammoth Lakes-02	Convict Creek	1980	5.69	3	382.12	2.6
238	Mammoth Lakes-03	Long Valley Dam (L Abut)	1980	5.91	10	537.16	4.2
284	Irpinia, Italy-01	Auletta	1980	6.9	10	476.62	12.9
292	Irpinia, Italy-01	Sturno (STN)	1980	6.9	7	382	6.5
298	Irpinia, Italy-02	Bovino	1980	6.2	44	356.39	9.6
313	Corinth, Greece	Corinth	1981	6.6	10	361.4	5.2
316	Westmorland	Parachute Test Site	1981	5.9	17	348.69	5.9

319	Westmorland	Westmorland Fire Sta	1981	5.9	6	193.67	3.6
320	Mammoth Lakes-10	Convict Creek	1983	5.34	6	382.12	2.2
338	Coalinga-01	Parkfield - Fault Zone 14	1983	6.36	28	246.07	4.6
457	Morgan Hill	Gilroy Array #3	1984	6.19	13	349.85	6.5
499	Hollister-04	Hollister Differential Array #3	1986	5.45	13	215.54	8.1
502	Mt. Lewis	Halls Valley	1986	5.6	12	281.61	1.8
549	Chalfant Valley-02	Bishop - LADWP South St	1986	6.19	14	303.47	3.3
564	Kalamata, Greece-01	Kalamata (bsmt)	1986	6.2	6	382.21	1.7
568	San Salvador	Geotech Investig Center	1986	5.8	2	489.34	1.1
634	Whittier Narrows-01	LA - Fletcher Dr	1987	5.99	11	329.06	2.8
674	Whittier Narrows-01	Pasadena - Brown Gym	1987	5.99	4	341.14	3.3
721	Superstition Hills-02	El Centro Imp. Co. Cent	1987	6.54	18	192.05	8.1
723	Superstition Hills-02	Parachute Test Site	1987	6.54	1	348.69	7.6
725	Superstition Hills-02	Poe Road (temp)	1987	6.54	11	316.64	10.5
728	Superstition Hills-02	Westmorland Fire Sta	1987	6.54	13	193.67	10.9
739	Loma Prieta	Anderson Dam (Downstream)	1989	6.93	20	488.77	5.2
761	Loma Prieta	Fremont - Emerson Court	1989	6.93	40	284.79	7.2
762	Loma Prieta	Fremont - Mission San Jose	1989	6.93	39	367.57	7.9
764	Loma Prieta	Gilroy - Historic Bldg.	1989	6.93	10	308.55	3.6
766	Loma Prieta	Gilroy Array #2	1989	6.93	10	270.84	2.3
767	Loma Prieta	Gilroy Array #3	1989	6.93	12	349.85	2.3
768	Loma Prieta	Gilroy Array #4	1989	6.93	14	221.78	4.5
776	Loma Prieta	Hollister - South & Pine	1989	6.93	28	282.14	7
778	Loma Prieta	Hollister Differential Array	1989	6.93	25	215.54	3.7
786	Loma Prieta	Palo Alto - 1900 Embarc.	1989	6.93	31	209.87	9.6
787	Loma Prieta	Palo Alto - SLAC Lab	1989	6.93	31	425.3	4.5
802	Loma Prieta	Saratoga - Aloha Ave	1989	6.93	8	380.89	3.9
803	Loma Prieta	Saratoga - W Valley Coll.	1989	6.93	8	347.9	4.1
806	Loma Prieta	Sunnyvale - Colton Ave.	1989	6.93	24	267.71	9.8
821	Erzican, Turkey	Erzincan	1992	6.69	0	352.05	2
850	Landers	Desert Hot Springs	1992	7.28	22	359	21.7
864	Landers	Joshua Tree	1992	7.28	11	379.32	21.3
900	Landers	Yermo Fire Station	1992	7.28	24	353.63	8.8
949	Northridge-01	Arleta - Nordhoff Fire Sta	1994	6.69	3	297.71	6
953	Northridge-01	Beverly Hills - 14145 Mulhol	1994	6.69	9	355.81	5.4
959	Northridge-01	Canoga Park - Topanga Can	1994	6.69	0	267.49	6.4
960	Northridge-01	Canyon Country - W Lost Cany	1994	6.69	11	325.6	3.1
963	Northridge-01	Castaic - Old Ridge Route	1994	6.69	20	450.28	5.1
964	Northridge-01	Compton - Castlegate St	1994	6.69	43	266.9	11.4

983	Northridge-01	Jensen Filter Plant Generator Building	1994	6.69	0	525.79	3.9
986	Northridge-01	LA - Brentwood VA Hospital	1994	6.69	13	416.58	6
988	Northridge-01	LA - Century City CC North	1994	6.69	16	277.98	7.1
995	Northridge-01	LA - Hollywood Stor FF	1994	6.69	20	316.46	6.1
1000	Northridge-01	LA - Pico & Sentous	1994	6.69	28	304.68	8.4
1002	Northridge-01	LA - S. Vermont Ave	1994	6.69	28	301.93	9.6
1004	Northridge-01	LA - Sepulveda VA Hospital	1994	6.69	0	380.06	4.5
1005	Northridge-01	LA - Temple & Hope	1994	6.69	29	452.15	7
1008	Northridge-01	LA - W 15th St	1994	6.69	26	329.52	9.3
1034	Northridge-01	Malibu - Point Dume Sch	1994	6.69	27	349.54	7.8
1039	Northridge-01	Moorpark - Fire Sta	1994	6.69	17	341.58	7.5
1044	Northridge-01	Newhall - Fire Sta	1994	6.69	3	269.14	2.8
1048	Northridge-01	Northridge - 17645 Saticoy St	1994	6.69	0	280.86	5.9
1063	Northridge-01	Rinaldi Receiving Sta	1994	6.69	0	282.25	3.9
1082	Northridge-01	Sun Valley - Roscoe Blvd	1994	6.69	6	320.93	5.8
1083	Northridge-01	Sunland - Mt Gleason Ave	1994	6.69	12	402.16	6
1085	Northridge-01	Sylmar - Converter Sta East	1994	6.69	0	370.52	3.6
1086	Northridge-01	Sylmar - Olive View Med FF	1994	6.69	2	440.54	2.5
1115	Kobe, Japan	Sakai	1995	6.9	28	256	11.6
1116	Kobe, Japan	Shin-Osaka	1995	6.9	19	256	4.1
1119	Kobe, Japan	Takarazuka	1995	6.9	0	312	2.1
1141	Dinar, Turkey	Dinar	1995	6.4	0	219.75	10.2
1190	Chi-Chi, Taiwan	CHY019	1999	7.62	50	497.53	24.5
1208	Chi-Chi, Taiwan	CHY046	1999	7.62	24	442.15	19.1
1605	Duzce, Turkey	Duzce	1999	7.14	0	281.86	7.1
1681	Northridge-04	Moorpark - Fire Sta	1994	5.93	14	341.58	3.2
1752	Northwest China-03	Jiashi	1997	6.1	10	240.09	2.7
2624	Chi-Chi, Taiwan-03	TCU073	1999	6.2	19	473.65	12
2655	Chi-Chi, Taiwan-03	TCU122	1999	6.2	18	475.46	2.8
2714	Chi-Chi, Taiwan-04	CHY046	1999	6.2	38	442.15	5.4
3473	Chi-Chi, Taiwan-06	TCU078	1999	6.3	6	443.04	2.6
3495	Chi-Chi, Taiwan-06	TCU109	1999	6.3	37	535.13	16.6
3605	Lazio Abruzzo, Italy	Cassino-Sant' Elia	1984	5.8	20	436.79	4.1
3710	Whittier Narrows-02	LA - E Vernon Ave	1987	5.27	12	283.14	4.7
3748	Cape Mendocino	Ferndale Fire Station	1992	7.01	17	387.95	5.8
3751	Cape Mendocino	South Bay Union School	1992	7.01	33	459.04	7.8
3979	San Simeon, CA	Cambria - Hwy 1 Caltrans Bridge	2003	6.52	7	362.42	6.3
4068	Parkfield-02, CA	PARKFIELD - HOG CANYON	2004	6	1	363.69	4.2
4074	Parkfield-02, CA	PARKFIELD - VINEYARD CANYON	2004	6	4	340.45	4
4111	Parkfield-02, CA	Parkfield - Fault Zone 7	2004	6	1	297.46	5.7

4117	Parkfield-02, CA	Parkfield - Fault Zone 15	2004	6	1	307.59	4.1
4129	Parkfield-02, CA	PARKFIELD - TEMBLOR	2004	6	12	524.69	3.6
4130	Parkfield-02, CA	Parkfield - Vineyard Cany 1E	2004	6	2	381.27	2.6
4219	Niigata, Japan	NIGH01	2004	6.63	0	480.4	4.2
4348	Umbria Marche, Italy	Castelnuovo-Assisi	1997	6	17	293	8.4
4410	Umbria Marche (aftershock 17), Italy	Gubbio-Piana	1998	5.1	18	492	6.6
4440	Friuli (aftershock 13), Italy	Buia	1976	5.9	-999	310.68	4.6
4451	Montenegro, Yugo.	Bar-Skupstina Opstine	1979	7.1	0	462.23	8.3
4457	Montenegro, Yugo.	Ulcinj - Hotel Albatros	1979	7.1	2	410.35	7.7
4458	Montenegro, Yugo.	Ulcinj - Hotel Olimpic	1979	7.1	4	318.74	8.1
4716	Wenchuan, China	Deyangbaima	2008	7.9	30	418.21	36.9
4757	Wenchuan, China	Dayiyinping	2008	7.9	29	378.93	53.2
4781	Wenchuan, China	Jiangyouchonghua	2008	7.9	27	430.47	18.4
4847	Chuetsu-oki	Joetsu Kakizakiku Kakizaki	2007	6.8	9	383.43	5.9
4853	Chuetsu-oki	Joetsu City	2007	6.8	26	294.71	14.7
4860	Chuetsu-oki	Sanjo Shinbori	2007	6.8	16	278.12	10.5
4863	Chuetsu-oki	Nagaoka	2007	6.8	4	514.3	9.5
4866	Chuetsu-oki	Kawanishi Izumozaki	2007	6.8	0	338.32	6.5
4880	Chuetsu-oki	Hinodecho Yoshida Tsubame City	2007	6.8	20	261.55	12
4894	Chuetsu-oki	Kashiwazaki NPP, Unit 1: ground surface	2007	6.8	0	329	5.7
5774	Iwate	Nakashinden Town	2008	6.9	29	276.3	11
5779	Iwate	Sanbongi Osaki City	2008	6.9	36	539.87	13.7
5814	Iwate	Furukawa Osaki City	2008	6.9	31	248.19	12.3
5823	El Mayor-Cucapah	Chihuahua	2010	7.2	18	242.05	25.1
5827	El Mayor-Cucapah	MICHOACAN DE OCAMPO	2010	7.2	13	242.05	21.2
5975	El Mayor-Cucapah	Calexico Fire Station	2010	7.2	19	231.23	18.6
5990	El Mayor-Cucapah	El Centro Array #7	2010	7.2	27	210.51	16.5
6005	El Mayor-Cucapah	Holtville Post Office	2010	7.2	36	202.89	16.2
6013	El Mayor-Cucapah	El Centro - Meadows Union School	2010	7.2	28	276.25	15.3
6060	Big Bear-01	North Palm Springs Fire Sta #36	1992	6.46	41	367.84	8
6877	Joshua Tree, CA	Indio - Jackson Road	1992	6.1	25	292.12	4.2
6888	Darfield, New Zealand	Christchurch Cathedral College	2010	7	20	198	10.4
6890	Darfield, New Zealand	Christchurch Cashmere High School	2010	7	18	204	8.7
6897	Darfield, New Zealand	DSLC	2010	7	5	295.74	11.7
6911	Darfield, New Zealand	HORC	2010	7	7	326.01	6.7
6923	Darfield, New Zealand	Kaiapoi North School	2010	7	31	255	9.3
6930	Darfield, New Zealand	LRSC	2010	7	9	295.74	12.2
6953	Darfield, New Zealand	Pages Road Pumping Station	2010	7	25	206	11.2
6961	Darfield, New Zealand	RKAC	2010	7	13	295.74	12.7
6969	Darfield, New Zealand	Styx Mill Transfer Station	2010	7	21	247.5	12.2

8062	Christchurch, New Zealand	Canterbury Aero Club	2011	6.2	14	280.26	3.8
8063	Christchurch, New Zealand	Christchurch Botanical Gardens	2011	6.2	6	187	3.8
8066	Christchurch, New Zealand	Christchurch Hospital	2011	6.2	5	194	4.6
8067	Christchurch, New Zealand	Christchurch Cashmere High School	2011	6.2	4	204	3.1
8130	Christchurch, New Zealand	Shirley Library	2011	6.2	6	207	4.3
8133	Christchurch, New Zealand	SLRC	2011	6.2	32	249.28	5.9
8134	Christchurch, New Zealand	Styx Mill Transfer Station	2011	6.2	11	247.5	5.6
8161	El Mayor-Cucapah	El Centro Array #12	2010	7.2	10	196.88	13.2
8486	Parkfield-02, CA	Hog Canyon	2004	6	5	376	4.2
8606	El Mayor-Cucapah	Westside Elementary School	2010	7.2	10	242	9.3
8658	40204628	San Jose; CHP Field Office Junction Ave; 1-story; ground level	2007	5.45	13	266.31	7.4
8886	14383980	Olinda - Carbon Canyon Rd	2008	5.39	2	378.17	1.9

Table 3.5 List of record metadata, Oakland, V_{s30} = 760 m/sec.

RSN	EQ name	Station name	EQ year	EQ mag	JB dist (km)	Station V_{s30} (m/sec)	Sig duration (sec)
1	Helena, Montana-01	Carroll College	1935	6	2	593.35	1.2
57	San Fernando	Castaic - Old Ridge Route	1971	6.61	19	450.28	6.2
72	San Fernando	Lake Hughes #4	1971	6.61	19	600.06	3.9
139	Tabas, Iran	Dayhook	1978	7.35	0	471.53	6.7
143	Tabas, Iran	Tabas	1978	7.35	2	766.77	8
156	Norcia, Italy	Cascia	1979	5.9	1	585.04	2.5
219	Livermore-02	Del Valle Dam (Toe)	1980	5.42	10	403.37	3
230	Mammoth Lakes-01	Convict Creek	1980	6.06	1	382.12	6.9
233	Mammoth Lakes-02	Convict Creek	1980	5.69	3	382.12	2.6
236	Mammoth Lakes-03	Convict Creek	1980	5.91	3	382.12	2.4
241	Mammoth Lakes-04	Long Valley Dam (Downst)	1980	5.7	13	537.16	2.2
248	Mammoth Lakes-06	Convict Creek	1980	5.94	6	382.12	2.6
318	Westmorland	Superstition Mtn Camera	1981	5.9	19	362.38	3.7
321	Mammoth Lakes-11	Convict Creek	1983	5.31	7	382.12	2.8
408	Coalinga-05	Oil Fields Fire Station - FF	1983	5.77	6	474.15	3.6
409	Coalinga-05	Oil Fields Fire Station - Pad	1983	5.77	6	474.15	3.6
410	Coalinga-05	Palmer Ave	1983	5.77	8	458.09	1.8
413	Coalinga-05	Skunk Hollow	1983	5.77	7	480.32	3.2
414	Coalinga-05	Sulphur Baths (temp)	1983	5.77	10	617.43	2.6
419	Coalinga-07	Sulphur Baths (temp)	1983	5.21	10	617.43	0.7
514	N. Palm Springs	Cabazon	1986	6.06	7	376.91	2
548	Chalfant Valley-02	Benton	1986	6.19	22	370.94	5.7
589	Whittier Narrows-01	Alhambra - Fremont School	1987	5.99	2	549.75	2.1
594	Whittier Narrows-01	Baldwin Park - N Holly	1987	5.99	4	544.68	4.3
621	Whittier Narrows-01	Glendora - N Oakbank	1987	5.99	14	362.31	4.1
632	Whittier Narrows-01	LA - Cypress Ave	1987	5.99	9	366.71	3
675	Whittier Narrows-01	Pasadena - CIT Athenaeum	1987	5.99	4	415.13	3
691	Whittier Narrows-01	San Marino - SW Academy	1987	5.99	2	379.43	2.9
763	Loma Prieta	Gilroy - Gavilan Coll.	1989	6.93	9	729.65	1.5
801	Loma Prieta	San Jose - Santa Teresa Hills	1989	6.93	14	671.77	6.3
802	Loma Prieta	Saratoga - Aloha Ave	1989	6.93	8	380.89	3.9
952	Northridge-01	Beverly Hills - 12520 Mulhol	1994	6.69	12	545.66	4.9
954	Northridge-01	Big Tujunga, Angeles Nat F	1994	6.69	19	550.11	5.8
990	Northridge-01	LA - City Terrace	1994	6.69	35	365.22	6

1004	Northridge-01	LA - Sepulveda VA Hospital	1994	6.69	0	380.06	4.5
1006	Northridge-01	LA - UCLA Grounds	1994	6.69	14	398.42	5.5
1012	Northridge-01	LA 00	1994	6.69	10	706.22	5.1
1016	Northridge-01	La Crescenta - New York	1994	6.69	18	411.55	5.5
1070	Northridge-01	San Gabriel - E Grand Ave	1994	6.69	39	401.37	6.4
1078	Northridge-01	Santa Susana Ground	1994	6.69	2	715.12	4.1
1126	Kozani, Greece-01	Kozani	1995	6.4	14	649.67	2.9
1281	Chi-Chi, Taiwan	HWA032	1999	7.62	43	573.04	8.3
1302	Chi-Chi, Taiwan	HWA057	1999	7.62	46	671.52	12.4
1402	Chi-Chi, Taiwan	NST	1999	7.62	38	491.08	8.5
1487	Chi-Chi, Taiwan	TCU047	1999	7.62	35	520.37	9.7
1612	Duzce, Turkey	Lamont 1059	1999	7.14	4	551.3	10.3
1626	Sitka, Alaska	Sitka Observatory	1972	7.68	35	649.67	12.6
1631	Upland	Pomona - 4th & Locust FF	1990	5.63	7	384.44	2.5
1633	Manjil, Iran	Abbar	1990	7.37	13	723.95	9
1642	Sierra Madre	Cogswell Dam - Right Abutment	1991	5.61	18	680.37	1.4
1647	Sierra Madre	San Marino - SW Academy	1991	5.61	16	379.43	1.8
1836	Hector Mine	Twentynine Palms	1999	7.13	42	635.01	10.6
2390	Chi-Chi, Taiwan-02	TCU078	1999	5.9	14	443.04	4.1
2399	Chi-Chi, Taiwan-02	TCU089	1999	5.9	10	671.52	3.3
2619	Chi-Chi, Taiwan-03	TCU067	1999	6.2	28	433.63	5.2
2628	Chi-Chi, Taiwan-03	TCU078	1999	6.2	0	443.04	2.2
2629	Chi-Chi, Taiwan-03	TCU079	1999	6.2	0	363.99	3.1
2703	Chi-Chi, Taiwan-04	CHY028	1999	6.2	18	542.61	4.6
3180	Chi-Chi, Taiwan-05	TCU054	1999	6.2	45	460.69	9.1
3192	Chi-Chi, Taiwan-05	TCU082	1999	6.2	44	472.81	7.9
3471	Chi-Chi, Taiwan-06	TCU075	1999	6.3	24	573.02	9.9
3472	Chi-Chi, Taiwan-06	TCU076	1999	6.3	24	614.98	7.7
3473	Chi-Chi, Taiwan-06	TCU078	1999	6.3	6	443.04	2.6
3685	Whittier Narrows-02	Arcadia - Campus Dr	1987	5.27	8	367.53	0.7
3734	Whittier Narrows-02	San Gabriel - E Grand Ave	1987	5.27	1	401.37	3.1
3943	Tottori, Japan	SMN015	2000	6.61	9	616.55	3.5
3979	San Simeon, CA	Cambria - Hwy 1 Caltrans Bridge	2003	6.52	7	362.42	6.3
4031	San Simeon, CA	Templeton - 1-story Hospital	2003	6.52	5	410.66	3.1
4065	Parkfield-02, CA	PARKFIELD - EADES	2004	6	1	383.9	2.8
4068	Parkfield-02, CA	PARKFIELD - HOG CANYON	2004	6	1	363.69	4.2
4069	Parkfield-02, CA	PARKFIELD - JACK CANYON	2004	6	9	576.21	4.6
4096	Parkfield-02, CA	Bear Valley Ranch, Parkfield, CA, USA	2004	6	3	527.95	2.3
4130	Parkfield-02, CA	Parkfield - Vineyard Cany 1E	2004	6	2	381.27	2.6
4132	Parkfield-02, CA	Parkfield - Vineyard Cany 2E	2004	6	4	467.76	2.7

4135	Parkfield-02, CA	Parkfield - Vineyard Cany 4W	2004	6	7	386.19	3.1
4137	Parkfield-02, CA	Parkfield - Vineyard Cany 6W	2004	6	13	392.24	4.6
4193	Niigata, Japan	NGNH29	2004	6.63	45	464.92	8.4
4213	Niigata, Japan	NIG023	2004	6.63	25	654.76	1.9
4218	Niigata, Japan	NIG028	2004	6.63	0	430.71	3.5
4219	Niigata, Japan	NIGH01	2004	6.63	0	480.4	4.2
4228	Niigata, Japan	NIGH11	2004	6.63	6	375	3.1
4229	Niigata, Japan	NIGH12	2004	6.63	10	564.25	5
4312	Umbria-03, Italy	Gubbio	1984	5.6	15	922	2.8
4442	Friuli (aftershock 13), Italy	San Rocco	1976	5.9	-999	649.67	2
4472	L'Aquila, Italy	Celano	2009	6.3	18	612.78	3.2
4480	L'Aquila, Italy	L'Aquila - V. Aterno - Centro Valle	2009	6.3	0	475	4.4
4482	L'Aquila, Italy	L'Aquila - V. Aterno -F. Aterno	2009	6.3	0	552	4
4489	L'Aquila, Italy	Montereale	2009	6.3	16	421.13	7
4513	L'Aquila (aftershock 1), Italy	L'Aquila - Parking	2009	5.6	5	717	3.7
4518	L'Aquila (aftershock 1), Italy	Celano	2009	5.6	20	612.78	4.6
4550	L'Aquila (aftershock 2), Italy	L'Aquila - V. Aterno - M. Pettino	2009	5.4	9	585.04	2.3
4553	L'Aquila (aftershock 2), Italy	L'Aquila - V. Aterno -F. Aterno	2009	5.4	10	552	3.4
4787	Wenchuan, China	Jiangyoudizhentai	2008	7.9	23	475.59	27.2
4848	Chuetsu-oki	Joetsu Ogataku	2007	6.8	17	414.23	4.9
4858	Chuetsu-oki	Tokamachi Chitosecho	2007	6.8	25	640.14	4.3
4869	Chuetsu-oki	Kawaguchi	2007	6.8	24	640.14	8.7
4873	Chuetsu-oki	Kashiwazaki City Takayanagicho	2007	6.8	10	561.59	3.5
4882	Chuetsu-oki	Ojiya City	2007	6.8	16	430.16	7.1
5274	Chuetsu-oki	NIG028	2007	6.8	15	430.71	11.1
5275	Chuetsu-oki	NIGH01	2007	6.8	16	480.4	10.9
5478	Iwate	AKT023	2008	6.9	12	555.96	6.7
5494	Iwate	AKTH18	2008	6.9	47	431	8.1
5618	Iwate	IWT010	2008	6.9	16	825.83	8.5
5623	Iwate	IWT015	2008	6.9	17	567.45	6.2
5656	Iwate	IWTH24	2008	6.9	3	486.41	8
5657	Iwate	IWTH25	2008	6.9	0	506.44	6.9
5663	Iwate	MYG004	2008	6.9	20	479.37	7
5678	Iwate	MYGH02	2008	6.9	5	398.59	3.7
5760	Iwate	YMT017	2008	6.9	35	410.57	9.6
5773	Iwate	Miyagi Great Village	2008	6.9	41	531.25	8.9
5775	Iwate	Tamati Ono	2008	6.9	29	561.59	8
5776	Iwate	Kami, Miyagi Miyazaki City	2008	6.9	25	477.55	7.6
5799	Iwate	Misato, Akita City - Tsuchizaki	2008	6.9	40	552.38	6.5
5804	Iwate	Yamauchi Tsuchibuchi Yokote	2008	6.9	26	561.59	6.8

5809	Iwate	Minase Yuzawa	2008	6.9	17	655.45	7.6
5813	Iwate	Mizusawaku Interior O ganecho	2008	6.9	8	413.04	11.8
5830	El Mayor-Cucapah	RANCHO SAN LUIS	2010	7.2	44	523.99	21.4
6878	Joshua Tree, CA	North Palm Springs Fire Sta #36	1992	6.1	21	367.84	4.5
6928	Darfield, New Zealand	LPCC	2010	7	25	649.67	7.5
8110	Christchurch, New Zealand	MQZ	2011	6.2	14	649.67	3.1
8166	Duzce, Turkey	IRIGM 498	1999	7.14	4	425	999
8486	Parkfield-02, CA	Hog Canyon	2004	6	5	376	4.2
8648	40204628	San Jose; Laneview School Warmwood Ln; 1-story; ground level	2007	5.45	8	363.45	3
8674	40204628	Mt. Hamilton Road	2007	5.45	4	471	1.1
8742	40204628	Santa Clara Co. Comm. Cntr., Santa Clara, CA, US	2007	5.45	17	463.82	3.5
8861	14383980	Serrano	2008	5.39	12	440.67	2.6

3.2.2 Los Angeles Site

The list of 50 records for the Los Angeles site, V_{s30} = 270 m/sec, return period = 500 year, is shown in Table 3.6. The scale factor for each record is also given in the table. The suite shown contains more than 40 records per return periods. Extra records were selected so that further selection based on duration can be performed. Table 3.7 presents the data for V_{s30} = 760 m/sec.

The 5%-damped RotD50 component response spectra for the ground-motion suites for the Los Angeles site are shown in Figure 3.11 and Figure 3.12, for the two different soil classes. The suite average and target spectrum for each return period are also shown in the plot. These two quantities are shown a separate set of figures in Figure 3.13 and Figure 3.14. As the figures show, the suite average matches the target spectrum in the period range of interest for all cases.

A complete list of record-metadata for the records selected for the Los Angeles site is given in Table 3.8 and Table 3.9. In these tables, RSN stands for Records Sequence Number, which is a unique record number in the NGA-West2 database; JB stands for Joyner and Boore distance metric; Sig duration is the significant duration as duration between 5% and 75% of the Arias Intensity; and SF is the scale factor used for each recording.

Table 3.6 Ground-motion suite metadata and scale factors, Los Angeles, V_{s30} = 270 m/sec, return period = 500 years.

Site label	Site Vs_{30} (m/sec)	Return period (yr)	RSN	EQ name	Station name	EQ year	EQ mag	JB dist (km)	Station Vs_{30} (m/sec)	Sig duration (sec)	SF
07 LosAngeles	270	500	6	Imperial Valley-02	El Centro Array #9	1940	6.95	6	213.44	14.7	2.24
07 LosAngeles	270	500	15	Kern County	Taft Lincoln School	1952	7.36	38	385.43	10.4	3.45
07 LosAngeles	270	500	161	Imperial Valley-06	Brawley Airport	1979	6.53	9	208.71	4	2.83
07 LosAngeles	270	500	179	Imperial Valley-06	El Centro Array #4	1979	6.53	5	208.91	3	1.47
07 LosAngeles	270	500	185	Imperial Valley-06	Holtville Post Office	1979	6.53	5	202.89	4.7	2.25
07 LosAngeles	270	500	292	Irpinia, Italy-01	Sturno (STN)	1980	6.9	7	382	6.5	1.83
07 LosAngeles	270	500	313	Corinth, Greece	Corinth	1981	6.6	10	361.4	5.2	2.31
07 LosAngeles	270	500	568	San Salvador	Geotech Investig Center	1986	5.8	2	489.34	1.1	1
07 LosAngeles	270	500	721	Superstition Hills-02	El Centro Imp. Co. Cent	1987	6.54	18	192.05	8.1	1.93
07 LosAngeles	270	500	766	Loma Prieta	Gilroy Array #2	1989	6.93	10	270.84	2.3	1.55
07 LosAngeles	270	500	787	Loma Prieta	Palo Alto - SLAC Lab	1989	6.93	31	425.3	4.5	2.33
07 LosAngeles	270	500	806	Loma Prieta	Sunnyvale - Colton Ave.	1989	6.93	24	267.71	9.8	2.64
07 LosAngeles	270	500	850	Landers	Desert Hot Springs	1992	7.28	22	359	21.7	3.46
07 LosAngeles	270	500	949	Northridge-01	Arleta - Nordhoff Fire Sta	1994	6.69	3	297.71	6	1.81
07 LosAngeles	270	500	959	Northridge-01	Canoga Park - Topanga Can	1994	6.69	0	267.49	6.4	1.42
07 LosAngeles	270	500	963	Northridge-01	Castaic - Old Ridge Route	1994	6.69	20	450.28	5.1	1.12
07 LosAngeles	270	500	986	Northridge-01	LA - Brentwood VA Hospital	1994	6.69	13	416.58	6	3.07
07 LosAngeles	270	500	988	Northridge-01	LA - Century City CC North	1994	6.69	16	277.98	7.1	2.35
07 LosAngeles	270	500	1048	Northridge-01	Northridge - 17645 Saticoy St	1994	6.69	0	280.86	5.9	1.27
07 LosAngeles	270	500	1082	Northridge-01	Sun Valley - Roscoe Blvd	1994	6.69	6	320.93	5.8	1.63
07 LosAngeles	270	500	1085	Northridge-01	Sylmar - Converter Sta East	1994	6.69	0	370.52	3.6	0.89
07 LosAngeles	270	500	1086	Northridge-01	Sylmar - Olive View Med FF	1994	6.69	2	440.54	2.5	0.85
07 LosAngeles	270	500	1119	Kobe, Japan	Takarazuka	1995	6.9	0	312	2.1	0.85
07 LosAngeles	270	500	1193	Chi-Chi, Taiwan	CHY024	1999	7.62	10	427.73	12.6	2.3
07 LosAngeles	270	500	1208	Chi-Chi, Taiwan	CHY046	1999	7.62	24	442.15	19.1	3.15
07 LosAngeles	270	500	1489	Chi-Chi, Taiwan	TCU049	1999	7.62	4	487.27	17.1	2.1
07 LosAngeles	270	500	1491	Chi-Chi, Taiwan	TCU051	1999	7.62	8	350.06	18.7	2.66
07 LosAngeles	270	500	1493	Chi-Chi, Taiwan	TCU053	1999	7.62	6	454.55	17.9	2.92
07 LosAngeles	270	500	1495	Chi-Chi, Taiwan	TCU055	1999	7.62	6	359.13	19.1	2.34
07 LosAngeles	270	500	1499	Chi-Chi, Taiwan	TCU060	1999	7.62	9	375.42	19.1	3.75
07 LosAngeles	270	500	1508	Chi-Chi, Taiwan	TCU072	1999	7.62	0	468.14	14.7	1.14
07 LosAngeles	270	500	1528	Chi-Chi, Taiwan	TCU101	1999	7.62	2	389.41	16.7	2.32

Site label	Site *Vs*$_{30}$ (m/sec)	Return period (yr)	RSN	EQ name	Station name	EQ year	EQ mag	JB dist (km)	Station *Vs*$_{30}$ (m/sec)	Sig duration (sec)	SF
07 LosAngeles	270	500	1546	Chi-Chi, Taiwan	TCU122	1999	7.62	9	475.46	17.9	2.31
07 LosAngeles	270	500	2655	Chi-Chi, Taiwan-03	TCU122	1999	6.2	18	475.46	2.8	2.99
07 LosAngeles	270	500	3751	Cape Mendocino	South Bay Union School	1992	7.01	33	459.04	7.8	3.08
07 LosAngeles	270	500	4117	Parkfield-02, CA	Parkfield - Fault Zone 15	2004	6	1	307.59	4.1	2.68
07 LosAngeles	270	500	4457	Montenegro, Yugo.	Ulcinj - Hotel Albatros	1979	7.1	2	410.35	7.7	2.49
07 LosAngeles	270	500	4757	Wenchuan, China	Dayiyinping	2008	7.9	29	378.93	53.2	3.86
07 LosAngeles	270	500	4860	Chuetsu-oki	Sanjo Shinbori	2007	6.8	16	278.12	10.5	1.86
07 LosAngeles	270	500	4894	Chuetsu-oki	Kashiwazaki NPP, Unit 1: ground surface	2007	6.8	0	329	5.7	0.58
07 LosAngeles	270	500	5774	Iwate	Nakashinden Town	2008	6.9	29	276.3	11	2.92
07 LosAngeles	270	500	5823	El Mayor-Cucapah	Chihuahua	2010	7.2	18	242.05	25.1	2.27
07 LosAngeles	270	500	5975	El Mayor-Cucapah	Calexico Fire Station	2010	7.2	19	231.23	18.6	1.94
07 LosAngeles	270	500	6059	Big Bear-01	Morongo Valley Fire Station	1992	6.46	28	396.41	7.7	3.68
07 LosAngeles	270	500	6890	Darfield, New Zealand	Christchurch Cashmere High School	2010	7	18	204	8.7	2.18
07 LosAngeles	270	500	6911	Darfield, New Zealand	HORC	2010	7	7	326.01	6.7	1.14
07 LosAngeles	270	500	8063	Christchurch, New Zealand	Christchurch Botanical Gardens	2011	6.2	6	187	3.8	1.15
07 LosAngeles	270	500	8134	Christchurch, New Zealand	Styx Mill Transfer Station	2011	6.2	11	247.5	5.6	3.13
07 LosAngeles	270	500	8161	El Mayor-Cucapah	El Centro Array #12	2010	7.2	10	196.88	13.2	1.54
07 LosAngeles	270	500	8606	El Mayor-Cucapah	Westside Elementary School	2010	7.2	10	242	9.3	1.93

Table 3.7 Ground-motion suite metadata and scale factors, Los Angeles, V_{s30} = 760 m/sec, return period = 500 years.

Site label	Site V_{s30} (m/sec)	Return period (yr)	RSN	EQ name	Station name	EQ year	EQ mag	JB dist (km)	Station V_{s30} (m/sec)	Sig duration (sec)	SF
07 LosAngeles	760	500	1	Helena, Montana-01	Carroll College	1935	6	2	593.35	1.2	3.13
07 LosAngeles	760	500	72	San Fernando	Lake Hughes #4	1971	6.61	19	600.06	3.9	2.97
07 LosAngeles	760	500	156	Norcia, Italy	Cascia	1979	5.9	1	585.04	2.5	2.66
07 LosAngeles	760	500	230	Mammoth Lakes-01	Convict Creek	1980	6.06	1	382.12	6.9	1.04
07 LosAngeles	760	500	233	Mammoth Lakes-02	Convict Creek	1980	5.69	3	382.12	2.6	2.56
07 LosAngeles	760	500	236	Mammoth Lakes-03	Convict Creek	1980	5.91	3	382.12	2.4	2.05
07 LosAngeles	760	500	408	Coalinga-05	Oil Fields Fire Station - FF	1983	5.77	6	474.15	3.6	2.37
07 LosAngeles	760	500	409	Coalinga-05	Oil Fields Fire Station - Pad	1983	5.77	6	474.15	3.6	2.21
07 LosAngeles	760	500	410	Coalinga-05	Palmer Ave	1983	5.77	8	458.09	1.8	1.71
07 LosAngeles	760	500	589	Whittier Narrows-01	Alhambra - Fremont School	1987	5.99	2	549.75	2.1	1.42
07 LosAngeles	760	500	632	Whittier Narrows-01	LA - Cypress Ave	1987	5.99	9	366.71	3	3.27
07 LosAngeles	760	500	691	Whittier Narrows-01	San Marino - SW Academy	1987	5.99	2	379.43	2.9	2.62
07 LosAngeles	760	500	763	Loma Prieta	Gilroy - Gavilan Coll.	1989	6.93	9	729.65	1.5	1.29
07 LosAngeles	760	500	801	Loma Prieta	San Jose - Santa Teresa Hills	1989	6.93	14	671.77	6.3	1.51
07 LosAngeles	760	500	1006	Northridge-01	LA - UCLA Grounds	1994	6.69	14	398.42	5.5	1.29
07 LosAngeles	760	500	1070	Northridge-01	San Gabriel - E Grand Ave	1994	6.69	39	401.37	6.4	2.45
07 LosAngeles	760	500	1078	Northridge-01	Santa Susana Ground	1994	6.69	2	715.12	4.1	1.56
07 LosAngeles	760	500	1402	Chi-Chi, Taiwan	NST	1999	7.62	38	491.08	8.5	1.33
07 LosAngeles	760	500	1549	Chi-Chi, Taiwan	TCU129	1999	7.62	2	511.18	16.6	0.65
07 LosAngeles	760	500	1631	Upland	Pomona - 4th & Locust FF	1990	5.63	7	384.44	2.5	2.5
07 LosAngeles	760	500	1633	Manjil, Iran	Abbar	1990	7.37	13	723.95	9	0.77
07 LosAngeles	760	500	2619	Chi-Chi, Taiwan-03	TCU067	1999	6.2	28	433.63	5.2	2.75
07 LosAngeles	760	500	3472	Chi-Chi, Taiwan-06	TCU076	1999	6.3	24	614.98	7.7	3.45
07 LosAngeles	760	500	3979	San Simeon, CA	Cambria - Hwy 1 Caltrans Bridge	2003	6.52	7	362.42	6.3	2.55
07 LosAngeles	760	500	4031	San Simeon, CA	Templeton - 1-story Hospital	2003	6.52	5	410.66	3.1	0.99
07 LosAngeles	760	500	4069	Parkfield-02, CA	PARKFIELD - JACK CANYON	2004	6	9	576.21	4.6	3.33
07 LosAngeles	760	500	4096	Parkfield-02, CA	Bear Valley Ranch, Parkfield, CA, USA	2004	6	3	527.95	2.3	2.97
07 LosAngeles	760	500	4132	Parkfield-02, CA	Parkfield - Vineyard Cany 2E	2004	6	4	467.76	2.7	1.74
07 LosAngeles	760	500	4137	Parkfield-02, CA	Parkfield - Vineyard Cany 6W	2004	6	13	392.24	4.6	3.81
07 LosAngeles	760	500	4213	Niigata, Japan	NIG023	2004	6.63	25	654.76	1.9	1.36
07 LosAngeles	760	500	4218	Niigata, Japan	NIG028	2004	6.63	0	430.71	3.5	0.74
07 LosAngeles	760	500	4228	Niigata, Japan	NIGH11	2004	6.63	6	375	3.1	0.86
07 LosAngeles	760	500	4229	Niigata, Japan	NIGH12	2004	6.63	10	564.25	5	1.25

Site label	Site V_{s30} (m/sec)	Return period (yr)	RSN	EQ name	Station name	EQ year	EQ mag	JB dist (km)	Station V_{s30} (m/sec)	Sig duration (sec)	SF
07 LosAngeles	760	500	4442	Friuli (aftershock 13), Italy	San Rocco	1976	5.9	-999	649.67	2	2.48
07 LosAngeles	760	500	4480	L'Aquila, Italy	L'Aquila - V. Aterno - Centro Valle	2009	6.3	0	475	4.4	0.83
07 LosAngeles	760	500	4740	Wenchuan, China	Maoxiandiban	2008	7.9	2	638.39	21.5	1.29
07 LosAngeles	760	500	4742	Wenchuan, China	Maoxiannanxin	2008	7.9	1	429.97	25.9	1.13
07 LosAngeles	760	500	5274	Chuetsu-oki	NIG028	2007	6.8	15	430.71	11.1	3.04
07 LosAngeles	760	500	5478	Iwate	AKT023	2008	6.9	12	555.96	6.7	1.13
07 LosAngeles	760	500	5494	Iwate	AKTH18	2008	6.9	47	431	8.1	3.75
07 LosAngeles	760	500	5618	Iwate	IWT010	2008	6.9	16	825.83	8.5	1.47
07 LosAngeles	760	500	5623	Iwate	IWT015	2008	6.9	17	567.45	6.2	2.35
07 LosAngeles	760	500	5656	Iwate	IWTH24	2008	6.9	3	486.41	8	0.91
07 LosAngeles	760	500	5657	Iwate	IWTH25	2008	6.9	0	506.44	6.9	0.35
07 LosAngeles	760	500	5678	Iwate	MYGH02	2008	6.9	5	398.59	3.7	1.79
07 LosAngeles	760	500	5773	Iwate	Miyagi Great Village	2008	6.9	41	531.25	8.9	2.37
07 LosAngeles	760	500	5775	Iwate	Tamati Ono	2008	6.9	29	561.59	8	1.86
07 LosAngeles	760	500	5809	Iwate	Minase Yuzawa	2008	6.9	17	655.45	7.6	1.89
07 LosAngeles	760	500	6878	Joshua Tree, CA	North Palm Springs Fire Sta #36	1992	6.1	21	367.84	4.5	2.85
07 LosAngeles	760	500	6928	Darfield, New Zealand	LPCC	2010	7	25	649.67	7.5	1.68

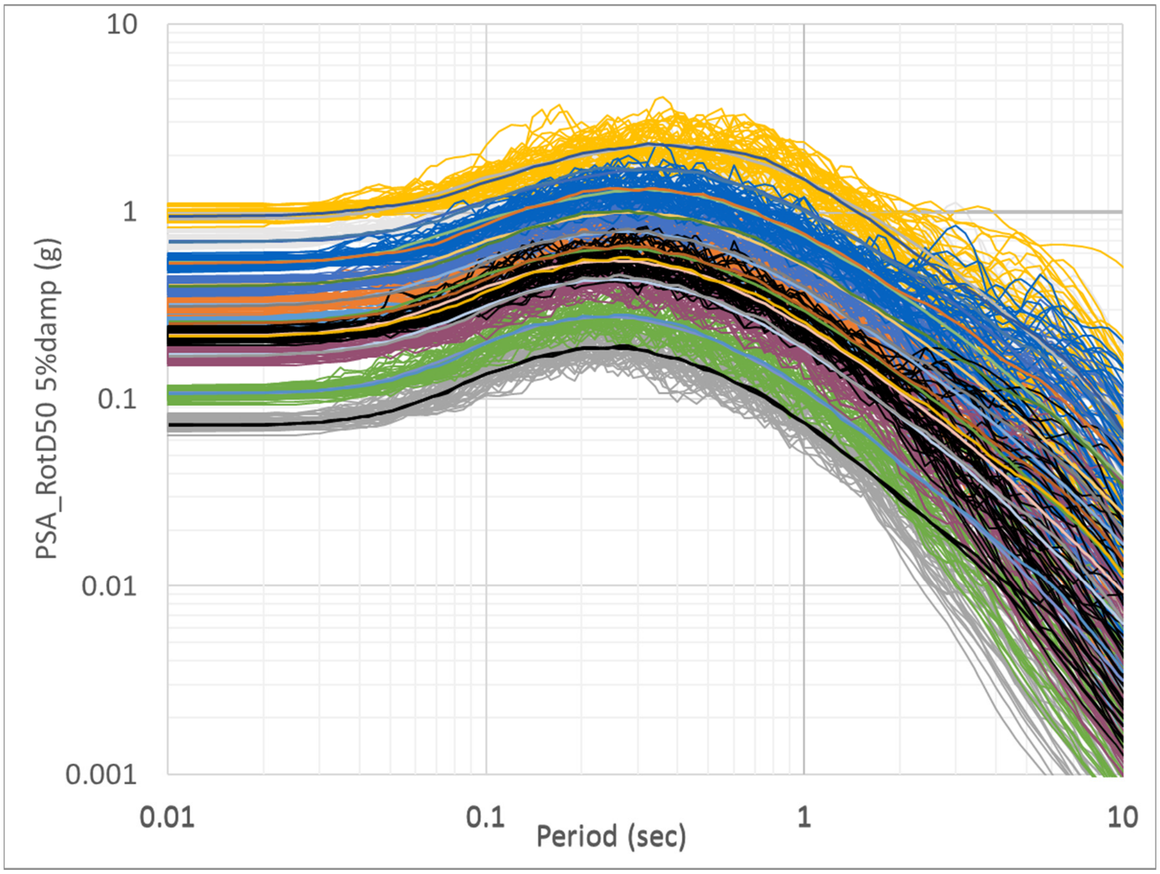

Figure 3.11 Ground-motion suites, Los Angeles, V_{s30} = 270 m/sec.

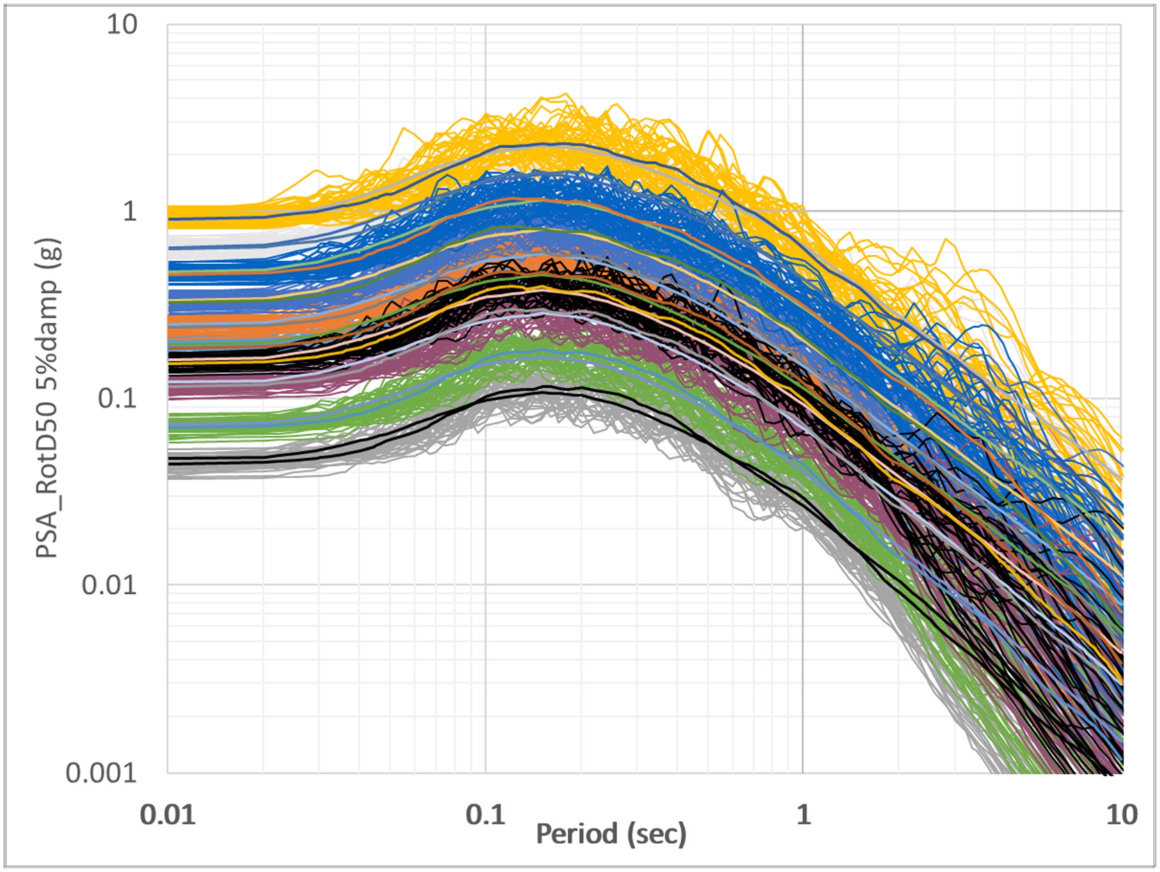

Figure 3.12 Ground-motion suites, Los Angeles, V_{s30} = 760 m/sec.

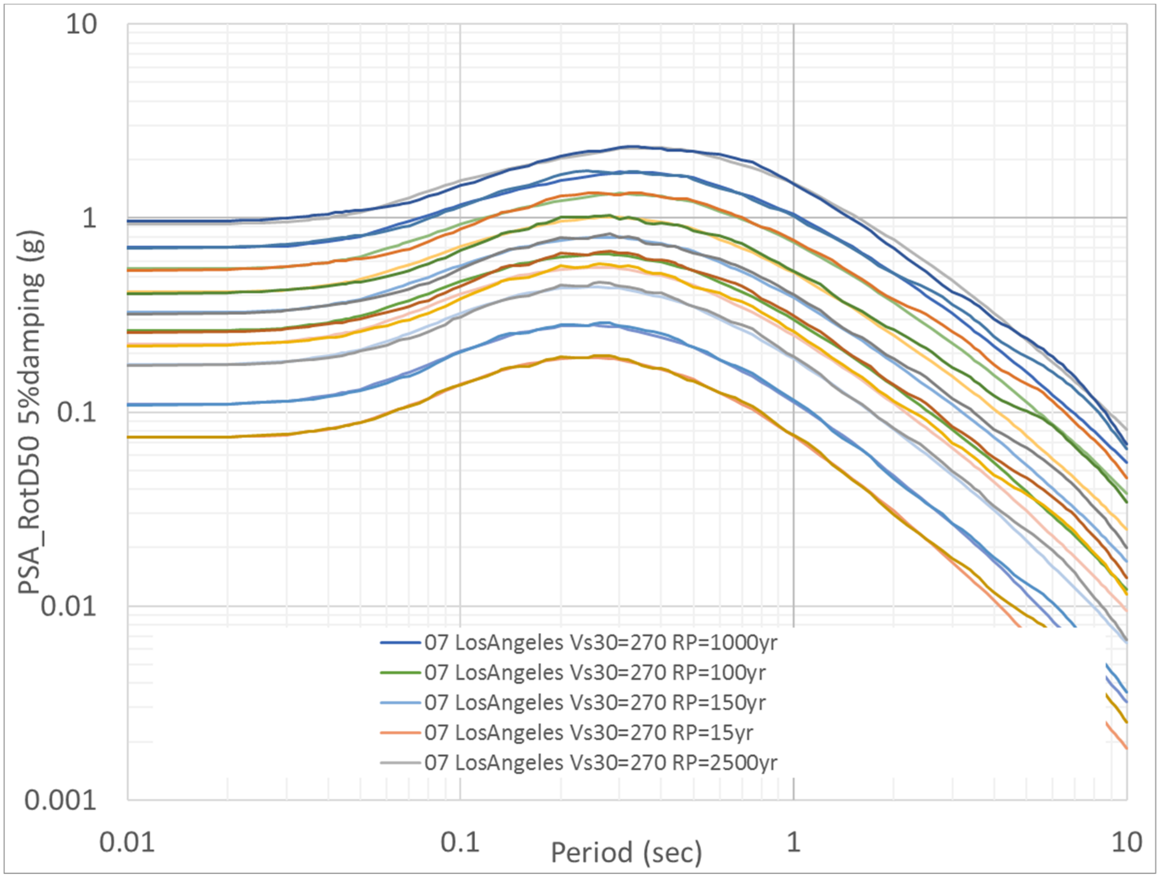

Figure 3.13 Suite average and target spectra for Los Angeles site, V_{s30} = 270 m/sec.

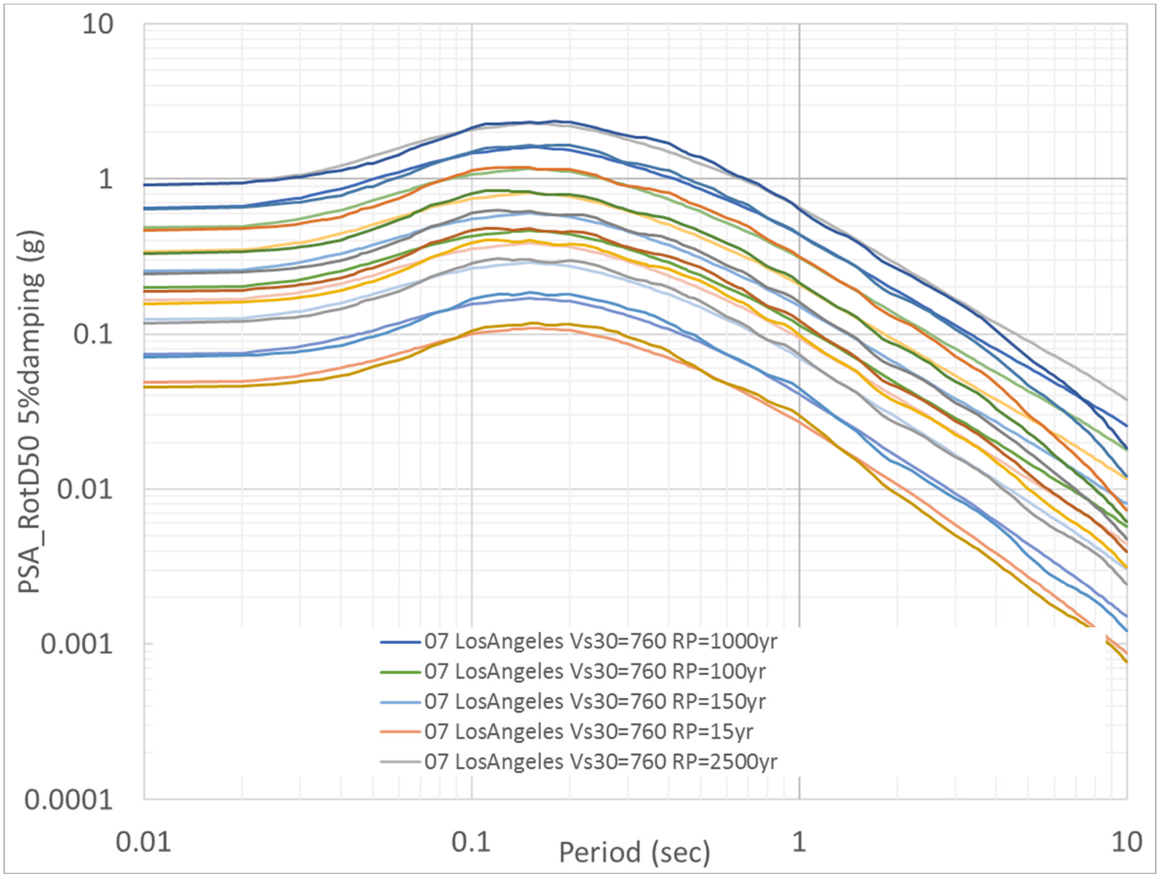

Figure 3.14 Suite average and target spectra for Los Angeles site, V_{s30} = 760 m/sec.

Table 3.8 List of record metadata, Los Angeles, V_{s30} = 270 m/sec.

RSN	EQ name	Station name	EQ year	EQ mag	JB dist (km)	Station Vs_{30} (m/sec)	Sig duration (sec)
6	Imperial Valley-02	El Centro Array #9	1940	6.95	6	213.44	14.7
15	Kern County	Taft Lincoln School	1952	7.36	38	385.43	10.4
21	Imperial Valley-05	El Centro Array #9	1955	5.4	14	213.44	8
57	San Fernando	Castaic - Old Ridge Route	1971	6.61	19	450.28	6.2
95	Managua, Nicaragua-01	Managua, ESSO	1972	6.24	4	288.77	4.6
96	Managua, Nicaragua-02	Managua, ESSO	1972	5.2	4	288.77	2.5
130	Friuli, Italy-02	Buia	1976	5.91	11	310.68	4.5
139	Tabas, Iran	Dayhook	1978	7.35	0	471.53	6.7
154	Coyote Lake	San Juan Bautista, 24 Polk St	1979	5.74	19	335.5	6.1
161	Imperial Valley-06	Brawley Airport	1979	6.53	9	208.71	4
162	Imperial Valley-06	Calexico Fire Station	1979	6.53	10	231.23	6.4
164	Imperial Valley-06	Cerro Prieto	1979	6.53	15	471.53	18.1
165	Imperial Valley-06	Chihuahua	1979	6.53	7	242.05	12.9
169	Imperial Valley-06	Delta	1979	6.53	22	242.05	23.4
175	Imperial Valley-06	El Centro Array #12	1979	6.53	18	196.88	9.7
179	Imperial Valley-06	El Centro Array #4	1979	6.53	5	208.91	3
180	Imperial Valley-06	El Centro Array #5	1979	6.53	2	205.63	3.7
184	Imperial Valley-06	El Centro Differential Array	1979	6.53	5	202.26	3.3
185	Imperial Valley-06	Holtville Post Office	1979	6.53	5	202.89	4.7
186	Imperial Valley-06	Niland Fire Station	1979	6.53	36	212	10.1
233	Mammoth Lakes-02	Convict Creek	1980	5.69	3	382.12	2.6
238	Mammoth Lakes-03	Long Valley Dam (L Abut)	1980	5.91	10	537.16	4.2
284	Irpinia, Italy-01	Auletta	1980	6.9	10	476.62	12.9
292	Irpinia, Italy-01	Sturno (STN)	1980	6.9	7	382	6.5
298	Irpinia, Italy-02	Bovino	1980	6.2	44	356.39	9.6
313	Corinth, Greece	Corinth	1981	6.6	10	361.4	5.2
316	Westmorland	Parachute Test Site	1981	5.9	17	348.69	5.9
320	Mammoth Lakes-10	Convict Creek	1983	5.34	6	382.12	2.2
457	Morgan Hill	Gilroy Array #3	1984	6.19	13	349.85	6.5
499	Hollister-04	Hollister Differential Array #3	1986	5.45	13	215.54	8.1
502	Mt. Lewis	Halls Valley	1986	5.6	12	281.61	1.8
549	Chalfant Valley-02	Bishop - LADWP South St	1986	6.19	14	303.47	3.3
564	Kalamata, Greece-01	Kalamata (bsmt)	1986	6.2	6	382.21	1.7

RSN	EQ name	Station name	EQ year	EQ mag	JB dist (km)	Station Vs_{30} (m/sec)	Sig duration (sec)
568	San Salvador	Geotech Investig Center	1986	5.8	2	489.34	1.1
634	Whittier Narrows-01	LA - Fletcher Dr	1987	5.99	11	329.06	2.8
674	Whittier Narrows-01	Pasadena - Brown Gym	1987	5.99	4	341.14	3.3
721	Superstition Hills-02	El Centro Imp. Co. Cent	1987	6.54	18	192.05	8.1
725	Superstition Hills-02	Poe Road (temp)	1987	6.54	11	316.64	10.5
728	Superstition Hills-02	Westmorland Fire Sta	1987	6.54	13	193.67	10.9
739	Loma Prieta	Anderson Dam (Downstream)	1989	6.93	20	488.77	5.2
761	Loma Prieta	Fremont - Emerson Court	1989	6.93	40	284.79	7.2
762	Loma Prieta	Fremont - Mission San Jose	1989	6.93	39	367.57	7.9
764	Loma Prieta	Gilroy - Historic Bldg.	1989	6.93	10	308.55	3.6
766	Loma Prieta	Gilroy Array #2	1989	6.93	10	270.84	2.3
768	Loma Prieta	Gilroy Array #4	1989	6.93	14	221.78	4.5
776	Loma Prieta	Hollister - South & Pine	1989	6.93	28	282.14	7
778	Loma Prieta	Hollister Differential Array	1989	6.93	25	215.54	3.7
787	Loma Prieta	Palo Alto - SLAC Lab	1989	6.93	31	425.3	4.5
803	Loma Prieta	Saratoga - W Valley Coll.	1989	6.93	8	347.9	4.1
806	Loma Prieta	Sunnyvale - Colton Ave.	1989	6.93	24	267.71	9.8
821	Erzican, Turkey	Erzincan	1992	6.69	0	352.05	2
850	Landers	Desert Hot Springs	1992	7.28	22	359	21.7
900	Landers	Yermo Fire Station	1992	7.28	24	353.63	8.8
949	Northridge-01	Arleta - Nordhoff Fire Sta	1994	6.69	3	297.71	6
953	Northridge-01	Beverly Hills - 14145 Mulhol	1994	6.69	9	355.81	5.4
959	Northridge-01	Canoga Park - Topanga Can	1994	6.69	0	267.49	6.4
960	Northridge-01	Canyon Country - W Lost Cany	1994	6.69	11	325.6	3.1
963	Northridge-01	Castaic - Old Ridge Route	1994	6.69	20	450.28	5.1
964	Northridge-01	Compton - Castlegate St	1994	6.69	43	266.9	11.4
983	Northridge-01	Jensen Filter Plant Generator Building	1994	6.69	0	525.79	3.9
986	Northridge-01	LA - Brentwood VA Hospital	1994	6.69	13	416.58	6
988	Northridge-01	LA - Century City CC North	1994	6.69	16	277.98	7.1
995	Northridge-01	LA - Hollywood Stor FF	1994	6.69	20	316.46	6.1
1000	Northridge-01	LA - Pico & Sentous	1994	6.69	28	304.68	8.4
1002	Northridge-01	LA - S. Vermont Ave	1994	6.69	28	301.93	9.6
1004	Northridge-01	LA - Sepulveda VA Hospital	1994	6.69	0	380.06	4.5
1005	Northridge-01	LA - Temple & Hope	1994	6.69	29	452.15	7
1008	Northridge-01	LA - W 15th St	1994	6.69	26	329.52	9.3
1034	Northridge-01	Malibu - Point Dume Sch	1994	6.69	27	349.54	7.8

RSN	EQ name	Station name	EQ year	EQ mag	JB dist (km)	Station Vs_{30} (m/sec)	Sig duration (sec)
1039	Northridge-01	Moorpark - Fire Sta	1994	6.69	17	341.58	7.5
1044	Northridge-01	Newhall - Fire Sta	1994	6.69	3	269.14	2.8
1048	Northridge-01	Northridge - 17645 Saticoy St	1994	6.69	0	280.86	5.9
1063	Northridge-01	Rinaldi Receiving Sta	1994	6.69	0	282.25	3.9
1082	Northridge-01	Sun Valley - Roscoe Blvd	1994	6.69	6	320.93	5.8
1085	Northridge-01	Sylmar - Converter Sta East	1994	6.69	0	370.52	3.6
1086	Northridge-01	Sylmar - Olive View Med FF	1994	6.69	2	440.54	2.5
1115	Kobe, Japan	Sakai	1995	6.9	28	256	11.6
1119	Kobe, Japan	Takarazuka	1995	6.9	0	312	2.1
1158	Kocaeli, Turkey	Duzce	1999	7.51	14	281.86	3.6
1176	Kocaeli, Turkey	Yarimca	1999	7.51	1	297	6.5
1182	Chi-Chi, Taiwan	CHY006	1999	7.62	10	438.19	5.1
1184	Chi-Chi, Taiwan	CHY010	1999	7.62	20	538.69	6.1
1190	Chi-Chi, Taiwan	CHY019	1999	7.62	50	497.53	24.5
1193	Chi-Chi, Taiwan	CHY024	1999	7.62	10	427.73	12.6
1203	Chi-Chi, Taiwan	CHY036	1999	7.62	16	233.14	10.4
1208	Chi-Chi, Taiwan	CHY046	1999	7.62	24	442.15	19.1
1244	Chi-Chi, Taiwan	CHY101	1999	7.62	10	258.89	11.8
1489	Chi-Chi, Taiwan	TCU049	1999	7.62	4	487.27	17.1
1491	Chi-Chi, Taiwan	TCU051	1999	7.62	8	350.06	18.7
1493	Chi-Chi, Taiwan	TCU053	1999	7.62	6	454.55	17.9
1495	Chi-Chi, Taiwan	TCU055	1999	7.62	6	359.13	19.1
1499	Chi-Chi, Taiwan	TCU060	1999	7.62	9	375.42	19.1
1504	Chi-Chi, Taiwan	TCU067	1999	7.62	1	433.63	9.1
1505	Chi-Chi, Taiwan	TCU068	1999	7.62	0	487.34	6.1
1508	Chi-Chi, Taiwan	TCU072	1999	7.62	0	468.14	14.7
1512	Chi-Chi, Taiwan	TCU078	1999	7.62	0	443.04	17.8
1513	Chi-Chi, Taiwan	TCU079	1999	7.62	0	363.99	19.2
1528	Chi-Chi, Taiwan	TCU101	1999	7.62	2	389.41	16.7
1545	Chi-Chi, Taiwan	TCU120	1999	7.62	7	459.34	20.7
1546	Chi-Chi, Taiwan	TCU122	1999	7.62	9	475.46	17.9
1605	Duzce, Turkey	Duzce	1999	7.14	0	281.86	7.1
1681	Northridge-04	Moorpark - Fire Sta	1994	5.93	14	341.58	3.2
1752	Northwest China-03	Jiashi	1997	6.1	10	240.09	2.7
2624	Chi-Chi, Taiwan-03	TCU073	1999	6.2	19	473.65	12
2655	Chi-Chi, Taiwan-03	TCU122	1999	6.2	18	475.46	2.8

RSN	EQ name	Station name	EQ year	EQ mag	JB dist (km)	Station Vs_{30} (m/sec)	Sig duration (sec)
2714	Chi-Chi, Taiwan-04	CHY046	1999	6.2	38	442.15	5.4
3275	Chi-Chi, Taiwan-06	CHY036	1999	6.3	45	233.14	8
3473	Chi-Chi, Taiwan-06	TCU078	1999	6.3	6	443.04	2.6
3495	Chi-Chi, Taiwan-06	TCU109	1999	6.3	37	535.13	16.6
3605	Lazio Abruzzo, Italy	Cassino-Sant' Elia	1984	5.8	20	436.79	4.1
3710	Whittier Narrows-02	LA - E Vernon Ave	1987	5.27	12	283.14	4.7
3751	Cape Mendocino	South Bay Union School	1992	7.01	33	459.04	7.8
3979	San Simeon, CA	Cambria - Hwy 1 Caltrans Bridge	2003	6.52	7	362.42	6.3
4068	Parkfield-02, CA	PARKFIELD - HOG CANYON	2004	6	1	363.69	4.2
4074	Parkfield-02, CA	PARKFIELD - VINEYARD CANYON	2004	6	4	340.45	4
4111	Parkfield-02, CA	Parkfield - Fault Zone 7	2004	6	1	297.46	5.7
4117	Parkfield-02, CA	Parkfield - Fault Zone 15	2004	6	1	307.59	4.1
4130	Parkfield-02, CA	Parkfield - Vineyard Cany 1E	2004	6	2	381.27	2.6
4219	Niigata, Japan	NIGH01	2004	6.63	0	480.4	4.2
4348	Umbria Marche, Italy	Castelnuovo-Assisi	1997	6	17	293	8.4
4410	Umbria Marche (aftershock 17), Italy	Gubbio-Piana	1998	5.1	18	492	6.6
4440	Friuli (aftershock 13), Italy	Buia	1976	5.9	-999	310.68	4.6
4457	Montenegro, Yugo.	Ulcinj - Hotel Albatros	1979	7.1	2	410.35	7.7
4716	Wenchuan, China	Deyangbaima	2008	7.9	30	418.21	36.9
4757	Wenchuan, China	Dayiyinping	2008	7.9	29	378.93	53.2
4781	Wenchuan, China	Jiangyouchonghua	2008	7.9	27	430.47	18.4
4798	Wenchuan, China	Anxiantashui	2008	7.9	0	376.1	27.3
4853	Chuetsu-oki	Joetsu City	2007	6.8	26	294.71	14.7
4860	Chuetsu-oki	Sanjo Shinbori	2007	6.8	16	278.12	10.5
4863	Chuetsu-oki	Nagaoka	2007	6.8	4	514.3	9.5
4866	Chuetsu-oki	Kawanishi Izumozaki	2007	6.8	0	338.32	6.5
4894	Chuetsu-oki	Kashiwazaki NPP, Unit 1: ground surface	2007	6.8	0	329	5.7
5774	Iwate	Nakashinden Town	2008	6.9	29	276.3	11
5779	Iwate	Sanbongi Osaki City	2008	6.9	36	539.87	13.7
5814	Iwate	Furukawa Osaki City	2008	6.9	31	248.19	12.3
5818	Iwate	Kurihara City	2008	6.9	13	512.26	6.4
5823	El Mayor-Cucapah	Chihuahua	2010	7.2	18	242.05	25.1
5827	El Mayor-Cucapah	MICHOACAN DE OCAMPO	2010	7.2	13	242.05	21.2
5975	El Mayor-Cucapah	Calexico Fire Station	2010	7.2	19	231.23	18.6
5988	El Mayor-Cucapah	Meloland, E Holton Rd.	2010	7.2	30	196	20.9
5990	El Mayor-Cucapah	El Centro Array #7	2010	7.2	27	210.51	16.5

RSN	EQ name	Station name	EQ year	EQ mag	JB dist (km)	Station Vs_{30} (m/sec)	Sig duration (sec)
6005	El Mayor-Cucapah	Holtville Post Office	2010	7.2	36	202.89	16.2
6013	El Mayor-Cucapah	El Centro - Meadows Union School	2010	7.2	28	276.25	15.3
6059	Big Bear-01	Morongo Valley Fire Station	1992	6.46	28	396.41	7.7
6060	Big Bear-01	North Palm Springs Fire Sta #36	1992	6.46	41	367.84	8
6877	Joshua Tree, CA	Indio - Jackson Road	1992	6.1	25	292.12	4.2
6890	Darfield, New Zealand	Christchurch Cashmere High School	2010	7	18	204	8.7
6897	Darfield, New Zealand	DSLC	2010	7	5	295.74	11.7
6911	Darfield, New Zealand	HORC	2010	7	7	326.01	6.7
6923	Darfield, New Zealand	Kaiapoi North School	2010	7	31	255	9.3
6953	Darfield, New Zealand	Pages Road Pumping Station	2010	7	25	206	11.2
6961	Darfield, New Zealand	RKAC	2010	7	13	295.74	12.7
6969	Darfield, New Zealand	Styx Mill Transfer Station	2010	7	21	247.5	12.2
8063	Christchurch, New Zealand	Christchurch Botanical Gardens	2011	6.2	6	187	3.8
8130	Christchurch, New Zealand	Shirley Library	2011	6.2	6	207	4.3
8133	Christchurch, New Zealand	SLRC	2011	6.2	32	249.28	5.9
8134	Christchurch, New Zealand	Styx Mill Transfer Station	2011	6.2	11	247.5	5.6
8161	El Mayor-Cucapah	El Centro Array #12	2010	7.2	10	196.88	13.2
8486	Parkfield-02, CA	Hog Canyon	2004	6	5	376	4.2
8606	El Mayor-Cucapah	Westside Elementary School	2010	7.2	10	242	9.3
8658	40204628	San Jose; CHP Field Office Junction Ave; 1-story; ground level	2007	5.45	13	266.31	7.4
8886	14383980	Olinda - Carbon Canyon Rd	2008	5.39	2	378.17	1.9

Table 3.9 List of record metadata, Los Angeles, V_{s30} = 760 m/sec.

RSN	EQ name	Station name	EQ year	EQ mag	JB dist (km)	Station Vs30 (m/sec)	Sig duration (sec)
1	Helena, Montana-01	Carroll College	1935	6	2	593.35	1.2
57	San Fernando	Castaic - Old Ridge Route	1971	6.61	19	450.28	6.2
72	San Fernando	Lake Hughes #4	1971	6.61	19	600.06	3.9
139	Tabas, Iran	Dayhook	1978	7.35	0	471.53	6.7
156	Norcia, Italy	Cascia	1979	5.9	1	585.04	2.5
219	Livermore-02	Del Valle Dam (Toe)	1980	5.42	10	403.37	3
230	Mammoth Lakes-01	Convict Creek	1980	6.06	1	382.12	6.9
233	Mammoth Lakes-02	Convict Creek	1980	5.69	3	382.12	2.6
236	Mammoth Lakes-03	Convict Creek	1980	5.91	3	382.12	2.4
237	Mammoth Lakes-03	Long Valley Dam (Downst)	1980	5.91	10	537.16	3.2
238	Mammoth Lakes-03	Long Valley Dam (L Abut)	1980	5.91	10	537.16	4.2
241	Mammoth Lakes-04	Long Valley Dam (Downst)	1980	5.7	13	537.16	2.2
248	Mammoth Lakes-06	Convict Creek	1980	5.94	6	382.12	2.6
318	Westmorland	Superstition Mtn Camera	1981	5.9	19	362.38	3.7
321	Mammoth Lakes-11	Convict Creek	1983	5.31	7	382.12	2.8
408	Coalinga-05	Oil Fields Fire Station - FF	1983	5.77	6	474.15	3.6
409	Coalinga-05	Oil Fields Fire Station - Pad	1983	5.77	6	474.15	3.6
410	Coalinga-05	Palmer Ave	1983	5.77	8	458.09	1.8
413	Coalinga-05	Skunk Hollow	1983	5.77	7	480.32	3.2
414	Coalinga-05	Sulphur Baths (temp)	1983	5.77	10	617.43	2.6
419	Coalinga-07	Sulphur Baths (temp)	1983	5.21	10	617.43	0.7
514	N. Palm Springs	Cabazon	1986	6.06	7	376.91	2
589	Whittier Narrows-01	Alhambra - Fremont School	1987	5.99	2	549.75	2.1
594	Whittier Narrows-01	Baldwin Park - N Holly	1987	5.99	4	544.68	4.3
621	Whittier Narrows-01	Glendora - N Oakbank	1987	5.99	14	362.31	4.1
632	Whittier Narrows-01	LA - Cypress Ave	1987	5.99	9	366.71	3
675	Whittier Narrows-01	Pasadena - CIT Athenaeum	1987	5.99	4	415.13	3
691	Whittier Narrows-01	San Marino - SW Academy	1987	5.99	2	379.43	2.9
763	Loma Prieta	Gilroy - Gavilan Coll.	1989	6.93	9	729.65	1.5
801	Loma Prieta	San Jose - Santa Teresa Hills	1989	6.93	14	671.77	6.3
811	Loma Prieta	WAHO	1989	6.93	11	388.33	7
825	Cape Mendocino	Cape Mendocino	1992	7.01	0	567.78	2.7
952	Northridge-01	Beverly Hills - 12520 Mulhol	1994	6.69	12	545.66	4.9
990	Northridge-01	LA - City Terrace	1994	6.69	35	365.22	6
1006	Northridge-01	LA - UCLA Grounds	1994	6.69	14	398.42	5.5
1070	Northridge-01	San Gabriel - E Grand Ave	1994	6.69	39	401.37	6.4
1078	Northridge-01	Santa Susana Ground	1994	6.69	2	715.12	4.1
1126	Kozani, Greece-01	Kozani	1995	6.4	14	649.67	2.9
1302	Chi-Chi, Taiwan	HWA057	1999	7.62	46	671.52	12.4

1402	Chi-Chi, Taiwan	NST	1999	7.62	38	491.08	8.5
1524	Chi-Chi, Taiwan	TCU095	1999	7.62	45	446.63	8.3
1549	Chi-Chi, Taiwan	TCU129	1999	7.62	2	511.18	16.6
1612	Duzce, Turkey	Lamont 1059	1999	7.14	4	551.3	10.3
1626	Sitka, Alaska	Sitka Observatory	1972	7.68	35	649.67	12.6
1631	Upland	Pomona - 4th & Locust FF	1990	5.63	7	384.44	2.5
1633	Manjil, Iran	Abbar	1990	7.37	13	723.95	9
1647	Sierra Madre	San Marino - SW Academy	1991	5.61	16	379.43	1.8
1836	Hector Mine	Twentynine Palms	1999	7.13	42	635.01	10.6
2390	Chi-Chi, Taiwan-02	TCU078	1999	5.9	14	443.04	4.1
2399	Chi-Chi, Taiwan-02	TCU089	1999	5.9	10	671.52	3.3
2619	Chi-Chi, Taiwan-03	TCU067	1999	6.2	28	433.63	5.2
2628	Chi-Chi, Taiwan-03	TCU078	1999	6.2	0	443.04	2.2
2629	Chi-Chi, Taiwan-03	TCU079	1999	6.2	0	363.99	3.1
2703	Chi-Chi, Taiwan-04	CHY028	1999	6.2	18	542.61	4.6
3180	Chi-Chi, Taiwan-05	TCU054	1999	6.2	45	460.69	9.1
3192	Chi-Chi, Taiwan-05	TCU082	1999	6.2	44	472.81	7.9
3471	Chi-Chi, Taiwan-06	TCU075	1999	6.3	24	573.02	9.9
3472	Chi-Chi, Taiwan-06	TCU076	1999	6.3	24	614.98	7.7
3473	Chi-Chi, Taiwan-06	TCU078	1999	6.3	6	443.04	2.6
3685	Whittier Narrows-02	Arcadia - Campus Dr	1987	5.27	8	367.53	0.7
3734	Whittier Narrows-02	San Gabriel - E Grand Ave	1987	5.27	1	401.37	3.1
3943	Tottori, Japan	SMN015	2000	6.61	9	616.55	3.5
3979	San Simeon, CA	Cambria - Hwy 1 Caltrans Bridge	2003	6.52	7	362.42	6.3
4031	San Simeon, CA	Templeton - 1-story Hospital	2003	6.52	5	410.66	3.1
4065	Parkfield-02, CA	PARKFIELD - EADES	2004	6	1	383.9	2.8
4068	Parkfield-02, CA	PARKFIELD - HOG CANYON	2004	6	1	363.69	4.2
4069	Parkfield-02, CA	PARKFIELD - JACK CANYON	2004	6	9	576.21	4.6
4096	Parkfield-02, CA	Bear Valley Ranch, Parkfield, CA, USA	2004	6	3	527.95	2.3
4130	Parkfield-02, CA	Parkfield - Vineyard Cany 1E	2004	6	2	381.27	2.6
4132	Parkfield-02, CA	Parkfield - Vineyard Cany 2E	2004	6	4	467.76	2.7
4135	Parkfield-02, CA	Parkfield - Vineyard Cany 4W	2004	6	7	386.19	3.1
4137	Parkfield-02, CA	Parkfield - Vineyard Cany 6W	2004	6	13	392.24	4.6
4193	Niigata, Japan	NGNH29	2004	6.63	45	464.92	8.4
4213	Niigata, Japan	NIG023	2004	6.63	25	654.76	1.9
4218	Niigata, Japan	NIG028	2004	6.63	0	430.71	3.5
4228	Niigata, Japan	NIGH11	2004	6.63	6	375	3.1
4229	Niigata, Japan	NIGH12	2004	6.63	10	564.25	5
4312	Umbria-03, Italy	Gubbio	1984	5.6	15	922	2.8
4442	Friuli (aftershock 13), Italy	San Rocco	1976	5.9	-999	649.67	2
4472	L'Aquila, Italy	Celano	2009	6.3	18	612.78	3.2
4480	L'Aquila, Italy	L'Aquila - V. Aterno - Centro Valle	2009	6.3	0	475	4.4
4482	L'Aquila, Italy	L'Aquila - V. Aterno -F. Aterno	2009	6.3	0	552	4
4489	L'Aquila, Italy	Montereale	2009	6.3	16	421.13	7
4513	L'Aquila (aftershock 1), Italy	L'Aquila - Parking	2009	5.6	5	717	3.7
4518	L'Aquila (aftershock 1), Italy	Celano	2009	5.6	20	612.78	4.6

4550	L'Aquila (aftershock 2), Italy	L'Aquila - V. Aterno - M. Pettino	2009	5.4	9	585.04	2.3
4553	L'Aquila (aftershock 2), Italy	L'Aquila - V. Aterno -F. Aterno	2009	5.4	10	552	3.4
4740	Wenchuan, China	Maoxiandiban	2008	7.9	2	638.39	21.5
4742	Wenchuan, China	Maoxiannanxin	2008	7.9	1	429.97	25.9
4787	Wenchuan, China	Jiangyoudizhentai	2008	7.9	23	475.59	27.2
4848	Chuetsu-oki	Joetsu Ogataku	2007	6.8	17	414.23	4.9
4858	Chuetsu-oki	Tokamachi Chitosecho	2007	6.8	25	640.14	4.3
4869	Chuetsu-oki	Kawaguchi	2007	6.8	24	640.14	8.7
4873	Chuetsu-oki	Kashiwazaki City Takayanagicho	2007	6.8	10	561.59	3.5
4882	Chuetsu-oki	Ojiya City	2007	6.8	16	430.16	7.1
5274	Chuetsu-oki	NIG028	2007	6.8	15	430.71	11.1
5478	Iwate	AKT023	2008	6.9	12	555.96	6.7
5494	Iwate	AKTH18	2008	6.9	47	431	8.1
5618	Iwate	IWT010	2008	6.9	16	825.83	8.5
5623	Iwate	IWT015	2008	6.9	17	567.45	6.2
5656	Iwate	IWTH24	2008	6.9	3	486.41	8
5657	Iwate	IWTH25	2008	6.9	0	506.44	6.9
5663	Iwate	MYG004	2008	6.9	20	479.37	7
5678	Iwate	MYGH02	2008	6.9	5	398.59	3.7
5760	Iwate	YMT017	2008	6.9	35	410.57	9.6
5773	Iwate	Miyagi Great Village	2008	6.9	41	531.25	8.9
5775	Iwate	Tamati Ono	2008	6.9	29	561.59	8
5799	Iwate	Misato, Akita City - Tsuchizaki	2008	6.9	40	552.38	6.5
5804	Iwate	Yamauchi Tsuchibuchi Yokote	2008	6.9	26	561.59	6.8
5809	Iwate	Minase Yuzawa	2008	6.9	17	655.45	7.6
5813	Iwate	Mizusawaku Interior O ganecho	2008	6.9	8	413.04	11.8
5830	El Mayor-Cucapah	RANCHO SAN LUIS	2010	7.2	44	523.99	21.4
6878	Joshua Tree, CA	North Palm Springs Fire Sta #36	1992	6.1	21	367.84	4.5
6928	Darfield, New Zealand	LPCC	2010	7	25	649.67	7.5
8110	Christchurch, New Zealand	MQZ	2011	6.2	14	649.67	3.1
8166	Duzce, Turkey	IRIGM 498	1999	7.14	4	425	999
8486	Parkfield-02, CA	Hog Canyon	2004	6	5	376	4.2
8630	40204628	Mt. Pleasant High School	2007	5.45	8	377	3.6
8648	40204628	San Jose; Laneview School Warmwood Ln; 1-story; ground level	2007	5.45	8	363.45	3
8709	40204628	Lick Observatory, Mt. Hamiliton, CA, USA	2007	5.45	13	710.29	2.6
8742	40204628	Santa Clara Co. Comm. Cntr., Santa Clara, CA, US	2007	5.45	17	463.82	3.5
8861	14383980	Serrano	2008	5.39	12	440.67	2.6

3.3 SIGNIFICANT DURATION

Significant duration was not considered in the ground-motion selection because a new set of ground motions was selected.

3.4 OVERVIEW OF PULSE-LIKE GROUND MOTIONS WITHIN GROUND-MOTION SETS

3.4.1 Summary of Investigation

The main goal of this report section is to investigate the inclusion of pulse-like ground motions within the PEER–CEA WG3 ground-motion sets. Pulse-like ground motions can be defined as those containing a double-sided velocity pulse within the recorded time series of a given earthquake recording. The presence of pulse motions is first documented for all record sets within the PEER–CEA WG3 ground-motion sets for soils with average shear-wave velocity (V_{S30}) of 270 m/sec. The characteristics of pulse motions within select ground-motion sets are then compared to relationships found within the literature on the topic of pulse-like ground motions. The metric used for evaluating the pulse-like ground motions is the pulse fraction (i.e., the fraction of pulse records out of the total number of ground motions for a given intensity).

The results of the study show that the WG3 ground-motion sets have an increasing number of pulse records with increasing seismic intensity or return period. Selected sites show reasonable agreement in terms of the fraction of pulse records when comparing to relationships published in the literature. Sites with high seismicity and known to be close to significant faults have a larger number of pulse records when compared to sites with low to moderate seismicity. The study illustrates that the ground-motion selection criteria used by WG3 include reasonable proportions of pulse-like ground motions despite not considering pulse-effects explicitly within the ground-motion selection criteria.

3.4.2 Fraction of Pulse-like Records for All Sites

The ten ground-motion sets for sites with V_{S30} = 270 m/sec within the WG3 ground-motion set were first monitored for the presence of pulse motions. The WG3 metadata for each ground-motion set includes the pulse period of each ground-motion record where a default value of "-999" is placed for ground motions without an identifiable pulse. The total number of pulse motions was obtained and then divided by the total number of ground motions for a given site and return period to obtain the pulse fraction (e.g., a pulse fraction of 0.25 means that 25% of the records contain an observable pulse). Pulse identification and characterization is computed using the work of Shahi and Baker [Baker 2007; Shahi and Baker 2011; Shahi and Baker 2013; and Shahi and Baker 2014] that uses a wavelet transform analysis and subsequent classification algorithm. The pulse fractions for all sites are shown in Table 3.10. The table shows that the fraction of pulse motions increases with increasing return period (e.g., intensity). Notably, ground motion suites range from 48 to 52 ground motions per return period, yet they have 50 ground motions on average.

To better illustrate some site-specific trends with respect to pulse-like ground motions, four exemplary sites will be used for discussion, namely: Sacramento, Bakersfield, San Francisco, and

San Bernardino. The sites of Sacramento and Bakersfield are selected to represent low and low-to-moderate seismicity sites, respectively. The San Francisco site is selected to represent a high seismicity site, while San Bernardino is selected to represent a very high seismicity site that is also a known near-fault site. The pulse fractions for the selected sites are compared with the average pulse fraction for all WG3 sites with V_{s30} = 270 m/sec in Figure 3.15.

Table 3.10 Pulse fraction of ground motion suites for all V_{s30} = 270 m/sec sites in the UHS set.

Return period (yr)	OAK-270**	SAC-270	SF-270	SJ-270	BF-270	LB-270	LA-270	NR-270	SB-270	SD-270
15	0.06	0*	0.08	0.04	0	0.06	0.06	0.04	0.05	0.02
25	0.12	0	0.08	0.14	0.04	0.10	0.08	0.08	0.11	0.12
50	0.20	0	0.18	0.21	0.04	0.16	0.14	0.14	0.18	0.18
75	0.24	0.02	0.19	0.24	0.06	0.20	0.20	0.20	0.27	0.18
100	0.24	0.02	0.26	0.28	0.08	0.22	0.20	0.22	0.31	0.20
150	0.31	0.02	0.31	0.31	0.08	0.22	0.24	0.22	0.37	0.24
250	0.35	0.02	0.31	0.33	0.08	0.27	0.29	0.30	0.43	0.25
500	0.35	0.02	0.41	0.41	0.14	0.33	0.35	0.34	0.49	0.29
1000	0.35	0.02	0.42	0.35	0.19	0.39	0.43	0.37	0.48	0.33
2500	0.35	0.02	0.35	0.38	0.27	0.38	0.38	0.38	0.54	0.39

* All pulse motions are identified according to NGA-West2 flatfile list, values of "0" indicate that no pulse motions are included for the given classification list, site and return period. ** OAK = Oakland, SAC = Sacramento, SF = San Francisco, SJ = San Jose, BF = Bakersfield, LB = Long Beach, LA = Los Angeles, NR = Northridge, SB = San Bernardino, and SD = San Diego.

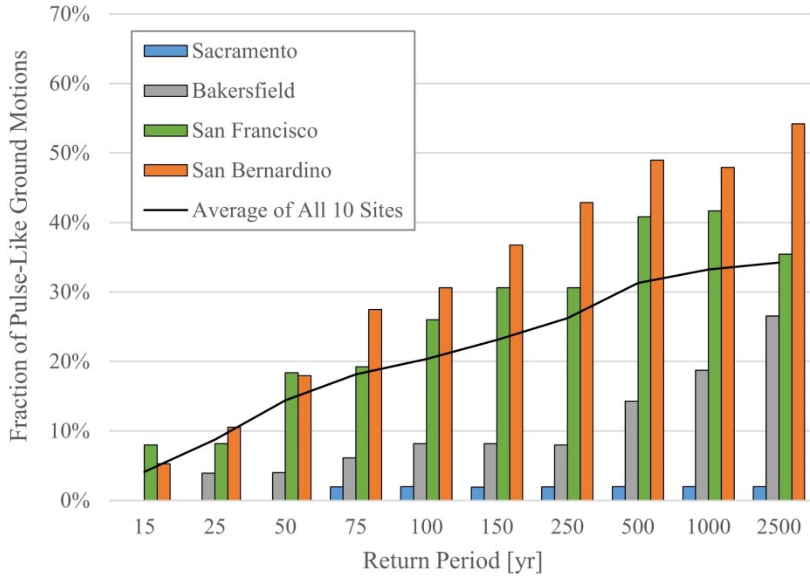

Figure 3.15 Pulse fraction of selected V_{S30} = 270 m/sec sites in the UHS set (NOTE: the solid black line illustrates the average pulse fraction of all sites for a given return period).

3.4.3 Comparing Pulse Fractions with Hayden et al. [2014].

The relationship proposed by Hayden et al. [2014] is used as a benchmark to assess the appropriateness of the pulse fractions for the four exemplary sites, where the appropriate pulse fraction can be estimated as a function of the closest site to source distance (R) and the epsilon of the design ground-motion parameter (ε). These two parameters are used to estimate the appropriate pulse fraction using Equation (3.1)

$$\text{pulse fraction} = \frac{1}{1+\exp\left[-3.87+1.04\left(R^{0.5}\right)+15.99\left(\varepsilon+3\right)^{-2}\right]} \tag{3.1}$$

The parameter epsilon (ε) is a standard normal variable (i.e., zero mean and variance of 1.0) representing the number of standard deviations above (+ve) or below (-ve) the mean value of a ground motion prediction equation of an intensity measure of interest. Hayden et al. [2014] suggest that the epsilon in peak ground velocity (PGV) be used, yet they acknowledge that PGV is not typically available in public seismic hazard databases (e.g., USGS). In light of this, they also suggest that the epsilon of 5% damped spectral acceleration (Sa) at a period of 1.0 sec can be used as an alternative for target magnitudes less than or equal to 7.0 based on the work of Bradley [2012]. A similar assumption is made for the current example. The values of R for Equation (3.1) are taken as the mean distance (D_{bar}) at a period of 0.2 sec from hazard deaggregation for each site and return period. The hazard deaggregation data for each site is presented in Table 3.11.

Table 3.11 Hazard deaggregation data used to estimate pulse characteristics for the four exemplary sites.

Return period (yr)	15	25	50	75	100	150	250	500	1000	2500
Sacramento, V_{S30} = 270 m/sec (low seismicity)										
D_{bar} [1]	90.7	81.7	71.9	67.2	63.9	58.9	53.0	45.6	38.8	30.6
M_{bar} [2]	6.4	6.5	6.5	6.5	6.5	6.5	6.5	6.5	6.4	6.3
ε_{bar} [3]	0.14	0.36	0.61	0.74	0.84	0.96	1.11	1.29	1.44	1.59
Bakersfield, V_{S30} = 270 m/sec (low-to-moderate seismicity)										
D_{bar}	62.8	52.0	42.2	37.6	34.8	31.8	28.8	24.8	21.6	18.3
M_{bar}	6.1	6.2	6.3	6.3	6.4	6.4	6.4	6.4	6.3	6.3
ε_{bar}	0.11	0.23	0.35	0.43	0.50	0.60	0.76	0.96	1.14	1.38
San Francisco, V_{S30} = 270 m/sec (high seismicity)										
D_{bar}	38.6	31.4	24.6	22.3	20.9	19.2	17.7	16.6	15.4	14.4
M_{bar}	6.3	6.4	6.6	6.7	6.7	6.8	6.9	6.9	7.0	7.0
ε_{bar}	-0.35	-0.20	0.03	0.17	0.28	0.45	0.67	0.97	1.27	1.62
San Bernardino, V_{S30} = 270 m/sec (very high seismicity)										
D_{bar}	28.0	21.2	15.8	13.5	12.4	11.0	10.2	8.9	8.2	7.6
M_{bar}	6.1	6.2	6.4	6.4	6.5	6.6	6.7	6.8	6.8	6.9
ε_{bar}	-0.23	-0.13	-0.03	0.04	0.12	0.25	0.46	0.77	1.09	1.46

[1] Mean source-to-site distance (km) for 5% damped spectral acceleration at T = 0.2 sec from hazard deaggregation.
[2] Mean magnitude for 5% damped spectral acceleration at T = 0.2 sec from hazard deaggregation.
[3] Mean epsilon for 5% damped spectral acceleration at T = 1.0 sec from hazard deaggregation (proxy to ε(PGV) [Bradley 2012]).

The pulse fractions within the UHS ground-motion sets are compared with those predicted by Hayden et al. [2014] in Figure 3.16. The figure shows that the low seismicity site of Sacramento has very few pulse records and agrees with the estimated values. Similar results are shown for the Bakersfield site in Figure 3.16(b). The high seismicity site of San Francisco [Figure 3.15(c)] shows that the UHS ground-motion sets have a larger pulse fraction than the estimate using Equation (3.1) at moderate return periods. This is most likely due to Equation (3.1) estimating pulse fraction as a function of source-to-site distance (R) where the WG3 record selection process did not consider this as a criterion for including or eliminating pulse-like ground motions. Most importantly, the very high seismicity and known near-source site of San Bernardino [Figure 3.15(d)] shows a very good agreement in terms of the fraction of pulse motions at all return periods.

In general, it can be seen from Figure 3.15 that, by including pulse ground motions, the number of pulse records included during the record selection process using non-pulse related selection criteria is in reasonable agreement with the relationship proposed by Hayden et al. [2014] in terms of pulse fraction.

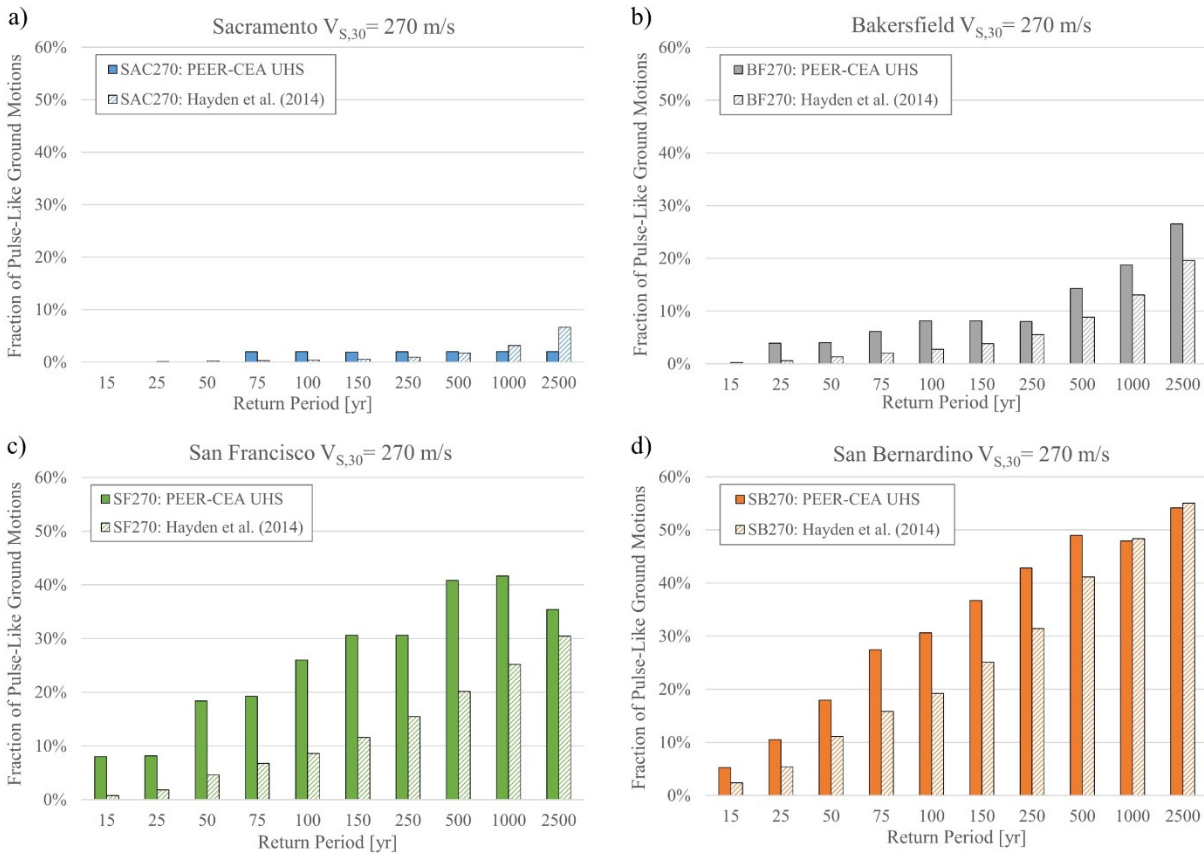

Figure 3.16 Pulse fraction of selected V_{S30} = 270 m/sec sites in the UHS set (solid bars) compared with relationship proposed by Hayden et al. [2014] (dashed bars): (a) Sacramento; (b) Bakersfield; (c) San Francisco; and (d) San Bernardino.

3.5 GROUND-MOTION SUITES USING ALTERNATIVE OPTIONS FOR TARGET SPECTRA AND VARIABILITY

For completeness, additional suites of ground motions were investigated, with different models for the target mean and the target dispersion. Two options for target mean were investigated: (1) the Uniform-Hazard Spectrum (UHS) (as shown in this chapter); and (2): the Conditional-Mean Spectrum (CMS). Three models of variability were investigated: Model A to keep the natural variability of the ground-motion suite selected on the basis of spectral shape; Model B to define a period-independent constant variability; and Model C to use the variability associated with the CMS – Defined by the Conditional Spectra (CS) described below. Because the ground motions are typically selected based on their spectral shape, the first method (Model A) of keeping the suite's natural variability leads to relatively low dispersion. This model can be applied to both target-mean models, the UHS or CMS. This variability model, along with the UHS target spectrum, was used in the selection and scaling of the ground-motion suites that were presented in this chapter. Model, B forces a constant variability over the user-defined period range. The amount of variability, can also be defined by the user. This model can be applied to both target-mean models, the UHS or CMS, as well. Model C, which is applicable only to the case of using the CMS as the target mean, uses the dispersion model associated with the CS developed by Baker and Jayaram [2008].

A comparison of the different target mean spectra is shown in Figure 3.17, for the UHS and CMS, respectively. Each plot shows the target UHS for both cases—in red—and the resulting average of each ground-motion suite at each return period. The plot of the UHS suites shows that the average of each suite closely matches the UHS for all periods of interest. The plot of the CMS shows that the average of the ground-motion suites is conditioned at one period and follows the expected shape of a CMS—exceeding the target UHS at low return periods and structural period, and is below the UHS at the higher return periods.

Figure 3.18 shows a sample ground-motion suite for all possible combinations of target mean —UHS or CMS—and variability—minimum, constant, or conditioned. For both bases, UHS and CMS, the minimum sigma case corresponds to the ground-motion suites selected on the basis of spectral shape. The coefficient of variability, COV, for each of these cases is shown in Figure 3.19. The value of 0.6 for the constant COV was selected as a representative value for demonstration purposes; a lower value is recommended. The complete set of ground-motion suites for a site and site class is shown in Figure 3.20. This figure shows the range of ground motions to be used in the ground-motion simulations provided by each method.

Based on the results of this study, WG5 selected the model which uses CS as the target for the mean and dispersion. This work is presented in Chapter 4.

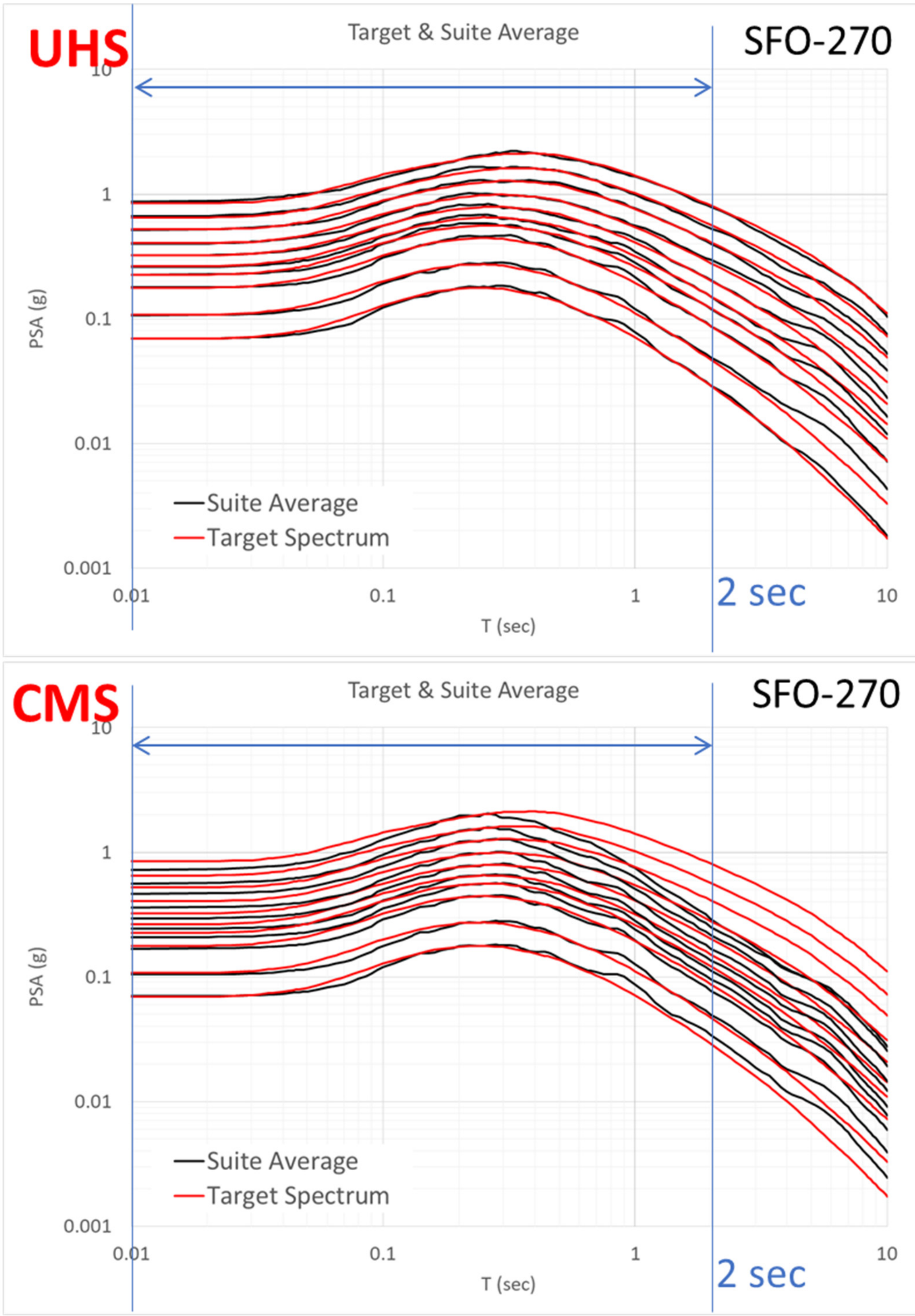

Figure 3.17 **Comparison of target suite average. The suite average in the second figure follows the CMS conditioned at *T** and corresponding target UHS. The UHS is shown as the target for both figures to show the difference between the resulting suite average for the two cases.**

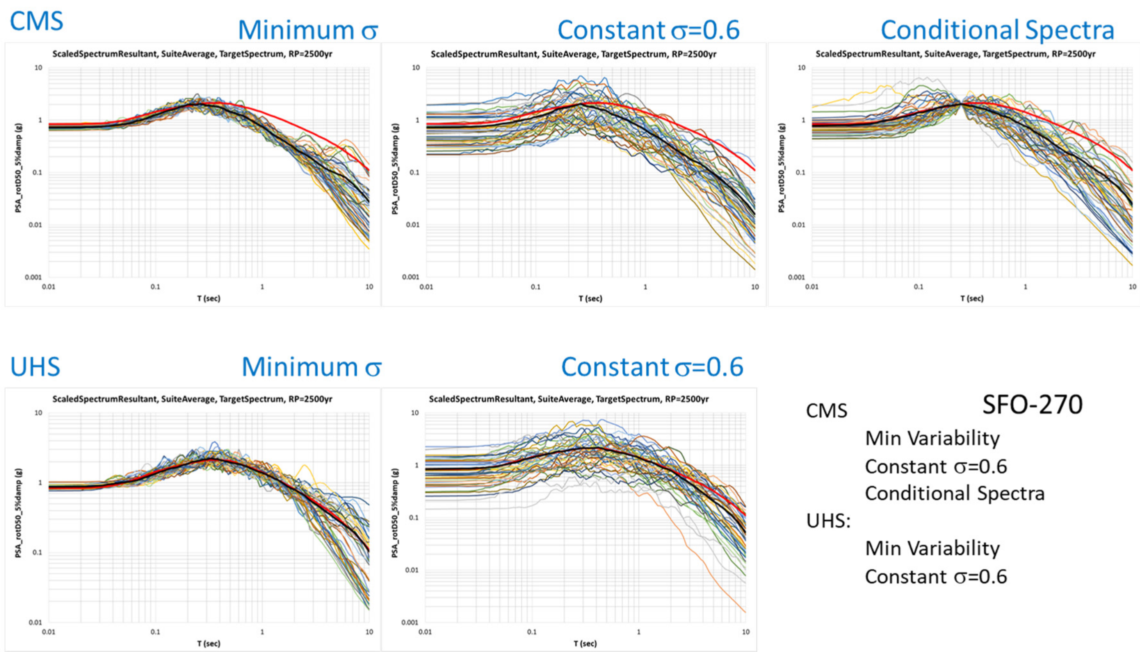

Figure 3.18 Sample ground-motion suite for different mean and variability models.

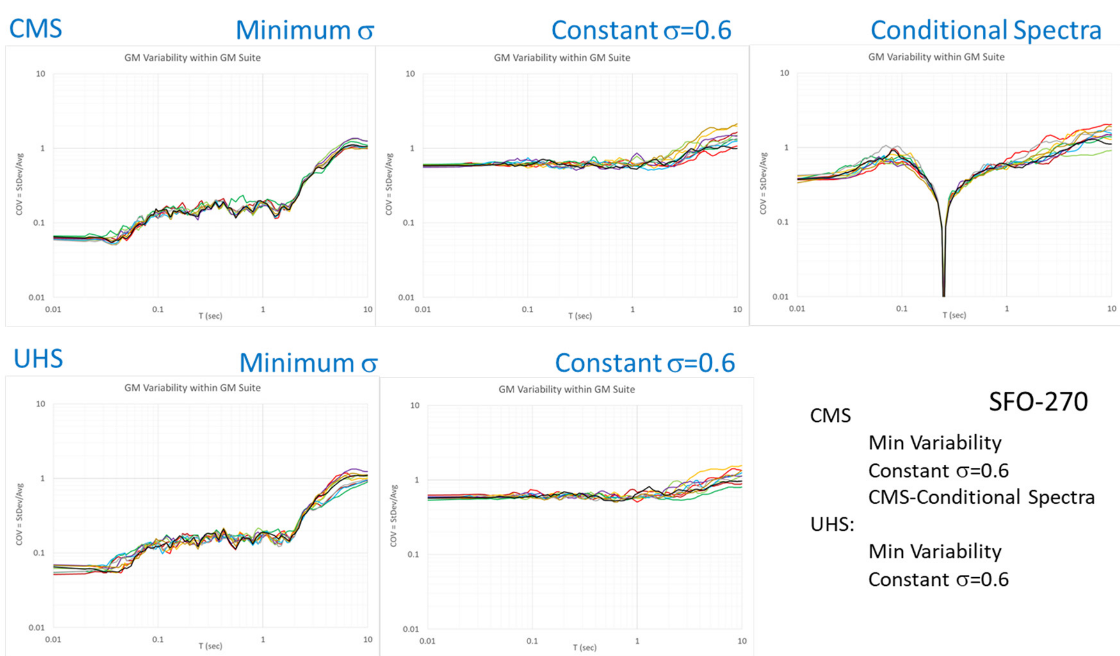

Figure 3.19 Sample of coefficient of variability in the ground-motion suite.

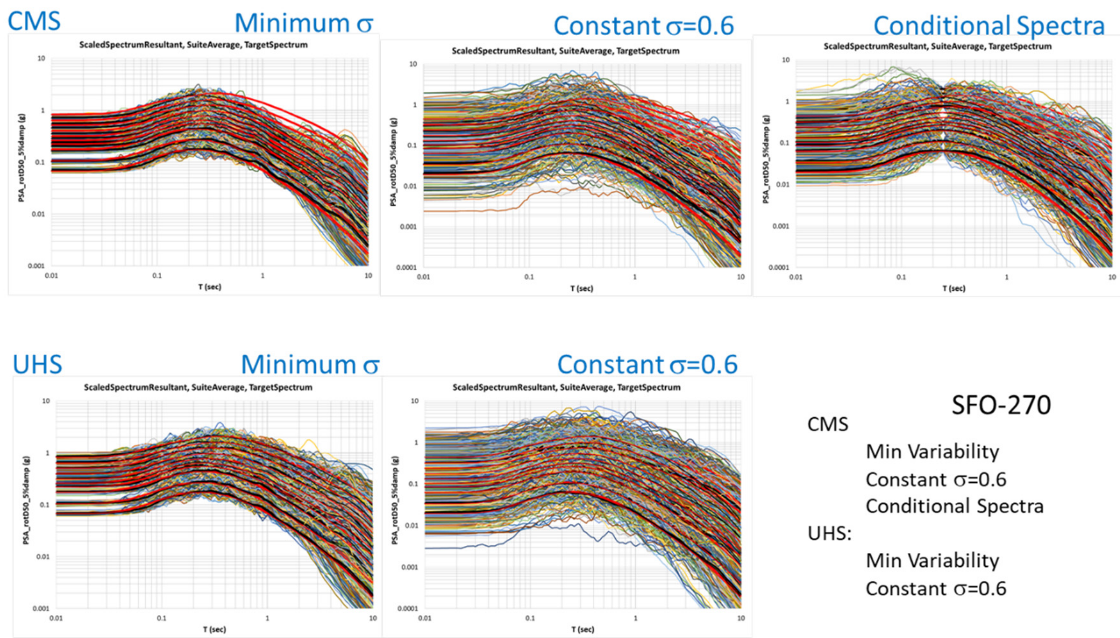

Figure 3.20 Sample of complete set of ground-motion suites for a site and site class.

4 Ground-Motion Selection and Modification for the Conditional-Spectrum-Based Records

This chapter provides the background on a secondary set of ground motions used within the PEER–CEA Project. Following sensitivity studies using structural analysis, the Project Team agreed that using a conditional spectrum hazard target with a short conditioning period would best represent the seismic hazard in terms of spectral shape for the needs of the project. This is including consistency with the IM used in the numerical studies behind the *FEMA P-1100* [2018] retrofit pre-standard, as well as the typical short-period spectral acceleration used within the insurance industry for residential wood-frame structures. Further discussion of the selection of conditioning period and sensitivity analyses are provided within the WG5's PEER–CEA report. Notably, only site conditions with a target V_{s30} of 270 m/sec were sought for the revised set of ground motions.

This chapter begins with discussion of the methodology behind selecting ground-motion sets using a conditional spectrum target in Section 4.1. The validation of the selection procedure and overview of ground-motion suites is discussed in Section 4.2 for all ten applicable sites (V_{s30} = 270 m/sec); see Chapter 2. The baseline sites selected for structural analysis are defined and reviewed for important ground-motion characteristics that were not explicitly considered in the record selection process in Sections 4.3 and 4.4. The ground-motion characteristics include significant duration and pulse-like ground-motion content. The chapter focuses on the site locations of Bakersfield, San Francisco, Northridge, and San Bernardino since these four sites have been adopted by WG5, whose tasks cover the range of seismicity covered by the *FEMA P-1100* plan sets for retrofit design.

4.1 METHODOLOGY

The ground motions were selected and scaled to fit a CS at each return period. The IM for conditioning was selected as the RotD50 spectral acceleration at a period of 0.25 sec. A CS consists of two parts representing central tendency and variance. The first, a CMS, represents the mean spectral intensity of the ground-motion suite [Baker 2011; Baker and Cornell 2006]. The target variance is captured through the use of a CS that incorporates the correlation of spectral acceleration values [Baker and Jayaram 2008; Jayaram and Baker 2008] for different rupture scenarios (M, R, and ε) at periods away from the conditioning period (T^*). The selection procedure was carried out using a modified version of the CS ground motion selection tool (CS-GMS tool) developed by Baker and Lee [2018]. The software tool can be used to select ground motions with a target response spectrum mean and variance. This tool builds upon an earlier algorithm proposed by Jayaram et al. [2011].

The target spectrum and variability using the CS-GMS tool developed by Baker and Lee [2018] is based on the following relationships and assumptions:

- The mean and standard deviation is computed internally by the CS-GMS tool for each site and return period using the BSSA14 ground-motion model [Boore et al. 2014]. Note: the epistemic uncertainty has already been considered in the PSHA process by employing multiple NGA-West2 models;
- The CMS is conditioned at a period of 0.25 sec, as selected by WG5; Because of the shape of both the UHS and CMS spectra at this relatively short period, it was determined that a second conditioning period was not needed. A sensitivity analysis of varying the conditional period was carried out by WG5 and is documented in WG5's PEER–CEA report;
- The variability is defined internally in the CS-GMS tool by the CS computation that includes period-dependent variability and no variability at $T^* = 0.25$ sec; and
- Correlations of spectral ordinates are computed internally by the CS-GMS tool using the relationship proposed by Baker and Jayaram [2008].

Developing the spectral targets for ground-motion selection requires entering several site-specific parameters within the CS-GMS tool. The first are the magnitude (M), distance (D), and epsilon (ε) that are representative of each site and return period. These values are taken as the expected values (i.e., M_{bar}, D_{bar}, and ε_{bar}) from PSHA deaggregation. Notably, D_{bar} represents the Joyner and Boore distance metric. The input values for the four baseline sites selected for structural analysis by the numerical modeling group are presented in Table 4.1. The additional settings using the CS-GMS tool assume a V_{s30} of 270 m/sec, California as the region, and assumes a strike–slip fault-type.

Following the definition of the target mean (CMS) and variability (CS), the ground-motion search and scaling criteria must be defined. Two site-dependent parameters are the ranges for magnitude (i.e., [M_{min}, M_{max}]) and source-to-site distance (i.e., [D_{min}, D_{max}]). Since the CS-GMS tool only allows for a single M-D-V_{S30} combination during searching, a representative range for magnitude and distance was selected for each site that was used for all return periods to maintain simplicity. These ranges of magnitude and distance are provided for the four baseline sites in Table 4.2, noting that these ranges are based on deaggregated PSHA results. The remaining search and scaling criteria remain constant for all sites and return periods. These are listed as follows:

- No lower or upper limits were put on V_{s30} values of ground motions;
- The period range for fitting both the CMS and CS was between 0.02 sec (T_{min}) and 2.0 sec (T_{max});
- The maximum scale factor was set to 5.0 with no lower bound limit on the minimum scale factor;
- The source database was the NGA-West2 [Ancheta et al. 2013];

- The spectrum component was the RotD50 of the two horizontal components; and
- All other inputs and settings were maintained at program defaults.

Table 4.1 Site- and return period-specific input parameters for developing the conditional mean spectra and conditional spectra using the CS-GMS tool (information for four baseline sites provided).

Site[1]	RP (yr)	M_{bar} [2]	D_{bar} [2] (km)	ε_{bar} [2]		Site	RP (yr)	M_{bar}	D_{bar} (km)	ε_{bar}
BAK	15	6.19	65.98	-0.15		SF	15	6.33	39.77	-0.46
BAK	25	6.27	54.73	-0.01		SF	25	6.47	32.13	-0.20
BAK	50	6.36	44.27	0.21		SF	50	6.64	25.00	0.16
BAK	75	6.40	39.44	0.35		SF	75	6.72	22.51	0.35
BAK	100	6.42	36.44	0.46		SF	100	6.78	20.99	0.49
BAK	150	6.43	33.19	0.60		SF	150	6.85	19.34	0.69
BAK	250	6.44	30.07	0.78		SF	250	6.92	17.73	0.93
BAK	500	6.43	26.02	1.02		SF	500	6.98	16.57	1.19
BAK	1000	6.42	22.80	1.24		SF	1000	7.04	15.36	1.49
BAK	2500	6.39	19.10	1.52		SF	2500	7.07	14.38	1.84
NR	15	6.11	31.37	-0.46		SB	15	6.13	28.97	-0.32
NR	25	6.18	24.39	-0.18		SB	25	6.23	21.78	-0.10
NR	50	6.25	19.03	0.21		SB	50	6.39	15.90	0.20
NR	75	6.29	16.97	0.43		SB	75	6.50	13.37	0.39
NR	100	6.32	15.93	0.57		SB	100	6.57	12.19	0.53
NR	150	6.35	14.61	0.78		SB	150	6.65	10.85	0.71
NR	250	6.38	13.66	0.98		SB	250	6.74	9.90	0.92
NR	500	6.42	12.27	1.29		SB	500	6.86	8.66	1.23
NR	1000	6.45	11.41	1.55		SB	1000	6.95	7.86	1.51
NR	2500	6.47	10.58	1.86		SB	2500	7.02	7.30	1.82

[1] BAK=Bakersfield, SF=San Francisco, NR=Northridge, and SB=San Bernardino; all sites are V_{s30} =270 m/sec.
[2] M_{bar}, D_{bar}, and ε_{bar} are taken from PSHA deaggregation information at a period of 0.25 sec.

Table 4.2 **Ranges of magnitude and distance used for record selection for each of the four baseline sites based on PSHA.**

Site	M_{min}	M_{max}	D_{min} (km)	D_{max} (km)
Bakersfield	6	8.5	30	100
San Francisco	5	8.5	0	50
Northridge	5	8	0	20
San Bernardino	5	8	0	30

4.2 GROUND-MOTION SUITES

The resulting ground-motion suites from the selection process targeting conditional mean spectra with conditional spectra variability are presented in this section. The ground-motion suites consist of ten return periods for each individual site. Each return period has 45 horizontal pairs of acceleration recordings. Ground-motion suites are produced for all ten sites assuming a target V_{s30} or 270 m/sec. The target spectral acceleration at the conditioning period (T^* = 0.25 sec), which serves as the anchor point for all records for a given site and return period, is shown in Table 4.3.

The two ground-motion selection criteria are the fit of the mean (RotD50) spectral acceleration of each site and return period to the target CMS and the record-to-record dispersion of each ground-motion set to the CS for each return period of interest. Figure 4.1(a) shows an example of the CMS fitting for all ten return periods for the San Francisco site. Similarly, the record-to-record variability of the 250-year return period is compared with the target CS in Figure 4.1(b). Notably, the variability is expressed as plus and minus lognormal standard deviation bounds.

In general, the record selection process provided excellent fits to the target mean (CMS) and variability (CS) estimated using the CS-GMS tool. The quality of this fit is dependent on the number of ground-motion pairs in a suite. The resulting mean and dispersion shown in this figure support the original choice by the WGs of having at least 40 record pairs per suite because they are consistent with the CS model. The mean (RotD50) spectral fit to the target CMS is provided for all ten sites and ten return periods in Appendix A.2. Comparisons of ground-motion variability to the target CS is provided for select return periods for the four baseline sites (Bakersfield, San Francisco, Northridge, and San Bernardino) in Appendix A.2. The target spectra for these ground-motion suites are given in Appendix A.3.

Table 4.3 Target spectral acceleration values at a conditioning period of 0.25 sec for all ten sites and return periods.

RP (yr)	OAK[1,2]	SAC	SF[3]	SJ	BAK[3]	LB	LA	NR[3]	SB[3]	SD
15	0.201	0.091	0.178	0.269	0.119	0.165	0.191	0.217	0.252	0.104
25	0.313	0.129	0.273	0.404	0.172	0.238	0.280	0.335	0.375	0.145
50	0.510	0.194	0.444	0.620	0.271	0.370	0.442	0.540	0.589	0.223
75	0.640	0.237	0.560	0.765	0.344	0.465	0.557	0.681	0.743	0.285
100	0.744	0.273	0.652	0.873	0.404	0.540	0.651	0.785	0.861	0.339
150	0.900	0.329	0.790	1.027	0.497	0.661	0.795	0.948	1.036	0.435
250	1.097	0.409	0.982	1.221	0.626	0.835	1.003	1.152	1.265	0.588
500	1.404	0.535	1.246	1.534	0.834	1.103	1.302	1.484	1.627	0.864
1000	1.737	0.690	1.564	1.852	1.070	1.422	1.657	1.828	2.021	1.187
2500	2.214	0.940	2.014	2.305	1.440	1.900	2.167	2.328	2.559	1.702

[1] Target intensity measure is the RotD50 spectral acceleration (g) for each horizontal ground-motion pair.
[2] OAK=Oakland, SAC=Sacramento, SF=San Francisco, SJ=San Jose, BAK=Bakersfield, LB=Long Beach, LA=Los Angeles, NR=Northridge, SB=San Bernardino, and SD=San Jose.
[3] This is one of four selected baseline sites for numerical analysis.

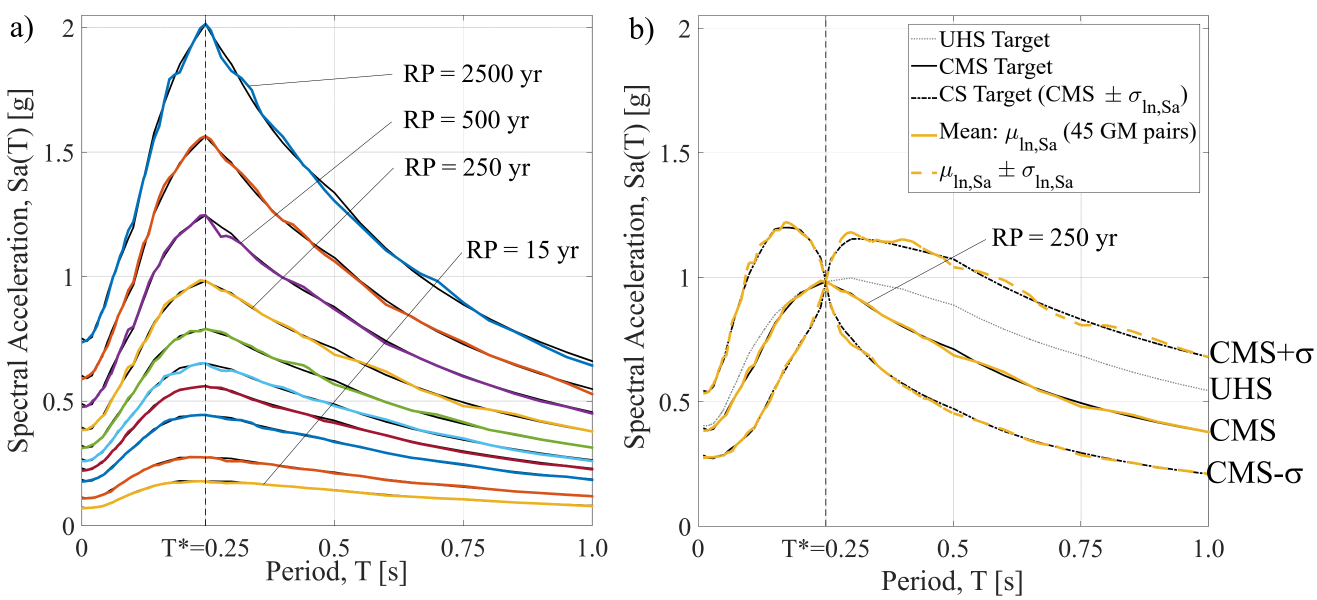

Figure 4.1 Example of record selection fitting for the San Francisco site: (a) Conditional mean spectra compared with mean spectral acceleration of each return period, and (b) illustration of fitting target variability for a single return period.

4.3 SIGNIFICANT DURATION OF SELECTED RECORDS

The CMS-CS based ground-motion sets were not selected based on the significant duration of the ground motions because duration models are typically conditional models and, hence, are meant to be used in evaluating a suite once it has been selected. This section provides an illustrative verification of the significant duration content of the record sets. The significant duration of a ground motion can be defined using numerous metrics [Bommer and Martinez-Pereira 1999], and the NGA-West2 database has a sub-set of these duration metrics provided for all records. The duration metric used here is the time interval between the 5% and 75% Arias Intensity and is referred to as D5-75 in this chapter. This duration metric was selected due to its wide use in the literature [Chandramohan et al. 2016] and its availability in the NGA-West2 database [Ancheta et al. 2013].

The significant duration statistics for the different ground-motion suites were collected. Since record selection targets the RotD50 spectral acceleration of two horizontal components, significant duration is reported herein as the average of the two horizontal components. A sample of the statistics monitored for significant duration is shown in Table 4.4 for the San Francisco site.

For comparison's sake, the prediction model proposed by Abrahamson and Silva [1996] and Stewart et al. [2002] (AS_1996) was calculated for each site and return period. The AS_1996 duration model provides a median and logarithmic standard deviation of the significant duration (e.g., horizontal D5-75 on soil in this case). The required inputs of magnitude and distance are taken as the mean values (M_{bar} and D_{bar}) at a period of 0.25 sec from PSHA deaggregation; see Table 4.1.

The calculations for the AS_1996 model were carried out using the function provided by the Baker Research Group; see *https://web.stanford.edu/~bakerjw/GMPEs.html for details*.

Figure 4.2 compares the median and logarithmic standard deviation bounds with the predictions of the AS_1996 model for the four baseline sites (i.e., Bakersfield, San Francisco, Northridge, and San Bernardino). The values are presented with the return period on the *x*-axis in logscale to compare all return periods simultaneously. The figure shows very good agreement with the prediction equation, considering that ground motions were not selected based on significant duration. The largest discrepancy is that the median D5-75 values for Bakersfield (the site with the lowest seismicity) are consistently above the AS_1996 prediction. This is most likely due these records having a minimum distance of 30 km (see Table 4.2) for record selection. This would logically force more longer duration ground motions to be selected to best match target spectral acceleration criteria.

Table 4.4 **Sample of extracted significant duration (D5-75) statistics for the San Francisco site.**

RP (yr)	Mean (μ) (sec)	Median (sec)	Std. dev. (σ) (sec)	COV (μ/σ)	Min	Max	β_{LN}	Lillie PassLN?[1]
15	8.46	7.90	4.67	0.55	1.43	23.93	0.62	0
25	8.07	7.85	4.09	0.51	1.53	20.01	0.57	1
50	9.00	8.09	5.33	0.59	2.06	23.93	0.65	1
75	9.16	8.54	5.37	0.59	1.76	23.93	0.64	1
100	7.52	6.68	4.70	0.62	1.35	27.77	0.60	0
150	8.23	7.03	5.39	0.65	0.91	26.33	0.70	0
250	8.41	6.93	5.34	0.64	0.72	28.56	0.65	1
500	8.10	6.26	5.24	0.65	1.43	23.93	0.63	0
1000	8.36	6.00	6.74	0.81	0.81	29.19	0.87	0
2500	7.28	5.47	6.16	0.85	0.40	34.29	0.84	1

[1] Testing for lognormal distribution using Lilliefors at 5% significance (0 = pass, 1= fail).

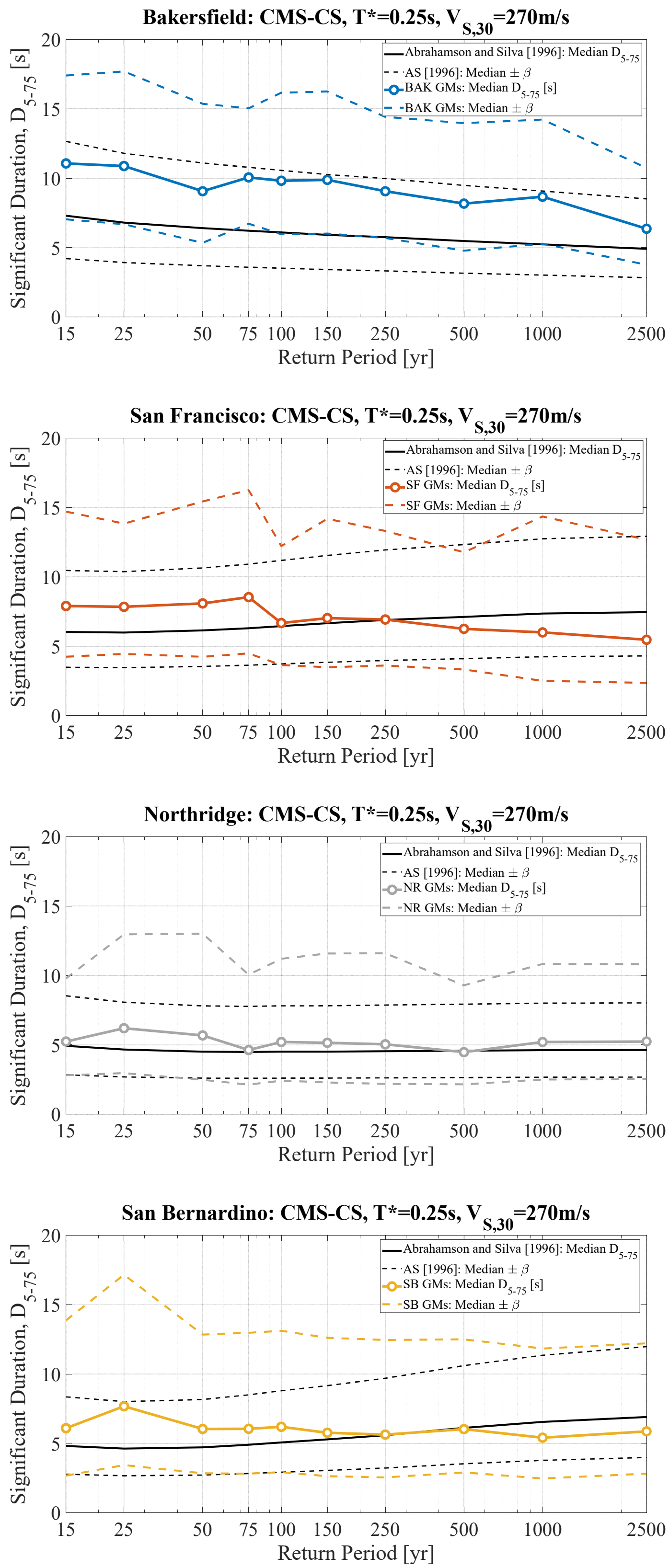

Figure 4.2 **Significant duration of ground-motion sets for baseline sites compared with prediction equation proposed by Abrahamson and Silva [1996].**

4.4 PULSE-LIKE GROUND MOTION CONTENT OF SELECTED RECORDS

This section investigates the pulse-like ground-motion content of the ground-motion suites selected to fit a CMS and conditional spectrum variability. This investigative effort is a direct result of strong concerns about pulse–motion content within the ground-motion sets during the project review process. The current project did not explicitly consider pulse-like ground-motions or forward directivity considerations within the hazard assessment or record selection process. This is specifically due to the current structures under consideration being inherently of short-period nature.

Extensive research has been conducted on the inclusion of pulse and near-source directivity effects in seismic hazard analysis as well as methods in order to properly select ground motion suites to include near-source effects; recent reviews are provided in NIST [2011], Almufti et al. [2015] and Tarbali et al. [2019]. Despite this, there is no accepted method for including these effects within these two stages of a seismic hazard representation, with existing research showing questionable significance for short-period structures. The ground-motion sets are reviewed for pulse content to illustrate the results of the current hazard assessment and record selection process.

4.4.1 Different Identification Methods for Pulse-Like Ground Motions

Numerous methods exist for identification of ground-motion recordings with strong velocity pulses. Identification of pulse motions is typically paired with an estimation of the pulse period (T_p), which represents the time interval for the predominant velocity pulse. The wavelet transform method [Baker, 2007] is that adopted for pulse classification within the NGA-West2 database (flatfiles available at *www.peer.berkeley.edu*). The pulse-like ground-motions identified within the NGA-West2 flatfiles are a subset of the larger list provided by Shahi and Baker [2014] using the same identification method. The approach of Hayden et al. [2014] uses peak-to-peak velocity (PPV) and normalized cumulative squared velocity (NCSV) to identify pulse motions and pulse periods. Recent work by Chang et al. [2019] uses the peak-to-point method (PPM) using the algorithm developed by Zhai et al. [2013] as well as the peak spectral velocity method [Alavi and Krawinkler 2004] for identifying pulse-like ground motions and pulse periods. An illustration of the methods is shown in Figure 4.3. Notably, this list of identification studies and methods is not exhaustive and represents recent efforts to classify pulse-like ground motions.

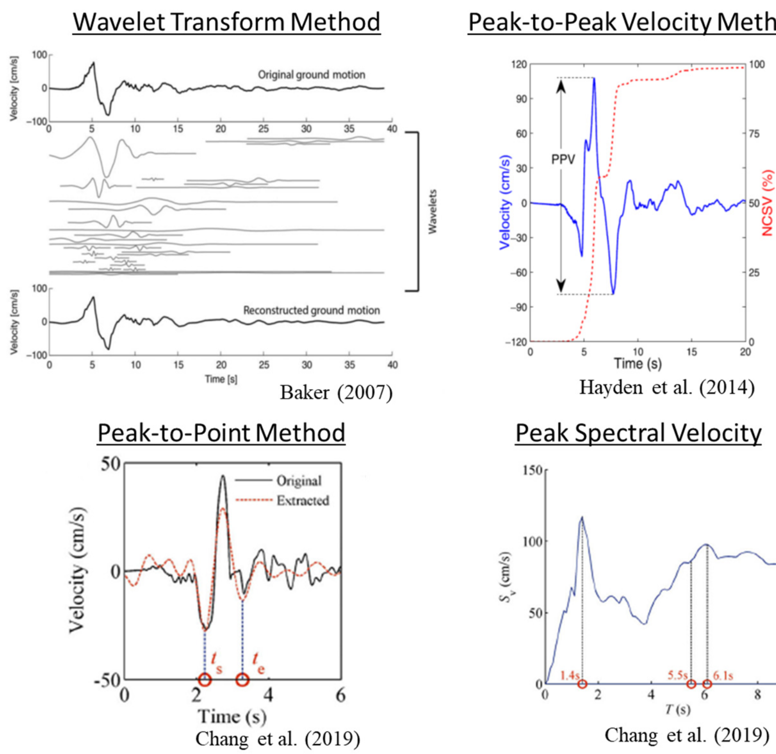

Figure 4.3 **Illustration of different methods for pulse–motion and pulse–period identification.**

4.4.2 Pulse-Like Motions within the NGA-West2 Database

Using the various pulse identification techniques mentioned in Section 4.4.1, the NGA-West2 database [Ancheta et al. 2013] was reviewed for pulse-motion content. The classification of pulse motions and pulse periods uses two defined sets of identified ground motions:

- NGA Flatfile – Only ground motions identified as pulse motions with corresponding pulse periods within the NGA-West2 database flatfile.
- Combined Set – A combined list of identified pulse motions using results from the NGA-West2 flatfile, Shahi and Baker [2014], Hayden et al. [2014], and Chang et al. [2019]. The various identified lists were sorted for repeated recordings.

The NGA Flatfile list serves as a control or baseline list. This represents the information that is most readily available and, arguably, an accepted list of identified pulse motions. The combined set of motions attempts to collect various identification methods to understand the range of pulse motions and pulse periods that could be applicable to short-period structures. When referring to short-period structures, the scope of the current project looks at elastic fundamental periods (T_1) in the range of 0.1 sec to 0.6 sec. Depending on the level of nonlinear behavior and structural system, pulse periods could be most damaging in the range of 1.25 [Shahi and Baker 2011] to 2.0 times [Tothong and Cornell 2008] the elastic fundamental period. Further, structures undergoing significant nonlinear demands could be affected by pulse periods much longer than the elastic (T_p > 2T_1) fundamental period depending on loading history and structural system [Champion and Liel 2012]. This suggests that a wide range of pulse periods can still be important for structural response when considering other intensity measures such as spectral shape and significant duration.

Figure 4.4 shows the distribution of identified pulse motions within the NGA-West2 flatfile (NGA_West2_Flatfile_RotD50_d050_public_version.xls last modified 3/15/2014) for the individual pulse identification sources and the combined set. The figure shows a considerable variation in the number of pulse ground motions and pulse–period distribution, depending on the classification method and study. When comparing the NGA flatfile to the combined set, a significant number of shorter period (T_p < 1.0 sec) pulse-like ground motions are identified using the other lists from other studies. Further, this pulse–period range is shown to have significant contribution from all identification studies in the combined set. Pulse periods beyond 1.0 sec are dominated by the list identified by Shahi and Baker [2014]. The information presented in Figure 4.4 is tabulated within Table 4.5 for completeness. The total identified pulse-like ground motions in Table 4.5 show a nearly 100% increase when comparing the NGA-West2 flatfile to the combined set used for comparison in this study (149 versus 295 total identified pulse-like ground motions).

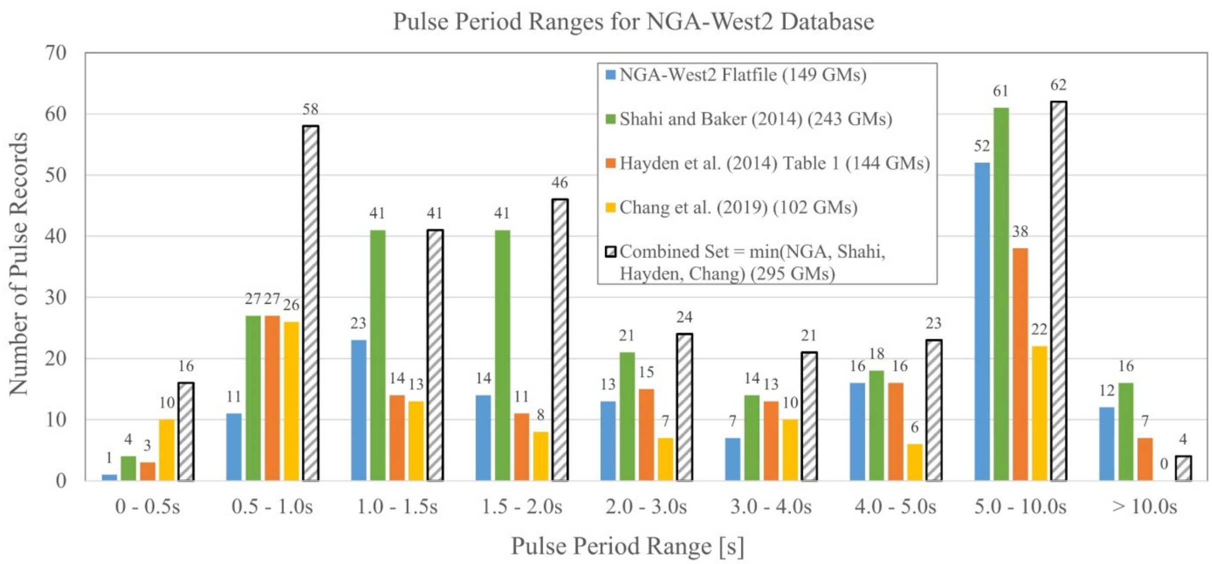

Figure 4.4 Comparing identified pulse ground motions and pulse periods from various identification methods and studies within the NGA-West2 database. Hatched bars represent the combined set from all studies assuming the minimum pulse period for repeated ground motions identified as pulse-like.

Table 4.5 **Number of pulse-like ground motions in NGA-West2 database according to different classification methods and studies.**

T_p range (sec)	NGA Flatfile	Shahi & Baker [2014]	Hayden et al. [2014]	Chang et al. [2019]	Combined
0–0.5	1	4	3	10	16
0.5–1.0	11	27	27	26	58
1.0–1.5	23	41	14	13	41
1.5–2.0	14	41	11	8	46
2.0–3.0	13	21	15	7	24
3.0–4.0	7	14	13	10	21
4.0–5.0	16	18	16	6	23
5.0–10.0	52	61	38	22	62
> 10.0	12	16	7	0	4
Total	149	243	144	102	295

4.4.3 Pulse Content of Selected Record Sets

The pulse-like ground-motion content of the record sets is expressed in terms of a pulse fraction. The pulse fraction is simply the ratio of pulse-like ground motions to the total number of ground motions for the site and return period under consideration. Notably, all ground-motion sets have 45 ground-motion pairs per return period (i.e., nine pulse records out of 45 has a pulse fraction of 0.2). The pulse fractions for the baseline sites (i.e., Bakersfield, San Francisco, Northridge, and San Bernardino) are compared for the two pulse classification sets in Figure 4.5 and Figure 4.6 for the NGA-West2 flatfile classification and the combined classification set, respectively; see Section 4.4.2 for definitions.

Comparing the different sites in Figure 4.5 (using the NGA flatfile classification) shows that the lower seismicity and far-field site of Bakersfield has only one pulse-like ground motion. The observed pulse motions increase with increasing seismicity of the sites, with more pulse motions observed for Northridge and San Bernardino (known near-field sites) when compared to San Francisco. The results using the combined classification set in Figure 4.6 show an increase in the observed pulse fraction when comparing to the NGA-West2 flatfile. However, the general trends across different sites and return periods are preserved, recalling that these are the same record sets viewed from a different set of classified pulse-like ground motions. The observed pulse fractions for all ten sites are provided in Table 4.6 and Table 4.7 for the NGA flatfile and combined classification sets, respectively.

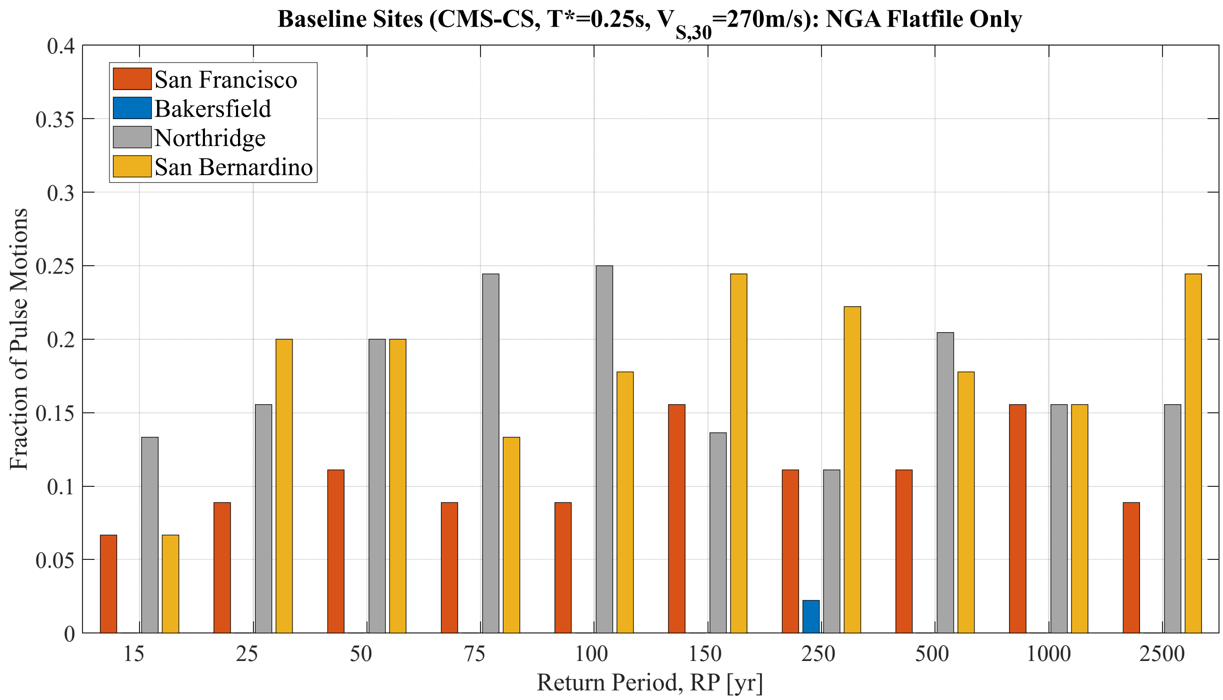

Figure 4.5 Fraction of pulse-like ground motions observed in the baseline ground-motion sets using records identified as pulse motions within the NGA-West2 flatfile.

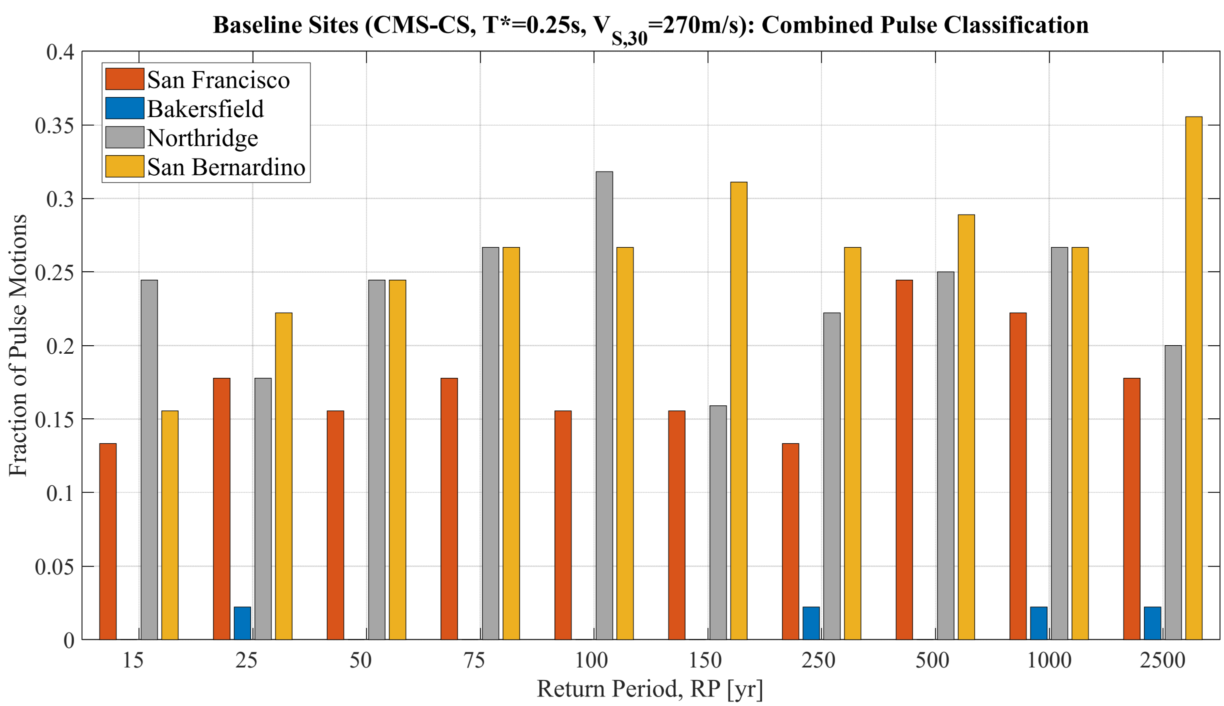

Figure 4.6 Fraction of pulse-like ground motions observed in the baseline ground-motion sets using records identified as pulse motions using the combined pulse classification set.

Table 4.6 Pulse fraction for each site and return period: NGA flatfile classification.

RP (yr)	OAK[1,2]	SAC	SF[3]	SJ	BAK[3]	LB	LA	NR[3]	SB[3]	SD
15	0.111	0.000	0.067	0.067	0.000	0.044	0.200	0.133	0.067	0.089
25	0.044	0.000	0.089	0.200	0.000	0.022	0.133	0.156	0.200	0.067
50	0.111	0.000	0.111	0.133	0.000	0.044	0.111	0.200	0.200	0.156
75	0.067	0.022	0.089	0.178	0.000	0.000	0.111	0.244	0.133	0.111
100	0.067	0.000	0.089	0.200	0.000	0.000	0.044	0.250	0.178	0.200
150	0.111	0.000	0.156	0.111	0.000	0.044	0.133	0.136	0.244	0.200
250	0.044	0.000	0.111	0.133	0.022	0.156	0.156	0.111	0.222	0.200
500	0.089	0.000	0.111	0.156	0.000	0.089	0.200	0.205	0.178	0.156
1000	0.111	0.000	0.156	0.111	0.000	0.111	0.156	0.156	0.156	0.222
2500	0.222	0.000	0.089	0.133	0.000	0.111	0.156	0.156	0.244	0.244

[1] Pulse fraction is based on a total of 45 ground motion pairs per return period.
[2] OAK=Oakland, SAC=Sacramento, SF=San Francisco, SJ=San Jose, BAK=Bakersfield, LB=Long Beach, LA=Los Angeles, NR=Northridge, SB=San Bernardino, and SD=San Jose.
[3] This is one of four selected baseline sites for numerical analysis.

Table 4.7 Pulse fraction for each site and return period: Combined classification set.

RP (yr)	OAK[1,2]	SAC	SF[3]	SJ	BAK[3]	LB	LA	NR[3]	SB[3]	SD
15	0.111	0.000	0.133	0.222	0.000	0.067	0.222	0.244	0.156	0.133
25	0.067	0.044	0.178	0.244	0.022	0.067	0.244	0.178	0.222	0.156
50	0.156	0.000	0.156	0.156	0.000	0.067	0.178	0.244	0.244	0.222
75	0.156	0.022	0.178	0.222	0.000	0.067	0.178	0.267	0.267	0.156
100	0.133	0.000	0.156	0.267	0.000	0.044	0.111	0.318	0.267	0.311
150	0.200	0.022	0.156	0.178	0.000	0.044	0.244	0.159	0.311	0.267
250	0.111	0.000	0.133	0.289	0.022	0.156	0.178	0.222	0.267	0.356
500	0.111	0.000	0.244	0.156	0.000	0.133	0.267	0.250	0.289	0.289
1000	0.200	0.000	0.222	0.178	0.022	0.156	0.222	0.267	0.267	0.378
2500	0.267	0.000	0.178	0.244	0.022	0.156	0.200	0.200	0.356	0.333

[1] Pulse fraction is based on a total of 45 ground motion pairs per return period.
[2] OAK=Oakland, SAC=Sacramento, SF=San Francisco, SJ=San Jose, BAK=Bakersfield, LB=Long Beach, LA=Los Angeles, NR=Northridge, SB=San Bernardino, and SD=San Jose.
[3] This is one of four selected baseline sites for numerical analysis.

In order to link the pulse fractions observed for the baseline record sets to what could be expected for each site's local site characteristics, the pulse fraction prediction relationship proposed by Hayden et al. [2014] is calculated for each site and return period. The relationship depends on the source-to-site distance (R) and the epsilon of the peak ground velocity $\left(\varepsilon_{\mathrm{PGV}}\right)$ as shown in Equation (4.1).

$$\text{pulse fraction} = \frac{1}{1+\exp\left[-3.87+1.04\left(R^{0.5}\right)+15.99\left(\varepsilon+3\right)^{-2}\right]} \tag{4.1}$$

The distance values are taken as the mean distance (D_{bar}) from PSHA deaggregation (at T = 0.25 sec). The values of $\varepsilon_{\mathrm{PGV}}$ are not available from PSHA results. Based on the findings of Bradley [2012] and the recommendations of Hayden et al. [2014], the epsilon of spectral acceleration at a period of 1.0 sec $\left\{\varepsilon\left[Sa\left(1\sec\right)\right]\right\}$ is used as a proxy for PGV with predominant magnitudes of 7 or less. These values are taken directly from the PSHA deaggregation results for each site and return period. Notably, other predictive relationships exist for estimating a target pulse fraction for a given site [NIST 2011; Shahi and Baker 2011; and Shahi and Baker 2014]. The relationship proposed by Hayden et al. [2014] was compared for a single site (Oakland) with Equation 19 of Shahi and Baker [2014] using an estimated magnitude-rupture length relationship based on data provided by Tarbali [2017]. As shown in Figure 4.7, the two relationships gave very similar results. The Hayden et al. [2014] relationship was selected due to ease of implementation for all sites.

The four baseline sites are compared with the relationship proposed by Hayden et al. [2014] in Figure 4.8 and Figure 4.9 for the NGA-West2 flatfile and combined classification sets, respectively. The most important observation for both figures is that the general fraction of pulse motions follows the trends in the predictive relationship that represents the typical trends for the individual site conditions. This highlights that the record selection process focusing on intensity measure-based targets (in this case target spectral acceleration, spectral shape, and variability) while selecting records with appropriate causal parameters for each site (e.g., M and R) includes a reasonable amount of pulse-like ground motions with respect to predictive equations. The lack of explicit agreement between observed pulse fractions and predictive relationships must consider that predictive pulse fractions can only be viewed as an indication rather than a deterministic target [Tarbali et al. 2019].

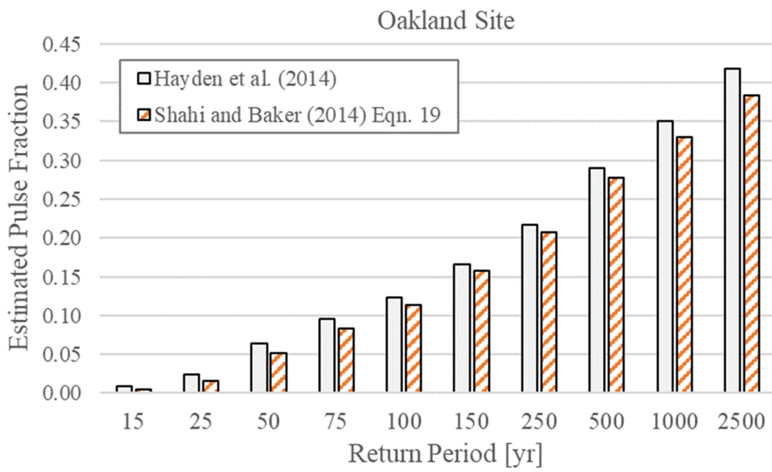

Figure 4.7 **Comparing predictive relationships for target pulse fractions for the Oakland site: Hayden et al. [2014] in solid bars versus Shahi and Baker [2014] in hatched bars.**

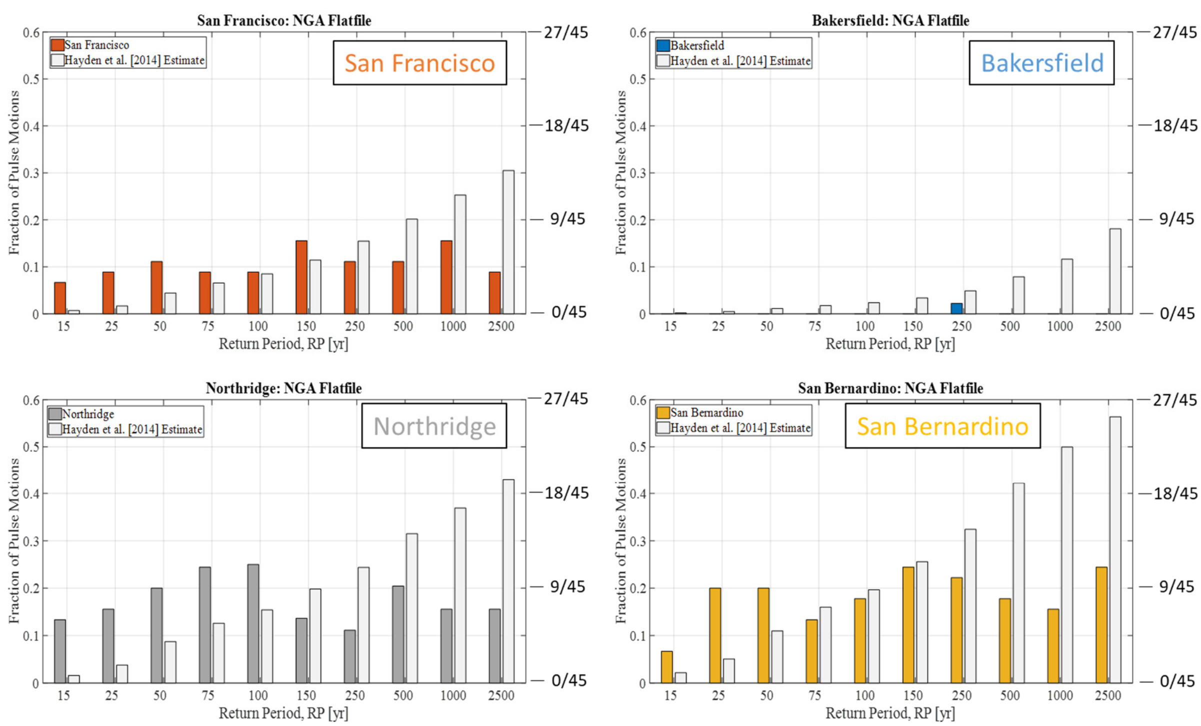

Figure 4.8 **Comparing pulse fraction of baseline ground-motion sets (colored bars) with the prediction relationship proposed by Hayden et al. [2014] (white bars): NGA-West2 flatfile pulse classification.**

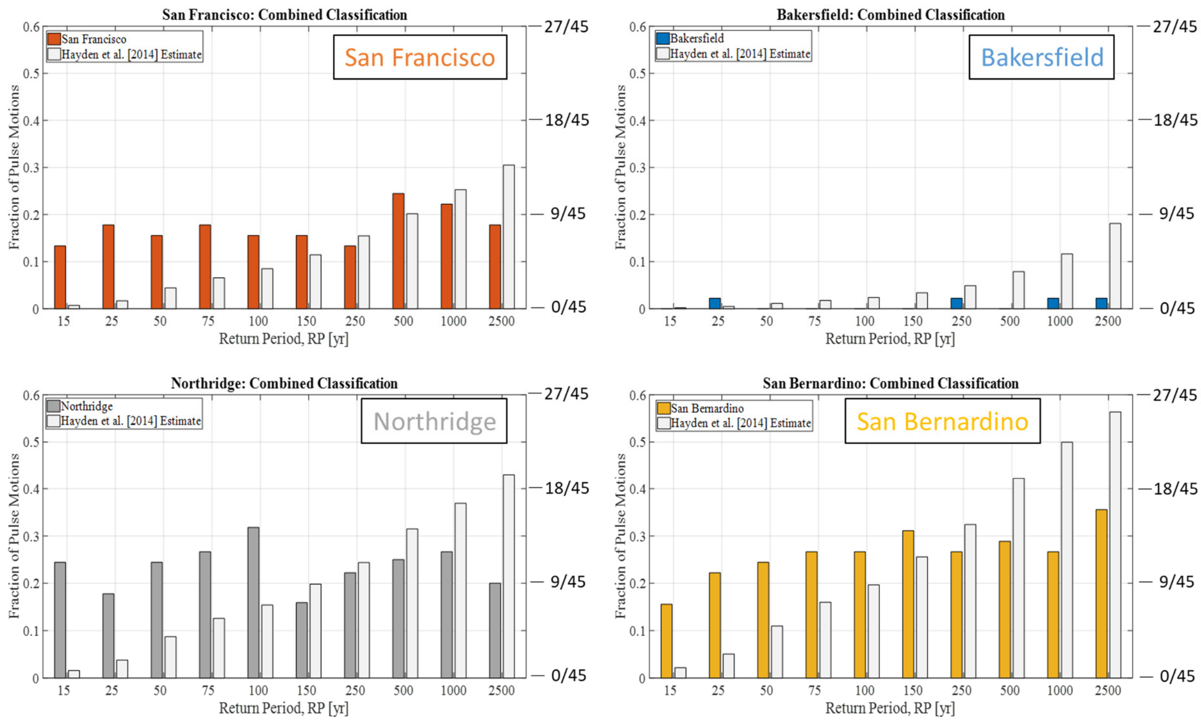

Figure 4.9 **Comparing pulse fraction of baseline ground-motion sets (colored bars) with the prediction relationship proposed by Hayden et al. [2014] (white bars): combined pulse classification set.**

5 Summary and Conclusions

This report summarizes the results of Working Group 3 (WG3), Task 3.1: *Selecting and Scaling Ground-Motion Records*, for the PEER–CEA wood-frame project. To achieve a proper representation of hazard and population distribution across the State of California, ten sites were selected and a site-specific probabilistic seismic hazard analysis (PSHA) was performed at each of these sites for both a soft soil (V_{s30} = 270 m/sec), which is more typical, and a stiff soil (V_{s30} = 760 m/sec), which represents a reference-site condition. The PSHA used the UCERF3 seismic-source model, which represents the latest seismic source model adopted by the USGS. The PSHA was carried out for structural periods ranging from 0.01 to 10 sec.

At each site and soil class, the results from the PSHA—hazard curves, hazard deaggregation, and uniform-hazard spectra (UHS)—were extracted for a series of ten return periods ranging from 15.5 to 2500 years. These return periods were selected in collaboration with the WG5 and WG6. For each case (site, soil class, and return period), the UHS was used as the target spectrum for selection and modification of a suite of ground motions. Additionally, another set of target spectra based on "Conditional Spectra" (CS), which are more realistic than UHS, as well the corresponding ground-motion suites, were developed. The Conditional Spectra are defined by a median (Conditional Mean Spectrum) and a period-dependent variance. A suite of 40 record pairs were selected and modified for each return period and target-spectrum type at each site and soil class. The choice of which ground-motion suite to use was left to WG5. Both suites are included in this report because it is important to consider the different methods of developing the ground-motion suites.

For the case of UHS as the target spectrum, the selected motions were scaled such that the average of the median spectrum (RotD50) of the ground-motion pairs follow the target UHS closely within the period range of interest to the analysts. For the case of the CS as the target spectrum, the ground-motion suites were selected and scaled using a modified version of the CS-GMS tool developed by Baker and Lee [2018]. The computation of CS requires a structural period for the conditional model. In collaboration with WG5 researchers, a conditioning period of 0.25 sec was selected as a representative of the fundamental mode of vibration of the buildings of interest in this study.

A detailed study of the pulse characteristics of the selected records in the ground-motion suites was also presented this report. The objective of this study was to quantify the fraction of records containing directivity pulses in each ground-motion suite and comparing it to a variety of predictive models. The comparison demonstrated that the general fraction of pulse motions follows the trends in the predictive relationship that represents the typical trends for the individual site conditions. The lack of explicit agreement between observed pulse fractions and predictive relationships must consider that predictive pulse fractions can only be viewed as an indication rather than a deterministic target.

This report presents a summary of the selected sites, the seismic-source characterization model and the ground-motion characterization model used in the PSHA, and selection and modification of suites of ground motions. The lists of selected and scaled motions are provided in appendices of this report, and the actual motions can be downloaded from the NGA-West2 website tool.

REFERENCES

Abrahamson N.A., Gregor N. (2015). Haz45, Seismic Hazard Analysis Software.

Abrahamson N.A., Silva W.J., Kamai R. (2014). Summary of the ASK14 ground motion relation for active crustal regions, *Earthq. Spectra*, 30(3): 1025–1055.

Abrahamson N.A., Silva W.J. (1996). *Empirical Ground Motion Models*, Report prepared for Brookhaven National Laboratory, New York, NY.

Al Atik L., Youngs R.R. (2014). Epistemic uncertainty for NGA-West2 models, *Earthq. Spectra*, 30(3): 1301–1318.

Alavi B., Krawinkler H. (2004). Behavior of moment-resisting frame structures subjected to near-fault ground motions, *Earthq. Eng. Struct. Dyn.*, 33(6): 687–706.

Almufti I., Motamed R., Grant D., Willford M. (2015). Incorporation of velocity pulses in design ground motions for a response history analysis using a probabilistic framework, *Earthq. Spectra*, 31(3): 1647–1666.

Ancheta T.D., Darragh R.B. Stewart J.P., Seyhan E., Silva W.J., Chiou B.S.-J., Wooddell K.E., Graves R.W., Kottke A.R., Boore D.M., Kishida T., Donahue J.L. (2013). PEER NGA-West2 database, *PEER Report No. 2013/03*, Pacific Earthquake Engineering Research Center, University of California, Berkeley, CA.

Baker J.W. (2007). Quantitative classification of near-fault ground motions using wavelet analysis, *Bull. Seismol. Soc. Am.*, 97(5): 1486–1501.

Baker J.W. (2011). Conditional mean spectrum: Tool for ground-motion selection, ASCE, *J. Struct. Eng.,* 137(3): 322–331.

Baker J.W., Cornell C.A. (2006). Spectral shape, epsilon and record selection, *Earthq. Eng. Struct. Dyn.*, 35: 1077–1095.

Baker J.W., Jayaram N. (2008). Correlation of spectral acceleration values from NGA ground motion models, *Earthq. Spectra*, 24(1): 299–317.

Baker J.W., Lee C. (2018). An improved algorithm for selecting ground motions to match a conditional spectrum, *J. Earthq. Eng.*, 22(4): 708–723.

Bommer J.J., Martinez-Pereira A. (1999). The effective duration of earthquake strong motion, *J. Earthq. Eng.*, 3: 127–172.

Boore D.M. (2010). Orientation-independent, nongeometric-mean measures of seismic intensity from two horizontal components of motion, *Bull. Seismol. Soc. Am.*, 100: 1830–1835.

Boore D.M., Stewart J.P., Seyhan E., Atkinson G.M. (2014). NGA-West2 equations for predicting PGA, PGV, and 5% damped PSA for shallow crustal earthquakes, *Earthq. Spectra*, 30(3): 1057–1085.

Bozorgnia Y., Abrahamson N.A., Al Atik L., Ancheta T.D., Atkinson G.M., Baker J.W., Baltay A., Boore D.M., Campbell K.W., Chiou B.S.-J., Darragh R., Day S., Donahue J., Graves R.W., Gregor N., Hanks T. Idriss I.M., Kamai R., Kishida T., Kottke A., Mahin S.A., Rezaeian S., Rowshandel B., Seyhan E., Shahi S., Shantz T., Silva W.J., Spudich P., Stewart J.P., Watson-Lamprey J., Wooddell K., Youngs R.R. (2014). NGA-West2 Research Project, *Earthq. Spectra*, 30(3): 973–987.

Bradley B.A. (2012). Empirical correlations between peak ground velocity and spectrum-based intensity measures, *Earthq. Spectra*, 28(1): 17–35.

Buyco K., Heaton T.H. (2019). 70%-Damped spectral acceleration as a ground motion intensity measure for predicting highly nonlinear response of structures, *Earthq. Spectra*, 35(2): 589–610.

Campbell K.W., Bozorgnia Y. (2014). NGA-West2 ground motion model for the average horizontal components of PGA, PGV, and 5% damped linear acceleration response spectra, *Earthq. Spectra*, 30(3): 1087–1115.

Champion C., Liel A. (2012). The effect of near-fault directivity on building seismic collapse risk, *Earthq. Eng. Struct. Dyn.*, 41: 1391–1409.

Chandramohan R., Baker J.W., Deierlein G.G. (2016). Quantifying the influence of ground motion duration on structural collapse capacity using spectrally equivalent records, *Earthq. Spectra*, 32(2): 927–950.

Chang Z., De Luca F., Goda K. (2019). Near-fault acceleration pulses and non-acceleration pulses: Effects on the inelastic displacement ratio, *Earthq. Eng. Struct. Dyn.*, 48:1256-1276.

Chiou B.S.-J. Youngs R.R. (2014). Update of the Chiou and Youngs NGA model for the average horizontal component of peak ground motion and response spectra, *Earthq. Spectra*, 30(3): 1117–1153.

FEMA (2012) *Next-Generation Methodology for Seismic Performance Assessment of Buildings*, *FEMA P-58*, prepared by the Applied Technology Council for the Federal Emergency Management Agency, Washington, D.C.

FEMA (2018). *Vulnerability-Based Seismic Assessment and Retrofit of One- and Two-Family Dwellings: Volume 1 - Prestandard, FEMA P-1100*, Prepared by the Applied Technology Council for the California Earthquake Authority (Sacramento, CA) and the Federal Emergency Management Agency (Washington, DC).

Hale C., Abrahamson N.A., Bozorgnia Y. (2018). Probabilistic seismic hazard analysis code verification, *PEER Report No. 2018/03*, Pacific Earthquake Engineering Research Center, University of California, Berkeley, CA.

Hayden C.P., Bray J.D., Abrahamson N.A. (2014). Selection of near-fault pulse motions, ASCE, *J. Geotech. Geoenviro. Eng.,* doi: 10.1061/(ASCE)GT.1943-5606.0001129, 0401430.

Idriss I.M. (2014). An NGA-West2 empirical model for estimating the horizontal spectral values generated by shallow crustal earthquakes, *Earthq. Spectra*, 30(3): 1155–1177.

Jayaram N., Baker J.W. (2008). Statistical tests of the joint distribution of spectral acceleration values, *Bull. Seismol. Soc. Am.*, 98(5): 2231–2243.

Jayaram N., Lin T., Baker J.W. (2011). A computationally efficient ground-motion selection algorithm for matching a target response spectrum and variance, *Earthq. Spectra*, 27(3): 797–815.

Keefer D.L., Bodily S.E. (1983). Three-point approximations for continuous random variables, *Manage. Sci.*, 29: 595–609.

NIST (2011). Selecting and scaling earthquake ground motions for performing response history analysis, *NIST GCR 11-917-15*, NEHRP Consultants Joint Venture, National Institute of Standards and Technology, Gaithersburg, MD.

Petersen M.D., Moschetti M.P., Powers P.M., Mueller C.S., Haller K.M., Frankel A.D., Zeng Y, Rezaeian S., Harmsen S.C., Boyd O.S., Field N., Chen R., Rukstales K.S., Luco N., Wheeler R.L., Williams R.A., Olsen A.H. (2014). Documentation for the 2014 update of the United States national seismic hazard maps, *U.S. Geological Survey Open-File Report 2014–1091*, 243 pgs., *https://dx.doi.org/10.3133/ofr20141091*.

Shahi S.K., Baker J.W. (2011). An empirically calibrated framework for including the effects of near-fault directivity in probabilistic seismic hazard analysis, *Bull. Seismol. Soc. Am.*, 101(2): 742–755.

Shahi S.K., Baker J.W. (2013). A probabilistic framework to include the effects of near-fault directivity in seismic hazard assessment, *PEER Report No. 2013/15*, Pacific Earthquake Engineering Research Center, University of California, Berkeley, CA.

Shahi S.K., Baker J.W. (2014). An efficient algorithm to identify strong-velocity pulses in multicomponent ground motions, *Bull. Seismol. Soc. Am.*, 104(5): 2456–2466.

Spudich P., Bayless J., Baker J.W., Chiou B.S.-J., Rowshandel B., Shahi S., Somerville P.G. (2013). Final report of the NGA-West2 Working Group, *PEER Report No. 2013/09*, Pacific Earthquake Engineering Research Center, University of California, Berkeley, CA

Stewart J.P., Chiou B.S.-J., Bray J.D., Graves R.W., Somerville P.G., Abrahamson N.A. (2002). Ground motion evaluation procedures for performance-based design, *Soil Dyn. and Earthq. Eng.*, 22(9–12): 765–772. [Publicly available documentation of Abrahamson and Silva 1996 model].

Tarbali K. (2017). *Ground Motion Selection for Seismic Response Analysis*, Ph.D. Dissertation, Department Civil and Natural Resources Engineering, University of Canterbury, Christchurch, New Zealand.

Tarbali K., Bradley B.A., Baker J.W. (2019). Ground motion selection in the near-fault region considering directivity induced pulse effects, *Earthq. Spectra*, 35(2): 759–786.

Tothong P., Cornell C.A. (2008). Structural performance assessment under near-source pulse-like ground motions using advanced ground motion intensity measures, *Earthq. Eng. Struct. Dyn.*, 37: 1013–1037.

USGS (2013). *The Uniform California Earthquake Rupture Forecast*, *Version 3* (*UCERF3*) – *The Time Independent Model*, U.S. Geological Survey, *USGS Open File Report 2013-1165*. Menlo Park, CA.

Vamvatsikos D., Cornell C.A. (2002). Incremental dynamic analysis, *Earthq. Eng. Struct. Dyn.*, 31(3): 491–514.

Zhai C., Chang Z., Li S., Chen Z., Xie L. (2013). Quantitative identification of near-fault pulse-like ground motions based on energy, *Bull. Seismol. Soc. Am.*, 103(5): 2591–2603.

LIST OF ELECTRONIC APPENDICES

Appendix A.1: **Set of Selected and Scaled Ground Motions for the Uniform-Hazard-Based Ground Motions at the Ten Sites**
For each site (Table 2.1 in report), site class, and return period:

a. Plot of individual-record response spectra (5% damped RotD50 PSA)
b. Plot of the UHS Target Spectrum and Suite Average (5%-damped RotD50 PSA)
c. Table of Record Metadata, Filenames and Scale Factor

Appendix A.2: **Set of Selected and Scaled Ground Motions for the CS-Based Ground Motions at the Ten Sites**
For each site (Table 2.1 in report), site class, and return period:

a. Plot of individual-record response spectra (5% damped RotD50 PSA)
b. Plot of the UHS Target Spectrum and Suite Average (5%-damped RotD50 PSA)
c. Table of Record Metadata, Filenames and Scale Factor

Appendix A.3: **Target Spectra for the two sets of ground-motion suites, UHS and CS (Digital Appendix – Microsoft Excel File)**

Appendix B.1: **List of Electronic Files**

Appendix B.2: **Hazard Curves (Digital Appendix – Microsoft Excel File)**

Appendix B.3: **UHS Deaggregation Results (Digital Appendix – Microsoft Excel File)**

Appendix C.1: **Presentation File at Panel Meeting of March 13, 2017**

Appendix C.2: **List of Action Items Decided at Panel Meeting of March 13, 2017**

The Pacifi c Earthquake Engineering Research Center (PEER) is a multi-institutional research and education center with headquarters at the University of California, Berkeley. Investigators from over 20 universities, several consulting companies, and researchers at various state and federal government agencies contribute to research programs focused on performance-based earthquake engineering.

These research programs aim to identify and reduce the risks from major earthquakes to life safety and to the economy by including research in a wide variety of disciplines including structural and geotechnical engineering, geology/seismology, lifelines, transportation, architecture, economics, risk management, and public policy.

PEER is supported by federal, state, local, and regional agencies, together with industry partners.

PEER Core Institutions

University of California, Berkeley (Lead Institution)
California Institute of Technology
Oregon State University
Stanford University
University of California, Davis
University of California, Irvine
University of California, Los Angeles
University of California, San Diego
University of Nevada, Reno
University of Southern California
University of Washington

PEER reports can be ordered at https://peer.berkeley.edu/peer-reports or by contacting

Pacific Earthquake Engineering Research Center
University of California, Berkeley
325 Davis Hall, Mail Code 1792
Berkeley, CA 94720-1792
Tel: 510-642-3437
Email: peer_center@berkeley.edu

ISSN 2770-8314
https://doi.org/10.55461/ZJDN7385